



**Supramolecular hydrogels based on bile acids and their  
derivatives**

par  
Meng Zhang

Département de chimie  
Faculté des arts et des sciences

Thèse présentée à la Faculté des études supérieures et postdoctorales  
en vue de l'obtention du grade de Philosophiae Doctor (Ph. D.)  
en chimie

Octobre 2016

© Meng Zhang, 2016



## Résumé

Les hydrogels moléculaires avec un réseau de fibres auto-assemblés sont utilisés dans différents domaines dont le relargage de médicaments, les senseurs, l'ingénierie tissulaire et la nano-modélisation. Les hydrogels moléculaires à base d'acides biliaries, qui sont une classe de biocomposés d'origine naturelle, montrent une biocompatibilité améliorée et sont de bons candidats pour des applications dans le domaine biomédical. Ces hydrogels présentent une bonne bio-dégradabilité et une diversité fonctionnelle grâce aux faibles interactions supramoléculaires et aux structures chimiques précisément contrôlées. Dans cette thèse, des nouveaux hydrogels moléculaires à base des acides biliaries et leurs dérivés ont été étudiés pour mieux comprendre la relation entre la structure chimique du gélifiant et la formation de gels moléculaires.

Un dimère de l'acide cholique avec un groupe diéthylènetriamine est insoluble dans l'eau. Par contre, il peut former des hydrogels grâce à un réseau tri-dimensionnel de fibres en présence de certains acides carboxyliques. L'addition d'acide carboxylique peut protoner le groupe amine secondaire et défaire les interactions intermoléculaires entre les dimères et favoriser la formation des liaisons hydrogènes acide-dimère. Seuls les acides carboxyliques faibles et hydrophiles causent la gélation des dimères. La résistance mécanique des hydrogels formés peut être modifiée par un choix judicieux d'acides. Les interactions hydrophobes et les liaisons hydrogènes entre les chaînes latérales d'acides carboxyliques peuvent améliorer les propriétés mécaniques des hydrogels. La *solubilité marginale* du complexe acide-dimère a été considérée comme un facteur critique pour la formation d'hydrogels.

Un autre système d'hydrogélification à base d'acides biliaries a été développé par l'introduction de dioxyde de carbone ( $\text{CO}_2$ ) dans des solutions aqueuses de certains sels d'acides biliaries, qui donne un hydrogel composé de molécules biologiques entièrement naturelles et fournit un réservoir commode du  $\text{CO}_2$  dans l'eau. Le groupement carboxylate des sels d'acides biliaries peut être partiellement protoné dans les solutions aqueuses, ce

qui amène la dissolution marginale dans l'eau et la formation d'hydrogels avec une structure fibreuse. L'aspect et les propriétés mécaniques des hydrogels dépendent de la concentration de  $\text{CO}_2$ . Le bullage avec  $\text{CO}_2$  pendant une ou deux secondes génère un hydrogel transparent avec des nanofibres. Le bullage supplémentaire forme des hydrogels plus forts. Mais réduit la transparence et la force mécanique des hydrogels. D'ailleurs, les hydrogels transparents ou opaques redeviennent des solutions transparentes quand ils sont chauffés avec bullage de  $\text{N}_2$ . La transition sol-gel est réversible et reproductible. La force mécanique et la transparence des hydrogels peuvent être améliorées par l'addition de sels inorganiques comme  $\text{NaCl}$  par l'effet de relargage. Toutes les composantes de ces hydrogels sont naturelles, donnant des hydrogels biocompatibles et potentiellement utiles pour des applications dans le domaine biomédical.

Le dimère mentionné ci-dessus possède des propriétés d'auto-assemblage dépendamment de sa concentration. Ceci a été étudié en utilisant un sel organique de dimère/acide formique avec un rapport molaire 1/1. Le sel du dimère s'auto-assemble dans l'eau et ainsi forme des nanofibres isolées et mono-dispersées à des concentrations faibles. Les fibres enchevêtrées donnent des réseaux fibreux 3D bien dispersés de façon aléatoire à des concentrations plus élevées. Quand la concentration du sel du dimère est supérieure à la concentration critique de gélation, le réseau fibreux est assez fort pour immobiliser la solution, qui provoque la formation d'un hydrogel isotrope. L'augmentation supplémentaire de la concentration du sel du dimère peut augmenter l'anisotropie de l'hydrogel et former ainsi un hydrogel nématique. La formation de domaines ordonnés des nanofibres alignées donne ces propriétés optiques à l'hydrogel. L'agitation de systèmes aqueux du sel de dimère favorise aussi la formation de nanofibres alignées.

**Mots clés:** Hydrogels moléculaires, acides biliaires, interactions supramoléculaires, réseau fibreux auto-assemblé, biocompatible, hydrogels introduit par  $\text{CO}_2$ , hydrogel nématique.

## Abstract

Molecular hydrogels are soft materials formed by the self-assembly of small molecules in aqueous solutions via supramolecular interactions. Although much effort has been made in the past several decades in the study of these hydrogels, the mechanism of their formation remains to be understood and the prediction of their formation is a challenge. The main purpose of this thesis is to develop novel molecular hydrogels derived from bile acids, which are naturally occurring biocompounds, and to find the relationship between the gelator structure and the gelation ability. Two new molecular gelation systems based on bile acids and their derivatives have been developed, which may be useful in biomedical applications. The *marginal solubility* of the solute in water has been found to be a prerequisite for the formation of such molecular hydrogels. The alignment of the nanofibers in the gels leads to the formation of nematic hydrogels.

The first gelation system is based on a cholic acid dimer as a gelator, which has two cholic acid molecules covalently linked by a diethylenetriamine spacer. This dimer is insoluble in water, but it forms hydrogels with 3-D fibrous networks in the presence of selected carboxylic acids. The carboxylic acids protonate the dimer, making it marginally soluble in water to yield hydrogels. Only weak and hydrophilic carboxylic acids were capable of inducing the gelation of the dimer and the mechanical strength of the hydrogels could be varied by judicious choice of the acids. Hydrophobic interactions and hydrogen bonding between the side chains of carboxylic acids improve the mechanical properties of hydrogels. The *marginal solubility* of the acid-dimer complex is regarded to be the critical factor for the formation of hydrogels.

Another hydrogelation system was developed by purging to the aqueous solutions of a series of bile salts with carbon dioxide (CO<sub>2</sub>), yielding hydrogels made of entire natural biological molecules and providing a convenient storage reservoir of CO<sub>2</sub> in water. Bile salts are well dissolved in water, while the solubility of bile acids is limited. The carboxylate group of bile salts may be partially protonated in aqueous solutions by bubbling CO<sub>2</sub>, making them only marginally soluble in water. This forms fibrous

structures. Both the appearance and mechanical properties of the hydrogels depend on the amount of CO<sub>2</sub> purged. Bubbling CO<sub>2</sub> initially induced the formation of transparent hydrogels with nanofibers. Continued purging with CO<sub>2</sub> strengthened the hydrogel mechanically, while further addition of CO<sub>2</sub> reduced the transparency and mechanical strength of the hydrogel. Both the transparent and opaque hydrogels reverted to transparent solutions when heated and bubbling N<sub>2</sub>. The sol-gel transition process was reversible and repeatable. The mechanical strength and transparency of the hydrogels could be improved by adding inorganic salts such as NaCl via a salting-out effect. All the hydrogel components are naturally biological compounds, making such hydrogels biocompatible and potentially useful in biomedical applications.

The cholic acid dimer linked with a diethylenetriamine spacer was able to assemble in water and form isolated nanofibers in the presence of certain carboxylic acids at a much lower concentration than the CMC of sodium cholate. These nanofibers entangle with each other to yield well-dispersed and randomly-directed 3-D fibrous networks at higher concentrations. When the concentration of dimer salt is above the minimum gelation concentration, the fibrous network is strong enough to immobilize the solution, leading to the formation of an isotropic hydrogel. Further increase of the dimer salt concentration may transit the hydrogels to be anisotropic, thus the formation of nematic hydrogels. The formation of ordered domains of the aligned nanofibers led to anisotropic optical properties of the hydrogels. Stirring the aqueous systems of dimer salt also promoted the alignment of the nanofibers. These molecular hydrogels with ordered aggregates may be useful in applications such as cell culture and mechano-optical sensing.

**Keywords:** Molecular hydrogels, bile acids, supramolecular interactions, self-assembled fibrous network, biocompatible, CO<sub>2</sub>-induced hydrogel, nematic hydrogel.

*To: my family members and Prof. Julian Zhu*

## Acknowledgements

First and foremost, I express my heartfelt thanks and deepest gratitude to my supervisor, Prof. Julian Zhu for offering me the opportunity to study in his group, for his guidance and patient support through my studies and research, and for his constant encouragement and unending enthusiasm to explore new fields. His super kindness, profound knowledge, great care of students, invaluable experience, and critical advice will be beneficially throughout my life. I also want to thank my co-supervisor, Prof. Karen Waldron for her help during my studies.

I would like to thank Prof. Christian Pellerin and Prof. William Skene for their critical comments and helpful suggestions in the committee meetings. I would like to extend my gratitude to Prof. C.Geraldine Bazuin for the helpful discussion during my experiments. I must also be grateful to all jury members of my thesis committee for taking their precious time and great expertise for reviewing this thesis.

This research would not have been possible without the financial support from Université de Montréal; the Natural Science and Engineering Research Council (NSERC Canada); and the Fonds Québécois de la Recherche sur la Nature et les Technologies (FQRNT). I would like to thank the Chinese Scholarship Council (CSC) for a scholarship.

I would like to thank all my colleagues in the Zhu group that with these precious memories. Very special thanks go to Prof. Zhao Zhang from Shanxi University, who was a visiting scholar in group Zhu in 2010 and trained me in organic synthesis, and to Yongguang Jia, Satu Strandman, Kun Zhang, Yu Shao, Wilms Baille, Nicolas Lévaray, and Eric Habib for all their help during my studies.

I would like to thank Sylvain Essiembre for his TGA training, Francine Belanger for the help with SAXS measurements, Marine-Christine Tang for helping capillary HPLC tests, Claude-Rosny Elie in the Schmitzer group for CD measurements, Hu Zhu in the Bazuin group for his help with AFM measurements. I also would like to thank Prof. Nanci Antonio and his group members for their help for TEM measurements.



I would like to thank Xiaoxiao Wang, Xuewei Zhang, Zhongkai Cui, Jingkui Chen, Na Xue, Zhida Wang, Xingping Qiu and other friends in Pavillon J. A. Bombardier for their support.

I would like to thank my parents and my sister. It would be impossible for me to finish the PhD program without their support and encouragements. Finally, I owe a huge thank you to my wife, Yongli Fan. Her love, patience and endless encouragements made my life better in so many ways. I owe the completion of this work to her enthusiasm and fresh perspective when things looked down.

## Table of contents

<b>Résumé .....</b>	<b>i</b>
<b>Abstract.....</b>	<b>iii</b>
<b>Acknowledgements .....</b>	<b>vi</b>
<b>Table of contents .....</b>	<b>viii</b>
<b>List of tables.....</b>	<b>xi</b>
<b>List of schemes.....</b>	<b>xii</b>
<b>List of figures .....</b>	<b>xiii</b>
<b>List of acronyms, abbreviations and symbols .....</b>	<b>xviii</b>
<b>Chapter 1 Introduction .....</b>	<b>1</b>
1.1 Definition and characteristics of gels.....	1
1.2 Classification of gels and molecular gels.....	3
1.3 Structure and gelation .....	6
1.4 Structure of molecular gelators .....	7
1.4.1 Alkanes and fatty acids .....	7
1.4.2 Aromatic derivatives .....	8
1.4.3 Steroidal derivatives.....	10
1.5 Molecular gels derived from bile acids.....	11
1.6 Scope and the structure of the present work .....	12
1.7 References .....	14
<b>Chapter 2 Supramolecular hydrogelation with bile acid derivatives: Structures, properties and applications .....</b>	<b>20</b>
Abstract .....	20
2.1. Introduction.....	21
2.2. Self-assemblies of bile salts and theories for molecular hydrogelation.....	23
2.3. Molecular hydrogels based on bile acids .....	26

2.3.1 Fibrillar aggregates from bile salts .....	26
2.3.2 Metallogels.....	27
2.3.3 Anionic hydrogelators.....	30
2.3.3.1 Bile acid sodium salts .....	30
2.3.3.2 Bile acid derivatives.....	32
2.3.4 Cationic gelators .....	34
2.3.4.1 Bile acid derivatives with primary amines.....	35
2.3.4.2 Bile acid derivatives with secondary amines .....	36
2.3.4.3 Bile acid derivatives with tertiary amines.....	37
2.3.4.4 Bile acid derivatives with quaternary ammoniums.....	38
2.3.5 Neutral gelators .....	39
2.3.5.1 Hydrogels in neat water .....	40
2.3.5.2 Hydrogels in aqueous solutions with organic solvents .....	40
2.3.6 Two-component hydrogels .....	42
2.4. Polymeric supramolecular hydrogels based on bile derivatives .....	45
2.5. Conclusions.....	47
2.6 Acknowledgements.....	47
2.7 References.....	48
<b>Chapter 3 Formation of molecular hydrogels from a bile acid derivative and selected carboxylic acids .....</b>	<b>62</b>
Abstract .....	62
3.1 Introduction.....	62
3.2 Results and discussions.....	64
3.3 Conclusions.....	71
3.4 Acknowledgements.....	72
3.5 Supporting information.....	72
3.5.1 Experimental part.....	72
3.5.2 Supporting data .....	74
3.6 References.....	78

<b>Chapter 4 Self-assembly of a bile acid derivative in aqueous solutions: From nanofibers to nematic hydrogels.....</b>	<b>82</b>
Abstract.....	82
4.1 Introduction.....	82
4.2 Experimental section.....	84
4.3 Results and discussion .....	85
4.4 Conclusions.....	95
4.5 Acknowledgments.....	96
4.6 References.....	96
<b>Chapter 5 Supramolecular hydrogels formed by CO<sub>2</sub> and bile salts in water .....</b>	<b>101</b>
Abstract.....	101
5.1 Introduction.....	101
5.2 Results and discussions.....	102
5.3 Conclusions.....	108
5.4 Acknowledgements.....	109
5.5 Supporting information.....	109
5.5.1 Experimental section.....	109
5.5.2 Supporting data .....	111
5.6 References.....	112
<b>Chapter 6 Conclusions and future work.....</b>	<b>116</b>
6.1 Conclusions.....	116
6.1.1 Novel molecular hydrogels derived from bile acids .....	116
6.1.2 A general rule for the formation of molecular gels.....	117
6.1.3 Nematic hydrogels .....	118
6.2 Perspectives.....	119
6.2.1 Molecular hydrogels induced by ammonia or amines .....	119
6.2.2 Two-component molecular hydrogels from bile salts and dopamine .....	120
6.2.3 Molecular hydrogels based on betulin and its derivatives .....	121
6.3 References.....	123

## List of tables

<b>Table 2.1</b> Two-component hydrogels based on bile acids .....	44
<b>Table 3.S1</b> The acids tested and the minimum gelation concentrations of the cholic acid dimer .....	74
<b>Table 6.1</b> Preliminary gelation tests of certain bile acids and a fatty acid in the presence of various amines .....	120

## List of schemes

<b>Scheme 2.1</b> Chemical structure of bile acids and certain bile acid conjugates. ....	23
<b>Scheme 3.S1</b> Synthesis of the dimer .....	74

## List of figures

- Figure 1.1** Schematic representation of two rheological tests of a gel. (A) The variation of  $G'$  and  $G''$  as a function of temperature, with the gel-sol phase transition temperature indicated by the dash line, and (B) the oscillatory stress sweep experiment result with the yield stress indicated by the dash line. ....3
- Figure 1.2** Schematic illustration for the formation of crystals, precipitates and molecular gels from compounds with low molecular weight. ....5
- Figure 1.3** Publications (left) and citations (right) per year on molecular gels based on a literature search on the Web of Science by using keywords “molecular gel”, “low-molecular-weight gel” and “supramolecular gel (excluding polymer gel)” (Jan. 2017). ....6
- Figure 1.4** Chemical structures of 12-hydroxystearic acid, stearic acid and eicosanoic acid. ....8
- Figure 1.5** chemical structures of certain aromatic molecular organogelators (A, B and C) and hydrogelators (D, E). ....9
- Figure 1.6** The chemical structures of certain molecular organogelators (A, B and C) and hydrogelators (D and E) derived from cholesterol. ....11
- Figure 1.7** The chemical structure (left) and 3-D model (right) of a primary bile acid, cholic acid. The different colors in the model (right) represent H (white), C (grey), and O (red). H atoms bound to C atoms were hidden to show a less-crowded image. ....12
- Figure 2.1** Schematic representation of various configurations of bile salt micelles with the hydroxyl groups shown as blue dots and carboxylate groups as red dots: (A) Primary micelles. (B) Secondary micelles. ....24
- Figure 2.2** Relationship between the value of packing parameter,  $p$ , and the morphologies of self-assemblies of amphiphiles in aqueous solutions. ....26
- Figure 2.3** Morphologies of self-assemblies from LCA at aqueous solutions (pH ~12.0). (A) Nanotubes with 0.1 wt% LCA. (B) Microtubes with 0.1 wt% LCA after vortexing and equilibration for a week. ....27

<b>Figure 2.4</b> Hydrogels from interaction between sodium cholate and different metal cations. ....	28
<b>Figure 2.5</b> The chemical structures of metallic hydrogelators based on bile acids. ....	30
<b>Figure 2.6</b> The chemical structures of anionic molecular gelators derived from bile acids. ....	33
<b>Figure 2.7</b> Schematic representation for the kinetic process of nanotube formation from the sugar-substituted LCA derivative <b>5</b> . ....	34
<b>Figure 2.8</b> The chemical structures of cationic molecular gelators derived from bile acids. ....	35
<b>Figure 2.9</b> Schematic representation of molecular arrangements of (A) nanotubes from wedge-shape <b>24</b> , and (B) narrow nanotubes by head-to-head arrangement (left) and wide nanotubes by head-to-tail arrangement (right) of compound <b>25</b> . ....	36
<b>Figure 2.10</b> Hydrogels made from <b>27</b> with various carboxylic acids. (A) 3-D fibrillar networks of the hydrogel from <b>27</b> with tartaric acid (both at 0.6 mM). (B) Schematic presentation of the interactions between <b>27</b> and carboxylic acids in hydrogels. ....	37
<b>Figure 2.11</b> Cryo-TEM image of the hydrogel from <b>28</b> (0.75 mM) in water with 20% acetic acid at different magnifications. ....	38
<b>Figure 2.12</b> The chemical structures of neutral molecular gelators derived from bile acids. ....	39
<b>Figure 2.13</b> Molecular hydrogels from the pegylated LCA derivative <b>38</b> and the fibrils morphology. ....	41
<b>Figure 2.14</b> pH-sensitivity of hydrogel from compound <b>46</b> in DMSO/H <sub>2</sub> O (1/1 by volume). ....	42
<b>Figure 2.15</b> Supramolecular hydrogels from polymers with bile acids. (A) Light responsive hydrogels from DCA- $\beta$ -CD and azobenzene-poly(acrylic acid). (B) Self-healable hydrogels from two polymer chains with CA and $\beta$ -CD, respectively. ....	46
<b>Figure 3.1</b> Molecular structure of the dimer based on cholic acid. ....	63
<b>Figure 3.2</b> Oscillatory stress sweep experiments of the hydrogel formed from the dimer (20 mM) and (A) monoprotic acids (40 mM) and (B) diprotic acids (20 mM). [-COOH] = 40 mM. ....	66



- Figure 3.3** TEM images of the fibrillar network in hydrogels formed by (A) 6 mM dimer and 12 mM acetic acid; (B) 1.2 mM dimer and 1.2 mM succinic acid; and (C) 0.6 mM dimer and 0.6 mM tartaric acid. (Black scale bar = 200 nm).....68
- Figure 3.4** Second derivative of the FT-IR spectra of (A) the dimer; (B) the aerogel of dimer-succinic acid (20 mM-20 mM).....69
- Figure 3.5** The schematic representation of the hydrogen bonds (A) between the dimers; and (B) between the dimer and carboxylic acid after gelation in water. ....70
- Figure 3.S1** Behavior of the dimer in the presence of certain carboxylic acids: (A) Homogeneous solution obtained from the dimer and trifluoroacetic acid; (B) Precipitation, which occurred after the addition of water into the mixture of the dimer and trifluoroacetic acid; (C) Viscous and cloudy liquid obtained from an aqueous solution of acetic acid and the dimer (both at 20 mM); (D) Transparent and stable hydrogel obtained from an aqueous solution of acetic acid (40 mM) and the dimer (20 mM). ....75
- Figure 3.S2** Viscoelastic properties of the dimer-acid hydrogel (20 mM dimer-40 mM acetic acid) in water: (A) Gelation over time; (B) Oscillatory stress sweep; (C) Frequency sweep; (D) Oscillatory temperature sweep.  $G'$  (closed circles),  $G''$  (open circles).....75
- Figure 3.S3** Viscoelastic properties of the hydrogels formed by the cholic acid dimer (20 mM) and various concentration of (A) Acetic acid. (B) Succinic acid.  $T_{gel-sol}$ : gel-sol transition temperature. ....76
- Figure 3.S4** AFM images (black scale bar = 200 nm) of the fibrillar network in hydrogels formed by (A) 6 mM dimer and 12 mM acetic acid (the white arrows indicate entwined nanofibers), and (B) 0.6 mM dimer and 0.6 mM tartaric acid. ....76
- Figure 3.S5** The CD spectra of the hydrogel samples formed with (A) 6 mM dimer and 12 mM acetic acid; (B) 0.6 mM dimer and 0.6 mM tartaric acid; and (C) 6 mM dimer and 6 mM tartaric acid. ....77
- Figure 3.S6**  $^1H$  NMR spectra of hydrogel of acetic acid-dimer (40 mM-20 mM) in  $D_2O$  at different temperatures. Peaks a, b, and c indicate the protons at methyl groups on the cholic acid dimer, peak d is from protons of the methyl group on acetic acid, peak

- e is from protons of trioxane added as an internal standard, the peaks at about 4.7 that varies with temperature are water solvent residual signals.....77
- Figure 3.S7** FT-IR spectra of (A) succinic acid; (B) the dimer; (C) aerogel of succinic acid-dimer (20 mM-20 mM).....78
- Figure 4.1** (A) The chemical structure of the formic acid/cholic acid dimer salt. The hydrogel made from 14 mM the dimer salt observed between the crossed polarized film (B) before and (C) after agitation. The POM images of hydrogels having the dimer salt at concentrations of (D) 15 mM, (E) 20 mM, and (F) 25 mM.....87
- Figure 4.2** Variation of the  $I_3/I_1$  ratio of pyrene fluorescence spectra as a function of the dimer salt concentration. The lines have been drawn as visual guides.....88
- Figure 4.3** Rheological properties of hydrogels at various concentrations of the dimer salt. (A) Gel-sol transition temperature, the blue line was drawn as a visual guide. (B) Storage modulus and yielding stress, the black and red lines were obtained from linear fitting with slope values marked besides the segments. ....89
- Figure 4.4** TEM images of self-assemblies of the dimer salt in water upon equilibration at concentrations of (A) 0.06 mM (sol), (B) 0.5 mM (sol), (C) 2 mM (sol), (D) 8 mM (gel), (E) 30 mM (nematic gel), and (F) 2 mM after stirring for 30 min (sol). (Black scale bar = 500 nm).....92
- Figure 4.5** SAXS result of a nematic hydrogel sample with 30 mM dimer salt. (A) 2-D SAXS pattern image. The white arrow indicates the director  $n$  of the nematic hydrogel. (B) SAXS diffractogram of the hydrogel (black open circles), theoretical fitting curve of for nanofibers of 20 nm diameter (red line), and theoretical fitting curve for 28 nm nanofibers (blue line). ....95
- Figure 5.1** (A) The chemical structure of NaLC, NaCDC, NaDC, and NaC. (B) An aqueous solution of 2 wt% NaDC. (C) A transparent hydrogel with 2 wt% NaDC by bubbling  $\text{CO}_2$  for 2 s, (D) An opaque hydrogel with 2 wt% NaDC by bubbling  $\text{CO}_2$  for 5 s. ....103
- Figure 5.2** TEM images of (A) aqueous solution with 10 mM NaDC, (B) transparent hydrogel with 10 mM NaDC and 4 mM  $\text{CO}_2$ , and (C) opaque hydrogel with 10 mM NaDC and 40 mM  $\text{CO}_2$ . (D) Schematic representation of the mechanism for the

formation of hydrogels from aqueous solutions of NaDC and further aggregation with increasing contents of CO<sub>2</sub>.....104

**Figure 5.3** Mechanical properties and morphology of hydrogels obtained from NaDC (23 mM) and CO<sub>2</sub>. (A) The variations of G' and pH value of the system with the concentration of CO<sub>2</sub>. (B) Variation of G' and G'' of the hydrogel at 40 mM CO<sub>2</sub> with the addition of NaCl in the mixture. The lines are drawn as visual guides. AFM images of hydrogels (C) with 40 mM CO<sub>2</sub> and (D) with 40 mM CO<sub>2</sub> and 200 mM NaCl. ....106

**Figure 5.4** FT-IR spectra of (A) DCA; (B) NaDC; and the freeze-dried aerogels of 23 mM NaDC with CO<sub>2</sub> at a concentration of (C) 16 mM, (D) 24 mM, (E) 48 mM, and (F) 64 mM. ....108

**Figure 5.S1** (A) An aqueous solution of NaC (3 wt%), (B) A hydrogel with 2 wt% NaCDC in water, (C) A hydrogel with 2 wt% NaLC in water. A, B and C were all purged with CO<sub>2</sub>. (D) A bluish viscous solution with 2 wt% NaLC in water, (E) A bluish stable hydrogel with 3 wt% NaLC. D and E were not purged with CO<sub>2</sub>. ....111

**Figure 5.S2** (A) Fluorescence spectra of pyrene (0.3 μM in water) with various concentrations of NaDC. (B) Variation of I<sub>3</sub>/I<sub>1</sub> of the pyrene fluorescence spectra with the concentration of NaDC. ....112

**Figure 6.1** Formation of hydrogels from NaDC and dopamine. ....121

**Figure 6.2** The synthetic route of betulonic acid from betulin. ....122

**Figure 6.3** The synthetic route of a series of potential molecular gelators based on betulin. ....123

## List of acronyms, abbreviations and symbols

$a_0$	Interfacial area of the hydrophilic head group
ACN	Acetonitrile
AFM	Atomic-force microscope
ATR	Attenuated total reflection
$C$	Concentration
CA	Cholic acid
CAC	Critical aggregation concentration
CD	Circular dichroism
CDCA	Chenodeoxycholic acid
CMC	Critical micellar concentrations
3-D	Three-dimensional
DCA	Deoxycholic acid
DCC	Dicyclohexylcarbodiimide
DHN	2,3-dihydroxynaphthalene
DMF	Dimethylformamide
DMSO	Dimethyl sulfoxide
DOX	Doxorubicin
FT-IR	Fourier transform infrared
$G'$	Storage modulus
$G''$	Loss modulus
HIV	Human immunodeficiency virus
HLB	Hydrophilic-lipophilic balance
$l_c$	Critical chain length
LCA	Lithocholic acid
LMWG	Low molecular weight gelator
MGC	Minimum gelation concentration
NaC	Sodium cholate
NaCDC	Sodium chenodeoxycholate

NaDC	Sodium deoxycholate
NaLC	Sodium lithocholate
NHS	N-hydroxysuccinimide
NMR	Nuclear magnetic resonance
$p$	Packing parameter
PBS	Phosphate buffer solution
PEG	Poly(ethylene glycol)
$pK_a$	Acid dissociation constant on logarithmic scale
PNIPAM	Poly(N-isopropylacrylamide)
POM	Polarized optical microscopy
$Q$	Scattering vector
$R$	Gas constant
SAFIN	Self-assembled fibrous network
SAXS	Small-angle X ray scattering
SEM	Scanning electron microscope
SWCNT	Single-walled carbon nanotube
TEM	Transmission electron microscopy
TEOS	Tetraethylorthosilicate
$T_{\text{gel-sol}}$	Gel-sol transition temperature
THF	Tetrahydrofuran
TRIS	Tris(hydroxymethyl)aminomethane
UDCA	Ursodeoxycholic acid
UV	Ultra-violet
$v$	Hydrophobic volume of the amphiphile
$\beta$ -CD	$\beta$ -cyclodextrin
$\Delta H$	Enthalpy change
$\lambda$	Wavelength
$\chi$	Flory-Huggins interaction parameter



# Chapter 1

## Introduction

### 1.1 Definition and characteristics of gels

Gels are soft materials that behave as solids despite being mostly composed of liquid. They have been known for centuries and are abundant and now widely used in fields such as food ingredients, contact lenses and cosmetic products.<sup>1</sup> The jelly-like look and feel of these materials make them easy to recognize by a simple “inversion” test: turning a pot of gel upside down, they can support their own weight without falling.<sup>2</sup> A gel is a solid-like material which can be easily deformed under stress, with temperature change or with time. The definition of gel remains a subject of debate, since gels may not remain physically stable.

In 1926, Dr. Dorothy Jordan Lloyd<sup>3</sup> noted that “...*the colloidal condition, the gel, is one which is easier to recognize than to define*”, and made the following statement, “*Only one rule seems to hold for all gels, and that is that they must be built up from two components, one of which is a liquid at the temperature under consideration, and the other of which, the gelling substance proper, often spoken of as the gelator, is a solid. The gel itself has the mechanical properties of a solid, i.e., it can maintain its form under the stress of its own weight, and under any mechanical stress, it shows the phenomenon of strain.*” This definition addressed the structural aspect of gels and described their viscoelastic properties, but mostly relied on the qualitative macroscopic observations. About 20 years later, Hermans<sup>4</sup> claimed that gels could be characterized by the following three points: “(1) *they are coherent colloid disperse system of at least two components; (2) they exhibit mechanical properties characteristic of the solid state; and (3) both the dispersed component and the dispersion medium extend themselves continuously throughout the whole system.*” This definition attempted to describe the gel by linking the microscopic and macroscopic properties but is still not accurate enough since not all gels are colloids and not all colloids are gels.<sup>5</sup> More recently, Terech and Weiss<sup>6</sup> defined gel

as a substance that: “(1) has a continuous structure with macroscopic dimensions that is permanent on the time scale of an analytical experiment and (2) is solid-like in its rheological behavior.” This may be the most comprehensive definition of gels while it is still cumbersome to apply.<sup>6</sup> Nevertheless, a simple method to distinguish a gel follows the definition proposed by Dr. Dorothy Jordan Lloyd: “...if it looks like ‘Jell-O’, it must be a gel!”<sup>5-6</sup>

Due to the structural and functional diversity of gels, there is a wide variety of experimental techniques to study them. A general and efficient methodology for the characterization of all kinds of gels is to begin with their rheological properties.<sup>6</sup> Rheology offers a convenient method to measure the viscoelastic properties of gel-like materials and quantify their mechanical strength.<sup>2,6</sup> It studies the deformation and flow of matters under the influence of an applied stress.<sup>7</sup> Rheometers generally measure two quantities: stress, the amount of force per unit area applied to the sample, and strain, the dimensionless degree to which the sample deforms.<sup>8</sup> When a gel sample is placed between two plates of a rheometer, applying a weak stress (or strain) to one of the plates in an oscillating fashion induces a subsequent oscillatory strain (or stress) in the sample with a phase difference. The values of storage and loss moduli ( $G'$  and  $G''$ , the contributions of elastic and viscous behavior to complex dynamic modulus, respectively) can be calculated from the values of stress ( $\delta_0$ ) and strain ( $\epsilon_0$ ), and their oscillatory phase difference ( $\theta$ ) from the following expressions:<sup>2</sup>

$$G' = \frac{\delta_0}{\epsilon_0} \cos\theta$$

$$G'' = \frac{\delta_0}{\epsilon_0} \sin\theta$$

Both  $G'$  and  $G''$  of a gel sample may increase with time through the sol-gel transition process via cross-linking or self-assembling behaviors and reach a plateau when the gelation process is completed. The viscous properties are dominant in its solution state and more energy is dissipated than stored ( $G'' > G'$ ), whereas the elastic properties dominant in its gel state and more energy is stored than dissipated ( $G' > G''$ ). Consequently, the point at which  $G' = G''$  may be defined as the gel point.<sup>9</sup> Certain gels



may be thermoresponsive and have the values of  $G'$  and  $G''$  crossed at a critical temperature (Fig. 1.1A),<sup>10</sup> which is the gel-sol phase transition temperature ( $T_{\text{gel-sol}}$ ) and indicates their thermo-stability.

A typical rheological experiment for gels is monitoring the moduli at a fixed frequency and temperature by varying the amplitude of oscillatory stress (Fig. 1.1B).<sup>2, 8, 11</sup> Both  $G'$  and  $G''$  remain constant when the applied stress is lower than a critical value, yield stress ( $\delta^*$ ).<sup>12</sup> Above the yield stress,  $G'$  decreases rapidly, indicating that the network in the gel is disrupted. The  $\delta^*$  is defined as the point where the  $G'$  decreases by 5-10%.<sup>12</sup> The storage modulus and yield stress reflect well the stiffness and toughness of a gel, respectively.<sup>13</sup> Gels with high values of  $G'$  and  $\delta^*$  may be regarded as strong gels since they could keep their initial shape under more strenuous conditions. A gel with good mechanical properties may be potentially used in many areas such as flexible optical devices.<sup>14-15</sup>

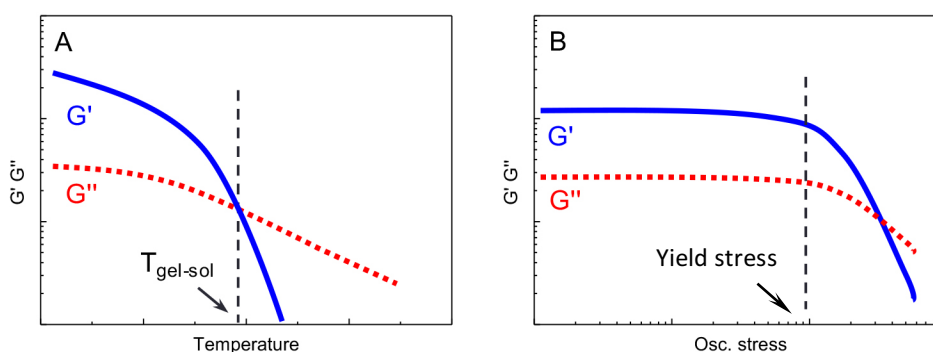


**Figure 1.1** Schematic representation of two rheological tests of a gel. (A) The variation of  $G'$  and  $G''$  as a function of temperature, with the gel-sol phase transition temperature indicated by the dash line, and (B) the oscillatory stress sweep experiment result with the yield stress indicated by the dash line.

## 1.2 Classification of gels and molecular gels

Gels can be classified in different ways according to the medium for gelation, the gelator source and structure, and the driving forces that create the 3-D networks.<sup>16</sup> For examples gels may be classified as hydrogels, organogels and liquid crystalline gels where

the medium for gelator is water, an organic solvent or a thermotropic liquid crystal, respectively.<sup>16-17</sup> If the liquid were replaced by a gas (typically air), the gels are called aerogels or xerogels.<sup>18</sup> Flory also suggested to classify gels into four different types on the basis of their microscopic structure:<sup>5,19</sup>

1. Gels with well-ordered lamellar structures. Some of these are lyotropic liquid crystals.
2. Gels with chemically cross-linked polymeric networks swollen with solvent. In these phases, the polymer chains are disordered.
3. Gels with polymeric networks in which the chain-chain interactions are physical instead of covalent bonding. The chains may be predominantly disordered, but regions of local order (especially where inter-chain interactions occur) may also exist.
4. Gels with particular disordered structures, including gels in which the networks are comprised of self-assembled fibrils from compounds with low molecular weights, i.e., molecular gels.

Molecular gels (or supramolecular gels) are soft materials that are derived from compounds with low molecular weights (usually < 2000 g/mol) in solvents.<sup>5-6</sup> These compounds are generally soluble marginally in certain solvents, and they can be dissolved to form homogeneous solutions under heating or sonication, and yield gels during the aging process at ambient conditions. Such a gelation process may be regarded as an intermediate transient state for a hot solution to form either crystals when the aggregates of solute molecules are highly ordered, or precipitates when the aggregates of solute molecules are amorphous,<sup>20</sup> as illustrated in Fig. 1.2.

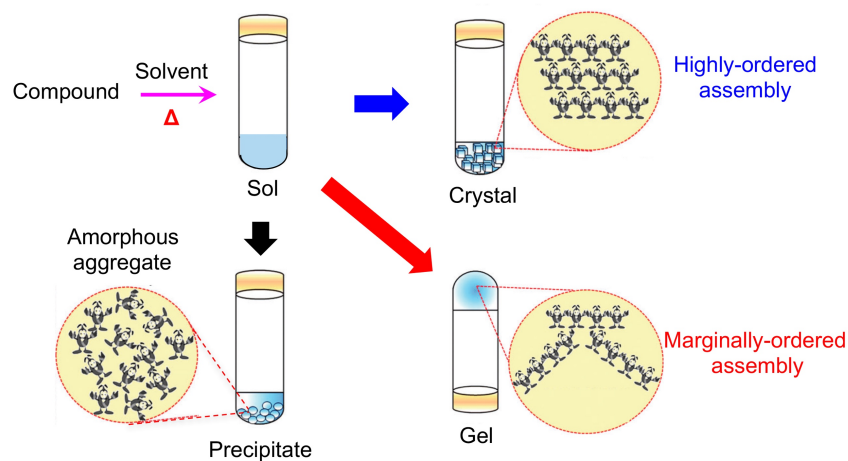


**Figure 1.2** Schematic illustration for the formation of crystals, precipitates and molecular gels from compounds with low molecular weight. (Adapted with permission from ref. 20. Copyright (2015) Royal Society of Chemistry.)

Most molecular gels formed by gelators with precisely controlled chemical structure are thermo-reversible and show better degradability and functional diversity than polymeric gels. Such materials may potentially be used in biomedical areas such as drug delivery and tissue engineering.<sup>21-22</sup> Some of them with good mechanical and optical properties may also be used in soft optical devices.<sup>14-15</sup> Supramolecular interactions, such as hydrogen bonding, hydrophobic interactions, electrostatic attraction, and metal coordination,<sup>11</sup> facilitate the self-assembly of solute molecules to form nanofibers and 3-D networks. These can immobilize the solution via surface tension to yield gels.<sup>23</sup> Molecular gels have attracted increasing attention over the past two decades. Fig. 1.3 shows the annual numbers of publications and citations to molecular gels in the Web of Science database from 1990 to 2016. The exponential growth of the publications and citations illustrate both the significant efforts to understand molecular gels and the increasing interest in this field.

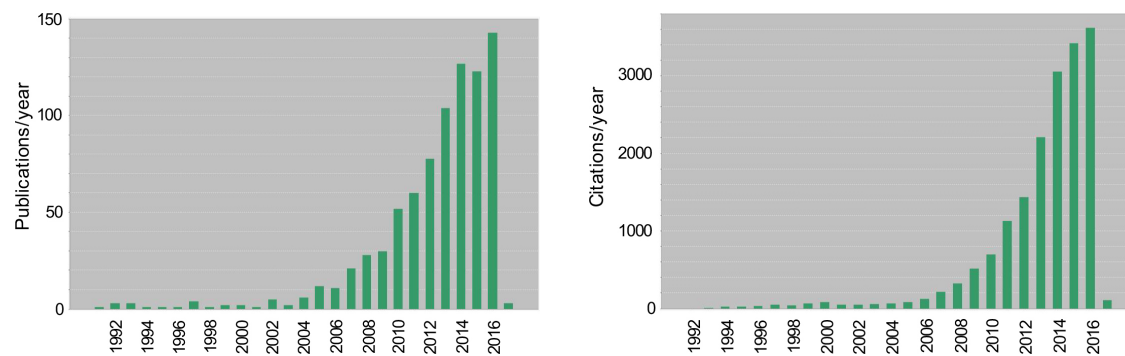


**Figure 1.3** Publications (left) and citations (right) per year on molecular gels based on a literature search on the Web of Science by using keywords “molecular gel”, “low-molecular-weight gel” and “supramolecular gel (excluding polymer gel)” (Jan. 2017).

### 1.3 Structure and gelation

The properties of molecular gels strongly depend on the chemical structure of gelators, and a slight variation on the molecular structure may result in totally different gelation behaviors. Terech and Weiss<sup>24</sup> summarized the properties of a series of low molecular weight organogelators in 1997 and they concluded the “serendipity” nature of the investigation of new gelators. To date, the relationship between the chemical structure of a given compound and its gelation behavior has remained unclear and most of the molecular gels reported have been found by trial-and-error.<sup>24-25</sup> A recent perspective published by Weiss in 2014 reaffirmed the serendipitous strategies of molecular gels, despite the decades of progress in this area and various applications.<sup>26</sup>

Efforts have been made to study a general relationship between the chemical structure of the gelators and the formation of molecular gels. The hydrophilic-lipophilic balance (HLB) was regarded to be important for the formation of molecular hydrogels.<sup>23, 27-28</sup> However, it is hard to obtain precise HLB values or establish an effective HLB scale for the formation of gels. The formation of hydrogels from compounds having long alkyl chains and a hydrophilic head group could be predicted by the packing parameter ( $p$ ), with the expression of  $p=v/(a_0l_c)$ , where  $v$  is the hydrophobic volume of the amphiphile,  $a_0$  is the interfacial area, and  $l_c$  is the maximum effective length that the hydrophobic chains

can assume.<sup>29-31</sup> However, it is not applicable for compounds with more complicated structures. For example, the packing parameter of bile salts calculated by this method did not fit the self-assembling behavior in aqueous solutions.<sup>32</sup> Formation of molecular organogels is a more complicated process than hydrogelation due to the structure diversity of organic solvents and their interactions with gelators. A review published by Lan *et al.*<sup>33</sup> reported that certain solvent parameters, such as dipole moment, dielectric constant and refractive index, may mediate the self-assembly of compounds in organic solvents into fibrous networks. Such research may be helpful for understanding the mechanism of assembly, but it still needs optimizing its general use. We studied the relationship between the gelator structure and gelation ability of a series of molecular hydrogels derived from bile acids to conclude that the marginal solubility of gelators of the species is a prerequisite for the formation of molecular hydrogels. Such a rule may also be applicable in the formation of molecular organogels. We will discuss the study in more details in Chapter 2.

## 1.4 Structure of molecular gelators

Despite the fact that most of molecular gels were found by trial-and-error, a vast amount of molecular gels, including hydrogels and organogels, has been reported to date.<sup>25, 34</sup> Their properties vary according to the structure of gelators.

### 1.4.1 Alkanes and fatty acids

Petroleum waxes with long-chain *n*-alkanes were found to form organogels in a series of organic solvents, such as short-chain *n*-alkanes.<sup>35</sup> They could be regarded as the organogelators with the simplest chemical structure.<sup>36</sup> Weiss and co-workers<sup>36-38</sup> conducted tests on the gelation behavior of long-chain *n*-alkanes in various organic solvents, including heptane, toluene, ethyl acetate, ethanol and silicon oil. The results indicated that long-chain *n*-alkanes (for example, C<sub>24</sub>H<sub>50</sub>, C<sub>28</sub>H<sub>58</sub>, C<sub>36</sub>H<sub>74</sub>) are effective gelators in these organic solvents and longer *n*-alkanes could show better gelation ability to yield stronger and more stable organogels. C<sub>36</sub>H<sub>74</sub> was the longest *n*-alkane examined

for gelation and it could gelate silicon oil to yield a gel which was stable for at least one week at a concentration of 0.19 wt%.<sup>36</sup> Some long-chain *n*-alkanes bearing one heteroatom (S and N), or fluorinated *n*-alkanes were also reported to form organogels in certain organic solvents.<sup>37,39</sup>

Fatty acids are compounds consisting of aliphatic chains with a terminal carboxylic acid group. Tachibana *et al.*<sup>40-41</sup> found that 12-hydroxystearic acid (12-HAS, Fig. 1.4) could be dissolved in CCl<sub>4</sub> and some aromatic solvents to form thermoreversible “jellies”, which behave as lyotropic liquid crystals. X-ray diffraction measurements revealed that such materials were composed of a number of small, ordered domains with a lamellar structure similar to crystals,<sup>40</sup> which were proven later to be the thin ribbons or microfibrils.<sup>41</sup> The carboxylic acid groups of fatty acids could be deprotonated in aqueous solutions at high pH. The deprotonated fatty acids may be regarded as amphiphiles which self-assemble in aqueous solutions to various structures. Stearic acid and eicosanoic acid (C<sub>17</sub>H<sub>35</sub>COOH and C<sub>19</sub>H<sub>39</sub>COOH, respectively, Fig. 1.4) formed opaque or translucent hydrogels in water in the presence of a series of amino compounds.<sup>42</sup> Acids that have shorter aliphatic chain than stearic acid or polar groups (such as 12-HSA) were not able to form hydrogels, which suggests that suitable hydrophilic-lipophilic balance is important for the formation of molecular hydrogels.

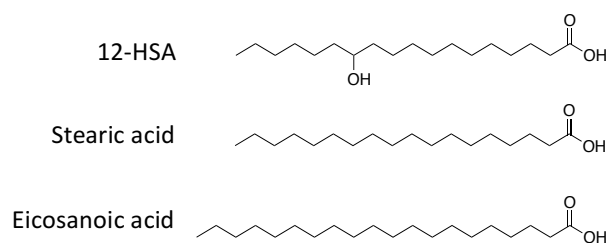


**Figure 1.4** Chemical structures of 12-hydroxystearic acid, stearic acid and eicosanoic acid.

### 1.4.2 Aromatic derivatives

Aromatic compounds such as benzene, pyrene, perylene and porphyrin derivatives can interact with each other by  $\pi$ - $\pi$  stacking, which is a typical driving force for the formation

of molecular gels. The simplest aromatic molecular gelators are the di-alkoxy-benzene derivatives (Fig. 1.5A) synthesized by Clavier *et al.* in 1999.<sup>43</sup> Organogels could be obtained from such compounds in various organic solvents, such as acetonitrile, propylene carbonate and DMF. Maitra *et al.*<sup>44</sup> also developed a series of organogelators from pyrene bearing a long alkyl chain, which were covalently linked via urethane, urea and amide groups (Fig. 1.5B and C). All these gelators self-assembled to form fibrous structures with hydrogen bonding and  $\pi$ - $\pi$  stacking interaction as the main driving forces, whereas the chiral gelator (Fig. 1.5C) was found to form chiral aggregates. These findings are helpful for the design of molecular gels with helical structures.

Certain aromatic derivatives with hydrophilic moieties can self-assemble in aqueous solutions to form molecular hydrogels. Stupp and co-workers<sup>45</sup> developed a molecular hydrogel based on amphiphilic perylene monoimide chromophore by covalently functionalizing perylene monoanhydride with a five-carbon linker to a carboxylate group (Fig. 1.5D). Such a compound could form several microns long nanoribbons with a high aspect ratio. Due to the visible-light absorbing properties of perylene monoimide units, these hydrogels afforded the capture of photons. Such a hydrogel could incorporate an electrocatalyst to make soft materials for the light-driven production of  $H_2$ , which may be useful in the production of solar fuels. A porphyrin derivative with sugar species (Fig. 1.5E) was also reported to form nanoribbons in water.<sup>46</sup>

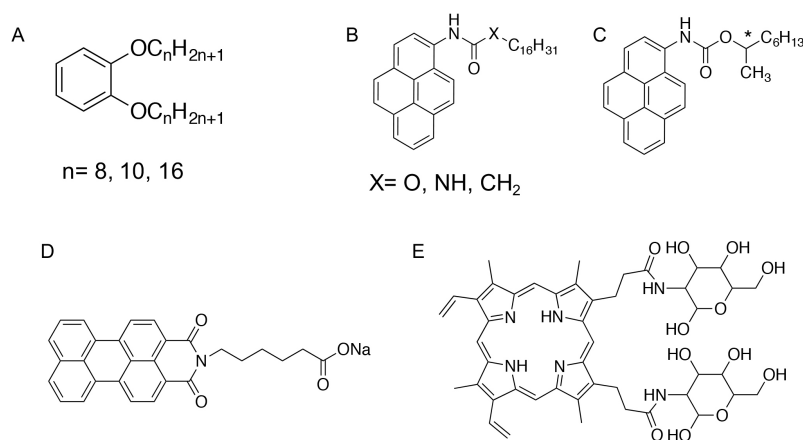


**Figure 1.5** Chemical structures of certain aromatic molecular organogelators (A, B and C) and hydrogelators (D, E).

### 1.4.3 Steroidal derivatives

Steroids are naturally occurring organic compounds with a tetracyclic ring skeleton, to which functional groups are attached. Cholesterol is an example of steroidal compounds and it is a constituent of the cell membranes to maintain the membrane fluidity, microdomain structure and permeability.<sup>47</sup> The hydroxyl group on its steroid unit can be easily derivatized. The first molecular gel based on cholesterol was an organogel developed by Weiss and co-workers in 1987.<sup>48</sup> They proposed that a compound comprised of an aromatic moiety bound to a steroidal unit via a functionalized linker may be used as a molecular organogelator.<sup>6</sup> Such a model works in a predictable way in many cases and has been widely used to design novel molecular organogels based on steroidal derivatives.<sup>47,49</sup>

Geiger *et al.*<sup>50</sup> synthesized a series of biphenyl-cholesterol compounds (Fig. 1.6A) that form organogels in *n*-octanol. The absorption and emission spectra of the compounds in organogels were similar to those in dilute solutions, indicating that the  $\pi$ - $\pi$  stacking interaction between biphenyl moieties was very weak and the steroidal part may be mostly responsible for the self-assembling behavior. Fang and co-workers<sup>51-52</sup> also developed a series of organogelators based on cholesterol derivatives (Fig. 1.6 B and C) which showed different properties and could have potential applications as sensors. Terthiophene-cholesterol derivatives (Fig. 1.6B) could form gels in several organic solvents upon intermolecular hydrogen bonding and van der Waals' interactions. One of such organogels could be dip-coated on a glass plate surface to make a fluorescent film that showed photobleaching under UV light in air. The UV-treated film was tested for use as turn-on fluorescent sensor for a series of volatile organic compounds such as acetic acid.<sup>51</sup> A nitrobenzoxadiazole-cholesterol compound (Fig. 1.6C) also formed organogels with highly ordered fibrous array structures, which showed remarkable thixotropic properties. The gel networks were disintegrated under a large shear stress but recovered immediately after removing the stress. Such organogels showed reversible fluorescence quenching behavior by the addition and evaporation of ammonia gas, and as a result, they could be used as a monitoring device for "ammonia leaking".



Certain amphiphilic compounds based on cholesterol self-assemble to form hydrogels in water. Dutta *et al.*<sup>28</sup> synthesized a series of cholesterol derivatives with amino acids as linkers and a quaternary ammonium group as a hydrophilic domain (Fig. 1.6D) to form hydrogels. Such gelators showed good gelation efficiencies and could form stable gels at concentrations lower than 1 wt%. Moreover, the biocompatibility tests of all these cholesterol-based hydrogels showed higher cell viability than the alkyl-chain-based molecular hydrogels. Liu *et al.*<sup>53</sup> also reported that a cholesterol derivative with a carboxylic acid group (Fig. 1.6E) forms hydrogels in aqueous ammonia solutions. Earlier studies on molecular gels based on cholesterol have been reviewed by the Fages<sup>49</sup> and Sievänen<sup>47</sup> groups, respectively.

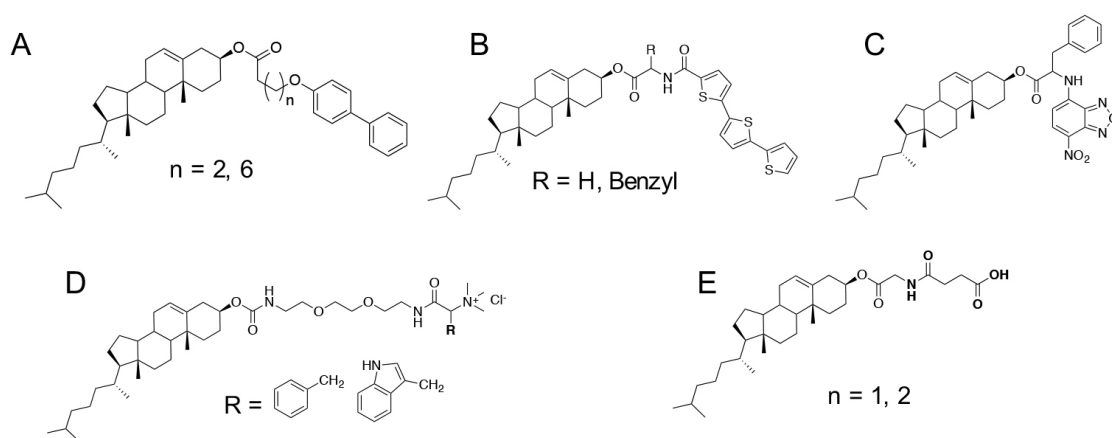


**Figure 1.6** The chemical structures of certain molecular organogelators (A, B and C) and hydrogelators (D and E) derived from cholesterol.

## 1.5 Molecular gels derived from bile acids

Molecular gels derived from biocompounds show improved biocompatibility and may avoid potential toxicity from the degradation products when used for biomedical applications. Bile acids, which are synthesized from cholesterol in the body of humans and most animals (Fig. 1.7) and facilitate the digestion and absorption of fats and fat-soluble nutrients,<sup>54-55</sup> have been widely studied for the gelation of both water and organic solvents.<sup>16</sup> Such gels may be potentially useful in areas such as drug delivery,<sup>56-58</sup> nanotemplating,<sup>59-62</sup> optical devices,<sup>33</sup> and dye adsorption.<sup>63</sup>

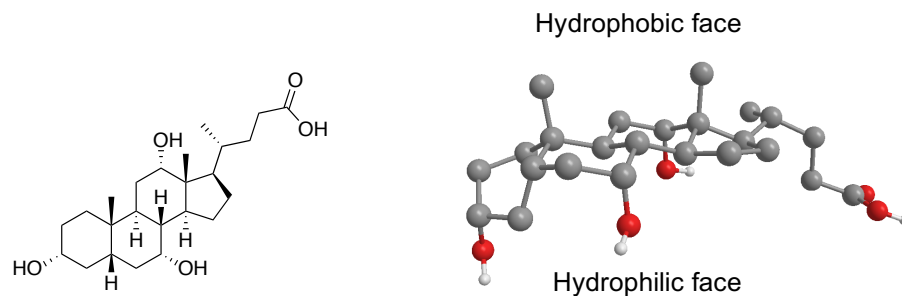


**Figure 1.7** The chemical structure (left) and 3-D model (right) of a primary bile acid, cholic acid. The different colors in the model (right) represent H (white), C (grey), and O (red). H atoms bound to C atoms were hidden to show a less-crowded image.

## 1.6 Scope and the structure of the present work

The main objective of this work was to develop novel molecular hydrogelation systems based on bile acids and their derivatives and to establish a generally gelation rule. To this end, we developed two different molecular hydrogel systems based on bile acids and studied their gelation behavior and properties under various conditions. The first gelation system is based on a cholic acid dimer with diethylenetriamine as a spacer. It is insoluble in water, but may interact with certain carboxylic acids to yield hydrogels. The properties of the hydrogels made from the dimer depend on the chemical structure of the carboxylic acids as well as the acid/dimer molar ratio. The other system is a molecular hydrogel prepared from a series of bile salts where the gelation is induced by carbon dioxide ( $\text{CO}_2$ ). Bile acid sodium salts are soluble in water and form a transparent and homogeneous aqueous solution. The carboxylate groups on a bile salt could be partially protonated in the presence of  $\text{CO}_2$ , leading to the formation of a bile acid that is insoluble in water. The system may be marginally soluble by the cooperation of a soluble bile salt and an insoluble bile acid, leading to the formation of hydrogels. Given the natural origin of bile acids and related compounds, the components in this gelation system are biocompatible so that the hydrogels may be potentially useful in biomedical applications.

This thesis consists of six chapters, including this introduction and a conclusion. All the work presented has been performed by the author of this thesis with the supervision of his supervisor, Prof. Julian Zhu, and the help of co-supervisor, Prof. Karen Waldron.

**Chapter 2** reviews the progress of molecular hydrogels based on bile acids and their derivatives. We summarize the literature work to elucidate the structure and property requirements of the molecular hydrogelators based on bile acids, their gelation capability and the properties of the resulting hydrogels and propose the idea of marginal solubility as a general prerequisite for the formation of molecular gels. This chapter has been published as a review. (M. Zhang, S. Strandman, K.C. Waldron, X.X. Zhu, Supramolecular hydrogelation with bile acid derivatives: Structures, properties and applications. *J. Mater. Chem. B*, **2016**, *4*, 7506-7520.)

**Chapter 3** shows the formation of hydrogels from a cholic acid dimer in the presence of various carboxylic acids. Gelation tests showed that only hydrophilic and weak carboxylic acids were capable of inducing the formation of hydrogels from the dimer. Supramolecular interactions such as protonation and hydrogen bonding with the acids made the dimer marginally soluble in water, leading to the formation of hydrogels. This chapter has been published as a communication. (M. Zhang, K.C. Waldron, X.X. Zhu, Formation of molecular hydrogels from a bile acid derivative and selected carboxylic acids. *RSC Adv.* **2016**, *6*, 35436-35440)

**Chapter 4** shows the continuous study of the gelation of the dimer with a carboxylic acid to better understand the gelation system. An organic salt of the dimer with formic acid in a ratio of 1:1 was capable of forming monodispersed nanofibers in aqueous solutions. It yielded hydrogels when the organic salt concentration was higher than the critical gelation concentration. Further increase of the dimer salt concentration made the hydrogels behave as lyotropic liquid crystals (nematic hydrogels). Ordered aggregates with parallel arrangement of nanofibers were found in these nematic hydrogels and they may be responsible for the anisotropic optical properties. This paper has been published as an article (M. Zhang, C. Fives, K.C. Waldron, X.X. Zhu, Self-assembly of an organic

salt based on a cholic acid dimer and formic acid in aqueous solutions: From nanofibers to nematic hydrogels. *Langmuir*, **2017**, 10.1021/acs.langmuir.6b04033)

**Chapter 5** presents the hydrogels from a series of bile salts induced by CO<sub>2</sub>. Bubbling CO<sub>2</sub> into the aqueous solutions of bile salts induced the formation of hydrogels, which reverted to solution upon heating with bubbling of N<sub>2</sub>. Bile salts self-assemble in water to form micelles, with hydroxyl and carboxylate groups on the surface. Bubbling CO<sub>2</sub> into a bile salt solution could reduce the pH and protonate the carboxylate groups. The micelles may be linked through hydrogen bonding between the protonated carboxylate groups, yielding either transparent hydrogels with nanofibers or opaque hydrogels with thicker nanoshreds. Mechanical strength may be improved by a salting-out effect upon the addition of inorganic salt such as NaCl. This paper has been submitted for publication. (M. Zhang and X.X. Zhu, Formation of supramolecular hydrogels of CO<sub>2</sub> and bile salts in water. Submitted to *Angew. Chem. Int. Ed.*)

**Chapter 6** is an overall summary of the previous chapters and includes suggestions for future work.

## 1.7 References

1. D. K. Smith. Supramolecular Gels: Building Bridges. *Nat. Chem.* **2010**, 2, 162-163.
2. M. O. Piepenbrock; G. O. Lloyd; N. Clarke; J. W. Steed. Metal- and Anion-Binding Supramolecular Gels. *Chem. Rev.* **2010**, 110, 1960-2004.
3. D. J. Lloyd, The Problem of Gel Structure. In *Colloid Chemistry*, Alexander, J., Ed. The Chemical Catalogue Company: New York, USA, 1926; pp 767-782.
4. P. H. Hermans, Gels. In *Colloid Science*, Kruyt, H. R., Ed. Elsevier: Amsterdam, 1949; Vol. 2, p 484.
5. R. G. Weiss; P. Terech. *Molecular Gels: Materials with Self-Assembled Fibrillar Networks*. Springer: Dordrecht, 2006.
6. P. Terech; R. G. Weiss. Low Molecular Mass Gelators of Organic Liquids and the Properties of Their Gels. *Chem. Rev.* **1997**, 97, 3133-3160.

7. T. G. Mezger. *The Rheology Handbook, 2nd Ed.* William Andrew Publishing: Norwich, NY, 2006.
8. D. T. N. Chen; Q. Wen; P. A. Janmey; J. C. Crocker; A. G. Yodh. Rheology of Soft Materials. *Annu. Rev. Condens. Matter Phys.* **2010**, *1*, 301-322.
9. S. Mortimer; A. J. Ryan; J. L. Stanford. Rheological Behavior and Gel-point Determination for a Model Lewis Acid-Initiated Chain Growth Epoxy Resin. *Macromolecules* **2001**, *34*, 2973-2980.
10. Y.-G. Jia; X. X. Zhu. Self-Healing Supramolecular Hydrogel Made of Polymers Bearing Cholic Acid and  $\beta$ -Cyclodextrin Pendants. *Chem. Mater.* **2015**, *27*, 387-393.
11. G. Yu; X. Yan; C. Han; F. Huang. Characterization of Supramolecular Gels. *Chem. Soc. Rev.* **2013**, *42*, 6697-6722.
12. T. G. Mezger. *The Rheology Handbook: For Users of Rotational and Oscillatory Rheometers.* Vincentz Network GmbH & Co KG: 2006.
13. Enateri V. Alakpa; V. Jayawarna; A. Lampel; Karl V. Burgess; Christopher C. West; Sanne C. J. Bakker; S. Roy; N. Javid; S. Fleming; Dimitris A. Lamprou; J. Yang; A. Miller; Andrew J. Urquhart; Pim W. J. M. Frederix; Neil T. Hunt; B. Péault; Rein V. Ulijn; Matthew J. Dalby. Tunable Supramolecular Hydrogels for Selection of Lineage-Guiding Metabolites in Stem Cell Cultures. *Chem* **2016**, *1*, 298-319.
14. A. Vidyasagar; K. Handore; K. M. Sureshan. Soft Optical Devices from Self-Healing Gels Formed by Oil and Sugar-Based Organogelators. *Angew. Chem. Int. Ed. Engl.* **2011**, *50*, 8021-8024.
15. G. John; S. R. Jadhav; V. M. Menon; V. T. John. Flexible Optics: Recent Developments in Molecular Gels. *Angew. Chem. Int. Ed. Engl.* **2012**, *51*, 1760-1762.
16. N. M. Sangeetha; U. Maitra. Supramolecular Gels: Functions and Uses. *Chem. Soc. Rev.* **2005**, *34*, 821-836.
17. T. Kato; N. Mizoshita; M. Moriyama; T. Kitamura. Gelation of Liquid Crystals with Self-Assembled Fibers. *Top. Curr. Chem.* **2005**, *256*, 219-236.
18. G. Nystrom; M. P. Fernandez-Ronco; S. Bolisetty; M. Mazzotti; R. Mezzenga. Amyloid Templated Gold Aerogels. *Adv. Mater.* **2015**.
19. P. J. Flory. Introductory Lecture. *Faraday Discuss Chem Soc* **1974**, *57*, 7.

20. S. Datta; S. Bhattacharya. Multifarious Facets of Sugar-Derived Molecular Gels: Molecular Features, Mechanisms of Self-Assembly and Emerging Applications. *Chem. Soc. Rev.* **2015**, *44*, 5596-5637.
21. T. R. Hoare; D. S. Kohane. Hydrogels in Drug Delivery: Progress and Challenges. *Polymer* **2008**, *49*, 1993-2007.
22. H. Storrie; M. O. Guler; S. N. Abu-Amara; T. Volberg; M. Rao; B. Geiger; S. I. Stupp. Supramolecular Crafting of Cell Adhesion. *Biomaterials* **2007**, *28*, 4608-4618.
23. L. A. Estroff; A. D. Hamilton. Water Gelation by Small Organic Molecules. *Chem. Rev.* **2004**, *104*, 1201-1218.
24. D. J. Abdallah; R. G. Weiss. Organogels and Low Molecular Mass Organic Gelators. *Adv. Mater.* **2000**, *12*, 1237-1247.
25. X. Du; J. Zhou; J. Shi; B. Xu. Supramolecular Hydrogelators and Hydrogels: From Soft Matter to Molecular Biomaterials. *Chem. Rev.* **2015**, *115*, 13165-13307.
26. R. G. Weiss. The Past, Present, and Future of Molecular Gels. What Is the Status of the Field, and Where Is It Going? *J. Am. Chem. Soc.* **2014**, *136*, 7519-7530.
27. T. Kar; S. Debnath; D. Das; A. Shome; P. K. Das. Organogelation and Hydrogelation of Low-Molecular-Weight Amphiphilic Dipeptides: pH Responsiveness in Phase-Selective Gelation and Dye Removal. *Langmuir* **2009**, *25*, 8639-8648.
28. S. Dutta; T. Kar; D. Mandal; P. K. Das. Structure and Properties of Cholesterol-Based Hydrogelators with Varying Hydrophilic Terminals: Biocompatibility and Development of Antibacterial Soft Nanocomposites. *Langmuir* **2013**, *29*, 316-327.
29. J. N. Israelachvili; D. J. Mitchell; B. W. Ninham. Theory of Self-Assembly of Hydrocarbon Amphiphiles into Micelles and Bilayers. *J. Chem. Soc., Faraday Trans. 2* **1976**, *72*, 1525-1568.
30. J. N. Israelachvili. *Intermolecular and Surface Forces*. Academic Press: London, 1991.
31. Z. Chu; C. A. Dreiss; Y. Feng. Smart Wormlike Micelles. *Chem. Soc. Rev.* **2013**, *42*, 7174-7203.
32. A. V. Verde; D. Frenkel. Simulation Study of Micelle Formation by Bile Salts. *Soft Matter* **2010**, *6*, 3815-3825.

33. Y. Lan; M. G. Corradini; R. G. Weiss; S. R. Raghavan; M. A. Rogers. To Gel or Not to Gel: Correlating Molecular Gelation with Solvent Parameters. *Chem. Soc. Rev.* **2015**, *44*, 6035-6058.
34. M. George; R. G. Weiss. Molecular Organogels. Soft Matter Comprised of Low-Molecular-Mass Organic Gelators and Organic Liquids. *Acc. Chem. Res.* **2006**, *39*, 489-497.
35. S. P. Srivastava; A. K. Saxena; R. S. Tandon; V. Shekher. Measurement and Prediction of Solubility of Petroleum Waxes in Organic Solvents. *Fuel* **1997**, *76*, 625-630.
36. D. J. Abdallah; R. G. Weiss. n-Alkanes Geln-Alkanes (and Many Other Organic Liquids). *Langmuir* **2000**, *16*, 352-355.
37. D. J. Abdallah; L. Lu; R. G. Weiss. Thermoreversible Organogels from Alkane Gelators with One Heteroatom. *Chem. Mater.* **1999**, *11*, 2907-2911.
38. D. J. Abdallah; S. A. Sirchio; R. G. Weiss. Hexatriacontane Organogels. The First Determination of the Conformation and Molecular Packing of a Low-Molecular-Mass Organogelator in Its Gelled State. *Langmuir* **2000**, *16*, 7558-7561.
39. C.-Y. Ku; P. Lo Nostro; S.-H. Chen. Structural Study of the Gel Phase of a Semifluorinated Alkane in a Mixed Solvent. *J. Phys. Chem. B* **1997**, *101*, 908-914.
40. T. Tachibana; T. Mori; K. Hori. Chiral Mesophases of 12-Hydroxyoctadecanoic Acid in Jelly and in the Solid State. I. A New Type of Lyotropic Mesophase in Jelly with Organic Solvents. *Bull. Chem. Soc. Jpn.* **1980**, *53*, 1714-1719.
41. T. Tachibana; T. Mori; K. Hori. Chiral Mesophases of 12-Hydroxyoctadecanoic Acid in Jelly and in the Solid State. II. A New Type of Mesomorphic Solid State. *Bull. Chem. Soc. Jpn.* **1981**, *54*, 73-80.
42. H. Basit; A. Pal; S. Sen; S. Bhattacharya. Two-Component Hydrogels Comprising Fatty Acids and Amines: Structure, Properties, and Application as a Template for the Synthesis of Metal Nanoparticles. *Chem. Eur. J.* **2008**, *14*, 6534-6545.
43. G. Clavier; M. Mistry; F. Fages; J.-L. Pozzo. Remarkably Simple Small Organogelators: Di-n-Alkoxy-Benzene Derivatives. *Tetrahedron Lett.* **1999**, *40*, 9021-9024.

44. U. Maitra; V. Kumar Potluri; N. M. Sangeetha; P. Babu; A. R. Raju. Helical Aggregates from a Chiral Organogelator. *Tetrahedron: Asymmetry* **2001**, *12*, 477-480.
45. A. S. Weingarten; R. V. Kazantsev; L. C. Palmer; M. McClendon; A. R. Koltonow; A. P. Samuel; D. J. Kiebalá; M. R. Wasielewski; S. I. Stupp. Self-Assembling Hydrogel Scaffolds for Photocatalytic Hydrogen Production. *Nat. Chem.* **2014**, *6*, 964-970.
46. J. H. Fuhrhop; C. Demoulin; C. Boettcher; J. Koenig; U. Siggel. Chiral Micellar Porphyrin Fibers with 2-Aminoglycosamide Head Groups. *J. Am. Chem. Soc.* **1992**, *114*, 4159-4165.
47. H. Svobodová; V. Noponen; E. Kolehmainen; E. Sievanen. Recent Advances in Steroidal Supramolecular Gels. *RSC Adv.* **2012**, *2*, 4985-5007.
48. Y. C. Lin; R. G. Weiss. Liquid-Crystalline Solvents as Mechanistic Probes. 24. A Novel Gelator of Organic Liquids and the Properties of Its Gels. *Macromolecules* **1987**, *20*, 414-417.
49. M. Zinic; F. Vogtle; F. Fages. Cholesterol-Based Gelators. *Top. Curr. Chem.* **2005**, *256*, 39-76.
50. H. C. Geiger; M. Lamson; D. J. Galka. Synthesis and Spectroscopic Characterization of Chiral Biphenyl-Cholesterol Gels. *Langmuir* **2014**, *30*, 13979-13986.
51. C. Yu; M. Xue; K. Liu; G. Wang; Y. Fang. Terthiophene Derivatives of Cholesterol-Based Molecular Gels and Their Sensing Applications. *Langmuir* **2014**, *30*, 1257-1265.
52. H. Yu; Y. Lu; X. Chen; K. Liu; Y. Fang. Functionality-Oriented Molecular Gels: Synthesis and Properties of Nitrobenzoxadiazole (NBD)-Containing Low-Molecular Mass Gelators. *Soft Matter* **2014**, *10*, 9159-9166.
53. K. Liu; N. Yan; J. Peng; J. Liu; Q. Zhang; Y. Fang. Supramolecular Gels Based on Organic Diacid Monoamides of Cholesteryl Glycinate. *J. Colloid Interface Sci.* **2008**, *327*, 233-242.
54. A. V. Verde; D. Frenkel. Simulation Study of Micelle Formation by Bile Salts. *Soft Matter* **2010**, *6*, 3815.
55. A. F. Hofmann. Bile Acids: The Good, the Bad, and the Ugly. *News Physiol. Sci.* **1999**, *14*, 24-29.
56. C. Valenta; E. Nowack; A. Bernkop-Schnurch. Deoxycholate-Hydrogels: Novel Drug Carrier Systems for Topical Use. *Int. J. Pharm.* **1999**, *185*, 103-111.



57. K. E. McNeel; S. Das; N. Siraj; Negulescu, II; I. M. Warner. Sodium Deoxycholate Hydrogels: Effects of Modifications on Gelation, Drug Release, and Nanotemplating. *J. Phys. Chem. B* **2015**, *119*, 8651-8659.
58. W. Liang; J. R. Guman-Sepulveda; S. He; A. Dogariu; J. Y. Fang. Microrheology and Release Behaviors of Self-Assembled Steroid Hydrogels. *J. Mater. Sci. Chem. Eng.* **2015**, *03*, 6-15.
59. G. Gundiah; S. Mukhopadhyay; U. G. Tumkurkar; A. Govindaraj; U. Maitra; C. N. R. Rao. Hydrogel Route to Nanotubes of Metal Oxides and Sulfates. *J. Mater. Chem.* **2003**, *13*, 2118.
60. Y. Qiao; Y. Lin; Y. Wang; Z. Yang; J. Liu; J. Zhou; Y. Yan; J. Huang. Metal-Driven Hierarchical Self-Assembled One-Dimensional Nanohelices. *Nano Lett.* **2009**, *9*, 4500-4504.
61. X.-J. Xu; G.-T. Fei; W.-H. Yu; X.-W. Wang; L. Chen; L.-D. Zhang. Preparation and Formation Mechanism of ZnS Semiconductor Nanowires Made by the Electrochemical Deposition Method. *Nanotechnology* **2006**, *17*, 426-429.
62. S. Bhat; U. Maitra. Nanoparticle-Gel Hybrid Material Designed with Bile Acid Analogues. *Chem. Mater.* **2006**, *18*, 4224-4226.
63. S. Song; L. Feng; A. Song; J. Hao. Room-Temperature Super Hydrogel as Dye Adsorption Agent. *J. Phys. Chem. B* **2012**, *116*, 12850-12856.

## Chapter 2

### Supramolecular hydrogelation with bile acid derivatives:

#### Structures, properties and applications\*

#### Abstract

Hydrogelation of small molecules in aqueous solutions results from a balance between solubilization and precipitation (or crystallization). The hydrophobic moieties of amphiphiles tend to aggregate and the hydrophilic units may stabilize the aggregates in aqueous solutions. Morphologies vary according to the chemical structure of the amphiphiles. The formation of nanofibers or worm-like micelles is a prerequisite for hydrogels. Molecular hydrogels often show better degradability and functional diversity than polymeric hydrogels and may be useful in biomedical applications. Bile acids have attracted increasing attention for designing various biomaterials, including molecular hydrogels. They are naturally occurring amphiphilic compounds that exist in our body and help with the dissolution and digestion of fat by the formation of micelles. This review highlights the recent progress in the field of molecular hydrogelators based on bile acids, including bile salts, anionic, cationic and neutral bile acid derivatives, two-component hydrogelation systems, and polymeric supramolecular hydrogels, along with their potential applications.

---

\*Published as a review: M. Zhang, S. Strandman, K.C. Waldron, X.X. Zhu, *J. Mater. Chem. B*, 2016, **4**, 7506-7520.

Contributions of authors other than supervisors

Meng Zhang: Literature searching, organization and analysis, manuscript writing.

Satu Strandman: Literature organization, manuscript revision.

## 2.1. Introduction

Molecular gels are a class of soft materials with self-assembled fibrous networks (SAFINs) in solvents. They are derived from compounds of low molecular weight ( $< 2000 \text{ gmol}^{-1}$ ) and formed by supramolecular interactions, such as hydrophobic interactions, hydrogen bonding, metal coordination, and electrostatic interactions.<sup>1-3</sup> Generally, the gelator molecules are marginally soluble in certain solvents but can be dissolved to form a homogeneous solution under heating. The supersaturated system upon subsequent cooling forms stable 3-D fibrous networks by self-assembly of the gelator molecules. Solvent molecules can be immobilized by the networks and the system appears solid-like. Compared with polymeric gels, most molecular gels are thermoreversible, formed by gelators of precisely controllable chemical structures, and show better biodegradability and functional diversity. They may be potentially useful in areas such as drug delivery,<sup>4-5</sup> tissue engineering,<sup>6-8</sup> sensors,<sup>9-10</sup> water decontamination,<sup>11</sup> and templating.<sup>12</sup> The application aspects of molecular gels were discussed in a review by Sangeetha and Maitra in 2005.<sup>13</sup>

Both organogels and hydrogels may be formed depending on the solvent used for gelation. Structures, properties and applications of organogelators and hydrogelators have been reviewed by Abdallah and Weiss<sup>14</sup> and Du *et al.*<sup>15</sup> The gelation ability of the molecular gelators is strongly dependent on their chemical structures but not in a predictable way. A review published by Terech and Weiss in 1997 summarized a series of molecular organogelators and their gelation ability in various organic solvents, and concluded the “serendipity” nature of molecular gelation.<sup>16</sup> More recently, a feature article by Weiss presented the current understanding of molecular gels and their future prospects.<sup>17</sup>

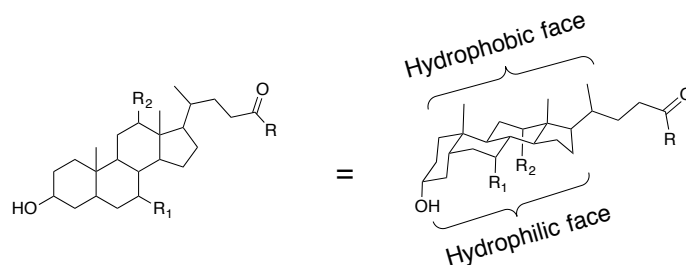
Molecular gelators based on biocompounds have drawn much attention because of their biological origin. These include nucleobases,<sup>18</sup> amino acids,<sup>19</sup> sugars,<sup>20</sup> and cholesterol,<sup>21</sup> and related reviews have been published on the structures and interactions of gelators, the properties of yielded organogels or hydrogels, and the potential applications. Among the biocompounds, bile acids are especially well suited for the

formation of both organo- and hydrogels, and most of the molecular gels based on bile acids could be obtained at a low gelator concentration.<sup>22</sup> Bile acids are a class of steroidal natural compounds found in humans and most animals and help in the adsorption and digestion of fats.<sup>23</sup> Materials based on bile acids often show improved biocompatibility and may be used for biomedical applications.<sup>24</sup> Bile acids are steroidal compounds with hydroxyl groups and a carboxylic acid group on the concave hydrophilic face and three methyl groups on the convex hydrophobic face (Scheme 2.1).<sup>25</sup> Taking advantage of their facial amphiphilicity in solutions, molecular umbrellas or pockets may be constructed with star-shaped oligomers of bile acids.<sup>26-27</sup> Linear oligomers of bile acids can fold into helical structures with nanometer-sized internal cavities in solvents.<sup>28-29</sup> Bile acid derivatives bearing multiple methacrylate groups are cross-linkable monomers and may be used for novel dental resins with good mechanical strength, low polymerization shrinkage and low cytotoxicity.<sup>30-31</sup> Bile salts are known to self-assemble in aqueous solutions to form micelles or nanofibers, making these compounds potential molecular gelators. Bile acids may also be modified to form molecular gelators.<sup>32</sup>

Review papers on the molecular gels based on bile acids have been published in the literature.<sup>22, 32-33</sup> These reviews focused on the properties and applications of bile acid molecular gels and paid more attention to organogels. It would be desirable to establish a general rule of the relationship between the molecular structure and the gelation ability of the gelator. New progress has been made since the last comprehensive review of molecular gels based on bile acids by Svobodová *et al.*<sup>32</sup> The current review attempts to establish a general understanding of the relationship between the structure of gelators and the properties of the yielded molecular gels. Molecular hydrogels are more biocompatible and less toxic than organogels due to the absence of organic solvents, and their porous nature from the 3-D fibrous networks can be used for the encapsulation and delivery of therapeutics including drug molecules, proteins and cells.<sup>34-35</sup> Certain molecular hydrogels exhibit viscous flow under shear stress (shear-thinning) and fast recovery when the applied stress is relaxed (self-healing), so they can be used as injectable hydrogels,<sup>36</sup> which are of practical interest since the loading of therapeutics is easy and a surgical procedure is not required for the insertion of such gels into tissue.<sup>37</sup> In this work we

attempt to systematically summarize the work on the structure and property requirements of the molecular hydrogelators based on bile acids, their gelation ability and the properties of the resulting hydrogels in order to find a general predictive rule for molecular gel formation. The progress in molecular hydrogels based on bile salts, including metallo gels, is discussed first, and then we focus on anionic, cationic, and neutral bile acid derivatives and two-component hydrogels with highlights of their applications. We intend to emphasize on the factors that are reported to affect the hydrogelation ability of bile acids and their derivatives.

**Scheme 2.1** Chemical structure of bile acids and certain bile acid conjugates.



	R	R <sub>1</sub>	R <sub>2</sub>
Cholic acid (CA)	OH	OH	OH
Deoxycholic acid (DCA)	OH	H	OH
Chenodeoxycholic acid (CDCA)	OH	OH	H
Lithocholic acid (LCA)	OH	H	H
Ursodeoxycholic acid (UDCA)	OH	$\beta$ -OH	H
Glycocholic acid	NH-CH <sub>2</sub> -COOH	OH	OH
Glycodeoxycholic acid	NH-CH <sub>2</sub> -COOH	H	OH
Taurocholic acid	NH-(CH <sub>2</sub> ) <sub>2</sub> -SO <sub>3</sub> H	OH	OH

## 2.2. Self-assemblies of bile salts and theories for molecular hydrogelation

All bile acids in the acidic form show limited solubility in water,<sup>38</sup> whereas deprotonation of the carboxylic acid group improves the solubility in aqueous solution and promotes the formation of various micelles and aggregates.<sup>39</sup> The critical micellar

concentrations (CMC) depend on their chemical structures and the presence of additives.<sup>40-48</sup> Primary micelles of bile salts are formed when the concentrations are close to the CMC, with hydrodynamic radii of 1-2 nm and aggregation numbers of 2-10 (Fig. 2.1A).<sup>23, 47</sup> Increasing the concentration of bile salts facilitates the interaction of the hydroxyl groups of bile salts in the primary micelles through hydrogen bonding, leading to the formation of secondary micelles with hydrodynamic radii of about 10 nm and aggregation numbers of 10-100 (Fig. 2.1B).<sup>23,47</sup> A further increase of the concentration of certain bile salts to around 40 wt%, such as sodium deoxycholate (NaDC), sodium taurocholate, and sodium glycodeoxycholate, induces the formation of hexagonal lyotropic liquid crystals.<sup>23, 39, 49-50</sup> The most hydrophobic bile acid, LCA, was reported to interact with ethylenediamine to form lyotropic liquid crystals at very low concentrations (1-4 wt%).<sup>51</sup>

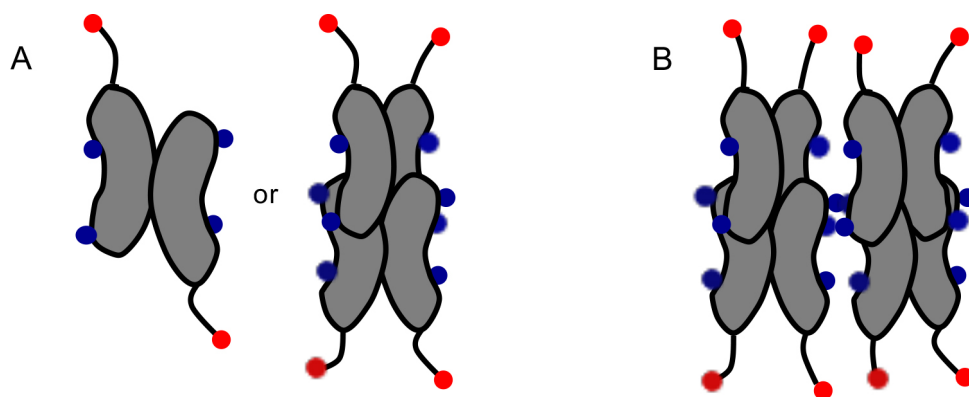


**Figure 2.1** Schematic representation of various configurations of bile salt micelles with the hydroxyl groups shown as blue dots and carboxylate groups as red dots: (A) Primary micelles. (B) Secondary micelles.

The gelation process is similar to that of crystallization or precipitation, where the molecules tend to aggregate into ordered or amorphous structures. Efforts have been made to illustrate a general rule for the formation of molecular hydrogels. Fan et al.<sup>52</sup> used the Flory-Huggins interaction parameter ( $\chi$ ) between a complex of melamine and di(2-ethylhexyl) phosphoric acid and a co-solvent of water with certain organic solvents to illustrate the relationship between the solubility and gelation capability. Stable opaque

hydrogels were obtained with intermediate values of  $\chi$  yielded, indicating that marginal solubility is important for the formation of molecular gels. The hydrophilic-lipophilic balance (HLB) of a molecule was reported to be crucial for the formation of molecular hydrogels.<sup>53-55</sup> Methods to evaluate the HLB of a compound with a specific structure have been proposed by Griffin<sup>56-57</sup> and Davies,<sup>58</sup> but it is difficult to obtain precise HLB values, or to establish an effective HLB scale for the formation of fibrils via self-assembly.<sup>53</sup>

The morphology of the self-assemblies of amphiphiles in aqueous solutions is related to the molecular packing parameter ( $p$ ) according to Israelachvili *et al.*:<sup>59-60</sup>

$$p = \frac{v}{a_0 l_c}$$

where  $v$  is the hydrophobic volume of the amphiphile,  $a_0$  is the interfacial area or the hydrophilic head group area on the amphiphile, and  $l_c$  is the critical chain length, which is the maximum effective length that the hydrophobic chains can assume. It was reported that the packing parameter  $p$  is effective to predict the morphologies of the self-assembly of amphiphiles in aqueous solution (Fig. 2.2).<sup>61-64</sup> Amphiphiles with a value of  $p$  between 1/3 and 1/2 may indicate the formation of worm-like cylindrical micelles (nanofibers or nanotubes),<sup>63</sup> which is essential for formation of molecular hydrogels. Other factors besides the structure, such as concentration and temperature, may also affect the morphology of amphiphile self-assemblies in aqueous solutions.<sup>65-66</sup> Unfortunately, calculation of the packing parameter of amphiphiles with steroid moieties may not be accurate,<sup>43</sup> making the prediction of the morphology difficult. Therefore, a general rule for the hydrogelation of bile acids cannot be extrapolated from the  $p$  value. While HLB values might be a better predictor, they are not readily available for most bile acids.

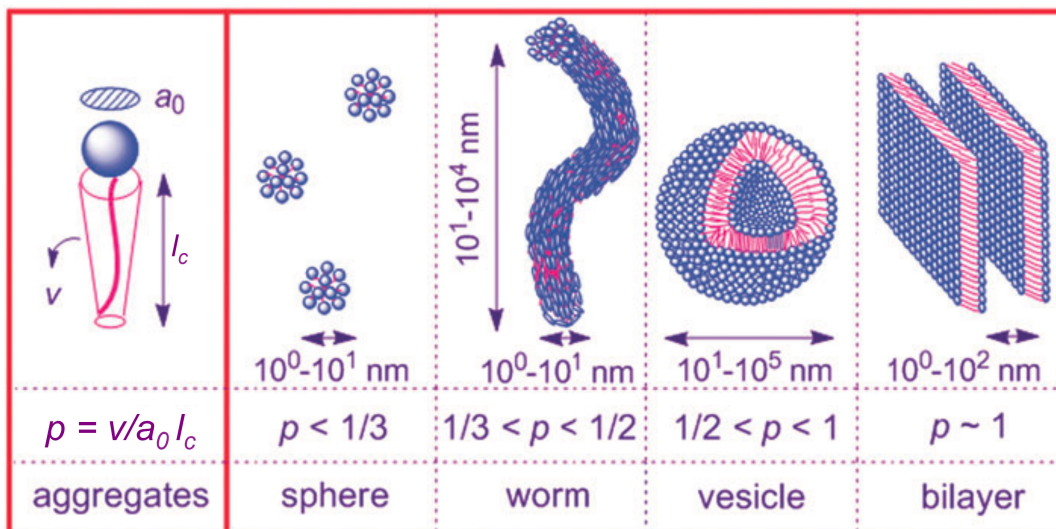


**Figure 2.2** Relationship between the value of packing parameter,  $p$ , and the morphologies of self-assemblies of amphiphiles in aqueous solutions. (Adapted with permission from ref. 63. Copyright (2013) Royal Society of Chemistry.)

## 2.3. Molecular hydrogels based on bile acids

### 2.3.1 Fibrillar aggregates from bile salts

A fibrous structure with nano-scale diameter is essential for the formation of 3-D networks in molecular gels, and isolated nanofibers may be observed from diluted molecular gelation systems. LCA can form tubular aggregates in aqueous solutions at room temperature. Terech *et al.*<sup>67-71</sup> reported the formation of long stiff tubules by LCA (0.1 wt%) in basic aqueous solutions with mean outer and inner diameters of 52 and 49 nm, respectively (Fig. 2.3A). The structures were confirmed by small-angle X ray scattering (SAXS) technique.<sup>71</sup> The kinetic process for the formation of such nanotubes was studied.<sup>69</sup> Structures such as fibrils, tapes, helical ribbons, and single- and multiple-walled nanotubes, can form immediately after the dissolution of LCA, while only monodisperse single-walled nanotubes were obtained as the final morphology. Such nanotubes may interact weakly to form entropic 3-D networks that behave as hydrogels.<sup>68</sup>



Fang and co-workers<sup>72-76</sup> reported the formation of microtubes with outer diameters in the range of 0.7 to 1.5  $\mu\text{m}$  from basic aqueous solutions after vortexing and equilibration for one week (Fig. 2.3B). The dissolution of LCA in basic aqueous solutions led to the formation of vesicles with outer diameter of about 1.5  $\mu\text{m}$ , which further aggregated into hollow cylindrical tubes with time. Such microtubes kept growing until all the vesicles were consumed and the elongated tubes coiled into 3-D spirals. It was also reported that NaDC or the sodium salt of other conjugated bile acids can self-assemble in aqueous solutions to form nanotubes or helical nanoribbons.<sup>77-79</sup>

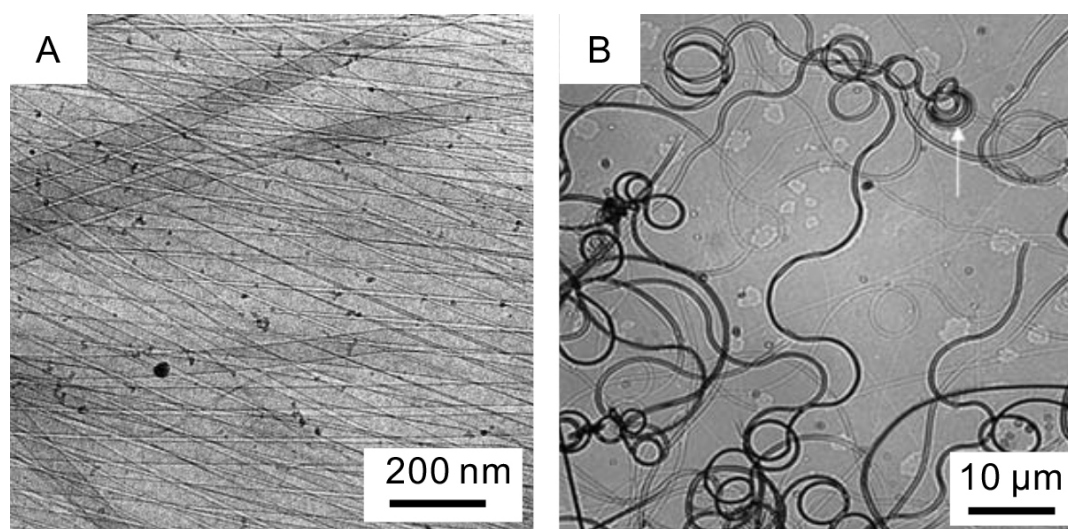


**Figure 2.3** Morphologies of self-assemblies from LCA at aqueous solutions (pH  $\sim$ 12.0). (A) Nanotubes with 0.1 wt% LCA. (B) Microtubes with 0.1 wt% LCA after vortexing and equilibration for a week. (Adapted with permission from ref. 70. Copyright (2002) American Chemical Society and from ref. 73. Copyright (2011) Royal Society of Chemistry.)

### 2.3.2 Metallogels

The first research reporting molecular hydrogels based on bile acids was an irreversible “clot (gel)” from sodium cholate (NaC) solution in the presence of various calcium salts ( $\text{CaCl}_2$ ,  $\text{Ca}(\text{NO}_3)_2$ ,  $\text{Ca}(\text{OAc})_2$ , etc.) upon heating to 50  $^\circ\text{C}$ .<sup>80-82</sup> In fact, NaC could interact with a series of metal cations ( $\text{Cu}^{2+}$ ,  $\text{Ag}^+$ ,  $\text{Hg}^{2+}$ ,  $\text{Zn}^{2+}$  etc.) to form hydrogels as shown in

Fig. 2.4.<sup>83-84</sup> Hydrogels may be obtained by the interaction between metal cations and other bile salts, such as NaDC, sodium chenodeoxycholate (NaCDC), sodium lithocholate (NaLC), and sodium glycocholate.<sup>85</sup>

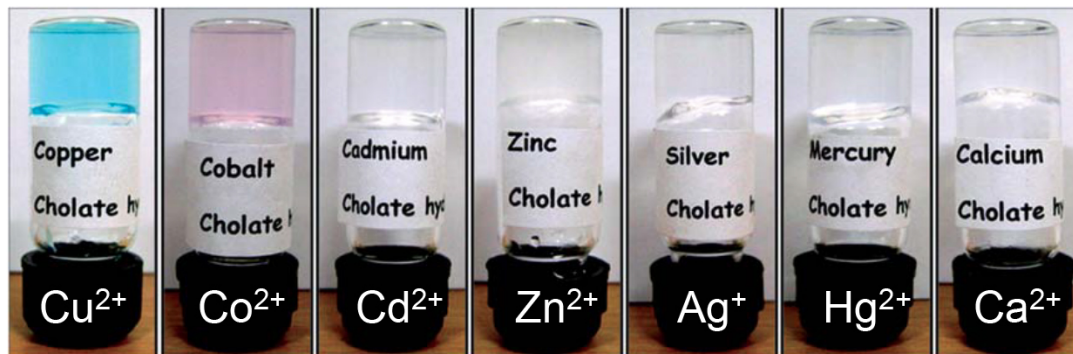


**Figure 2.4** Hydrogels from interaction between sodium cholates and different metal cations. (Adapted with permission from ref. 83. Copyright (2012) Royal Society of Chemistry.)

Trivalent lanthanides were reported to be able to interact with bile salts to induce the formation of hydrogels, which is driven by the combination of multiple supramolecular interactions, such as metal coordination, hydrogen bonding, hydrophobic interaction, and van der Waals' forces.<sup>72,86-88</sup>  $\text{La}^{3+}$  shows excellent gelation ability for the aqueous solution of NaC and the molar ratio between NaC and water can be 1: 92 000 in a stable hydrogel.<sup>72</sup> Banerjee *et al.*<sup>86</sup> conducted a systematic study on the hydrogelation of NaC with a series of trivalent lanthanides and showed that the size of the trivalent lanthanide affected the mechanical properties of the resulting hydrogels.<sup>86</sup> Aqueous solutions with 15 mM NaC and 5 mM lanthanide cations yielded hydrogels with storage moduli ( $G'$ ) of the hydrogels ranging from 38.6 kPa for  $\text{Nd}^{3+}$  (the largest cation) to 8.4 kPa for  $\text{Yb}^{3+}$  (the smallest). The hydrogels or xerogels from NaC with  $\text{Eu}^{3+}$  or  $\text{Tb}^{3+}$  showed enhanced luminescence properties in the presence of the probes, pyrene or 2,3-dihydroxynaphthalene (DHN), and the color of the emitted light from hydrogels under UV irradiation may be varied at different  $\text{Eu}^{3+}/\text{Tb}^{3+}$  ratios.<sup>86-87</sup> Similar luminescent hydrogels were also obtained by the interaction between  $\text{Eu}^{3+}$  and NaDC.<sup>88</sup> Laishram *et al.*<sup>89</sup> found a series of luminescent

hydrogels emitting red, blue, and green light, respectively, and mixed them at carefully controlled ratios to yield white light emitting luminescent hydrogels under irradiation of a long wavelength UV lamp.

An LCA derivative bearing a pyridine unit (**1**, Fig. 2.5) was reported to interact with  $\text{Cu}^{2+}$  to yield supramolecular hydrogels in water containing 30-50% organic solvent like methanol, acetonitrile, or acetone.<sup>90</sup> The metallic hydrogels were responsive to certain stimuli: the gelation process was favored by sonication or shaking, and the gel-to-sol phase transition may be triggered by addition of compounds such as pyridine and ammonium hydroxide. A CA amide derivative bearing a phenanthroline unit (**2**, Fig. 2.5) showed limited solubility in pure water, but formed a translucent hydrogel in a mixture of methanol and water (1:1 v/v). SEM images of the hydrogels showed fibers with diameters about 0.5  $\mu\text{m}$ .<sup>91</sup> The phenanthroline units interacted with  $\text{Zn}^{2+}$  at a ratio of 2:1 to form a dimeric complex (**3**, Fig. 2.5), which showed different gelation behaviors. The dimeric complex formed translucent hydrogels within several minutes after being dissolved, but was unstable and transformed into transparent liquids when left at room temperature. In the hydrogel initially formed, the dimeric complex self-assembled to form globules with diameters of 0.5-3.0  $\mu\text{m}$ , and no morphology variation was observed from the spontaneous gel-to-sol phase transition. The sterically demanding interactions between phenanthroline and metal ions changed the molecular arrangement of the CA derivative and did not favor the formation of fibrous structure.

Metallogels based on bile acids can be used as a template to induce the formation of nanostructures. For example, nanoparticles or nanoclusters of metals (Au, Ag, Pd) or metal sulfides (CdS, ZnS) were synthesized in a  $\text{Ca}^{2+}$ -cholate hydrogel, yielding hybrid soft materials.<sup>83,92</sup> The hybrid  $\text{Ca}^{2+}$ -cholate xerogel with Pd nanoparticles was reported to be an effective catalyst for the Suzuki reaction, and the catalytic activity may be retained for several months.<sup>92</sup> The addition of  $\text{Na}_2\text{S}$  to the supramolecular  $\text{Zn}^{2+}$ -cholate hydrogel induced the formation of ZnS helical nanotubes, with potential use as semi-conductor materials.<sup>84</sup> Tetraethylorthosilicate (TEOS) was hydrolyzed and assembled on the surface of the nanohelices, yielding  $\text{SiO}_2$  helices by further polymerization and mineralization.<sup>84</sup> The cations in metallogels based on bile acids could also be reduced to yield metal

nanoparticles.<sup>85,93</sup> Shen *et al.*<sup>85</sup> developed a series of metallo gels by mixing metal cations of Ag and Au with various bile salts, and obtained Ag and Au nanoparticles/nanoclusters by natural light irradiation of the hydrogels. The hydrogels remained in the gel state after the irradiation and showed higher mechanical strength in the presence of nanoaggregates. The same strategy was used to form Cu nanoparticles in the metallo gels of bile salts, where cysteine was used as a chemical reducing agent.<sup>94</sup> Such hydrogels with encapsulated red emissive Cu nanoclusters demonstrated good catalytic performance in a methylene blue-hydrazine reduction system, and may be potentially used as an alternative for treating organic pollutants in water.

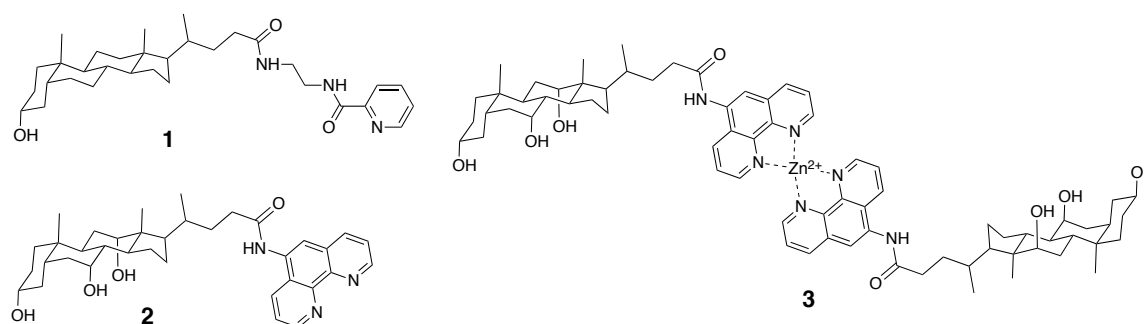


**Figure 2.5** The chemical structures of metallic hydrogelators based on bile acids.

### 2.3.3 Anionic hydrogelators

#### 2.3.3.1 Bile acid sodium salts

Bile salts have been shown to be effective anionic hydrogelators. NaDC is the most studied bile salt hydrogelator, which is sensitive to pH and yields hydrogels at about neutral pH.<sup>95</sup> The mechanical properties depend on the pH of solution, such as in the case of NaDC (115.8 mM) in a phosphate buffer solution (PBS).<sup>96</sup> The value of  $G'$  increased from 12 to 61 Pa when the pH changed from 7.3 to 6.8, but then decreased (54 Pa) at an even lower pH (6.7). The gelation process of NaDC at neutral pH studied by fluorescence spectroscopy with pyrene as a probe showed that clusters (primary or secondary micelles, as shown in Fig. 2.1) in the solution interact with each other to form larger aggregates (nanofibers or worm-like micelles) that induce the gelation process.<sup>97</sup> Research by Blow

and Rich<sup>98</sup> indicated that increasing the ionic strength in aqueous solutions by adding sodium salts (NaCl or Na<sub>2</sub>SO<sub>4</sub>) favored the gelation of NaDC due to the salting-out effect, and sufficiently high ionic strength could induce the gelation of NaDC without the addition of acidic compound. Jover *et al.*<sup>96</sup> reported that the G' of the hydrogel from NaDC (173.7 mM) in PBS increased from 50 Pa to 1000 Pa when the concentration of NaCl increased from 0 to 0.64 M. Decreasing pH or increasing ionic strength of the aqueous solutions of NaDC leads to the protonation of the carboxylate group, and intermolecular hydrogen bonds between carboxylic acid groups may result in gelation.<sup>96</sup> The pH-dependent gelation behavior was also found with NaLC, whereas no gelation was observed for NaC, nor for the sodium salts of conjugated bile acids.<sup>95</sup>

Additives such as amino acids have been shown to affect the mechanical properties of hydrogels based on NaDC. For example, Rich and Blow<sup>99</sup> reported that NaDC was able to interact with glycine to form a “gel with considerable rigidity”. Xin and co-workers<sup>100-102</sup> also reported that L-lysine and L-arginine destroyed the fibrillar networks of NaDC hydrogel formed in the presence of sodium halide. The authors claimed that the addition of both amino acids broke the hydrogen bonds in the hydrogels.<sup>101</sup> It is possible that the basic nature of lysine and arginine may raise the pH of mixture and increase the NaDC deprotonation degree and solubility, leading to disruption of the hydrogels. The organic buffer compound tris(hydroxymethyl)aminomethane (TRIS) also induced the gelation of NaDC in aqueous solutions of basic pH.<sup>103-104</sup>

Hydrogels based on NaDC may be potentially used as drug delivery agents. Valenta *et al.*<sup>105</sup> developed a drug carrier system by using thixotropic hydrogels of NaDC in PBS and mannitol as an additive. The model drug rutin was accommodated in such hydrogels and released through either an artificial membrane (dialysis tubing) or excised rat skin to aqueous solution via the dialysis process. The release rate of the drug from the NaDC hydrogel was about three times as high as that from certain polymer hydrogels, whereas their microbial stability was similar. Advantages of the NaDC hydrogels such as enhanced penetration and thixotropy make them a promising, alternative drug carrier system for topical pharmaceuticals as well as for cosmetic applications. A hydrogel made of NaDC in a Tris buffer solution was able to load a fluorescein probe and released it into aqueous

solutions, where the release rate was varied by shearing the hydrogel.<sup>103</sup> Fang and co-workers<sup>106</sup> reported that a NaDC hydrogel swelled in aqueous solutions to load probes such as doxorubicin hydrochloride (DOX) and then released them to water at different rates according to the pH of the surrounding environment, where higher pH values caused a higher release rate.

### 2.3.3.2 Bile acid derivatives

Modified bile acids in their anionic form may also form hydrogels under suitable conditions. Galantini and co-workers<sup>107-108</sup> reported a CA derivative (**4**, Fig. 2.6) as an effective molecular hydrogelator, by first forming stable vesicles in basic aqueous solutions at room temperature when the concentration was higher than 0.5 mM. Upon heating, the vesicles aggregated to form a necklace morphology in 42 h when the temperature was increased to 40 °C, and nanotubes were shown as the final morphology after being equilibrated for 96 h.<sup>107</sup> This compound was also found to form a hydrogel at room temperature in bicarbonate buffer solution (30 mM, pH ~10) when the concentration was above 3.0 mM. The hydrogel was thermo-sensitive and became a solution of self-assemblies with tubular morphology when heated to 34-36 °C.<sup>108</sup> Gubitosi *et al.*<sup>109</sup> also found that a sugar-substituted LCA (**5**, Fig. 2.6) formed a hydrogel at high concentrations and showed interesting morphology evolution behavior. Such a compound self-assembled in water to form initially tubular scrolls via the rolling of layers. Further rolling of the scrolls resulted in single-walled tubules, showing decreasing average diameters with uniform dispersion upon equilibration (Fig. 2.7).

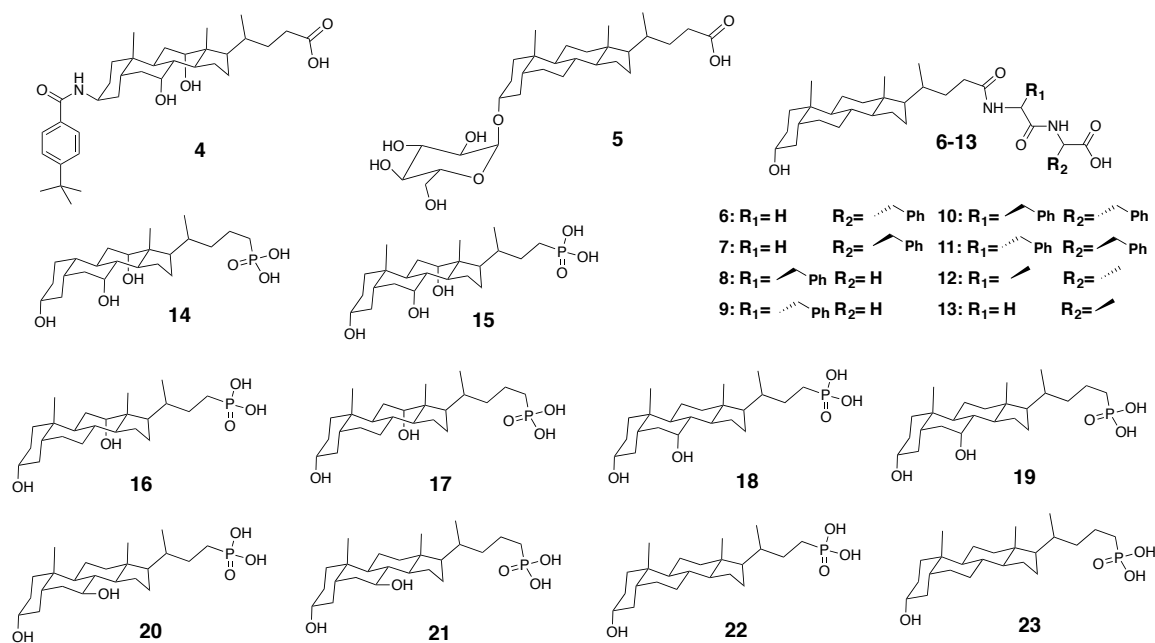


**Figure 2.6** The chemical structures of anionic molecular gelators derived from bile acids.

Maity *et al.*<sup>110</sup> designed and synthesized a series of compounds based on bile acids and numerous peptides composed of glycine, alanine, and phenylalanine, and studied their gelation ability in basic aqueous solutions. Only derivatives based on LCA (**6-13**, Fig. 2.6) formed hydrogels in aqueous solutions of pH higher than 7. Stereochemistry was reported to affect the gelation behavior: stereoisomers **6** and **7** showed different gelation abilities. Transparent and stable hydrogels were obtained with **6** in PBS at pH 7, while milky white suspensions were formed with **7** under the same conditions. Both compounds were effective hydrogelators in aqueous solutions with pH about 8 and the resulting hydrogels were thixotropic and injectable.<sup>110</sup>

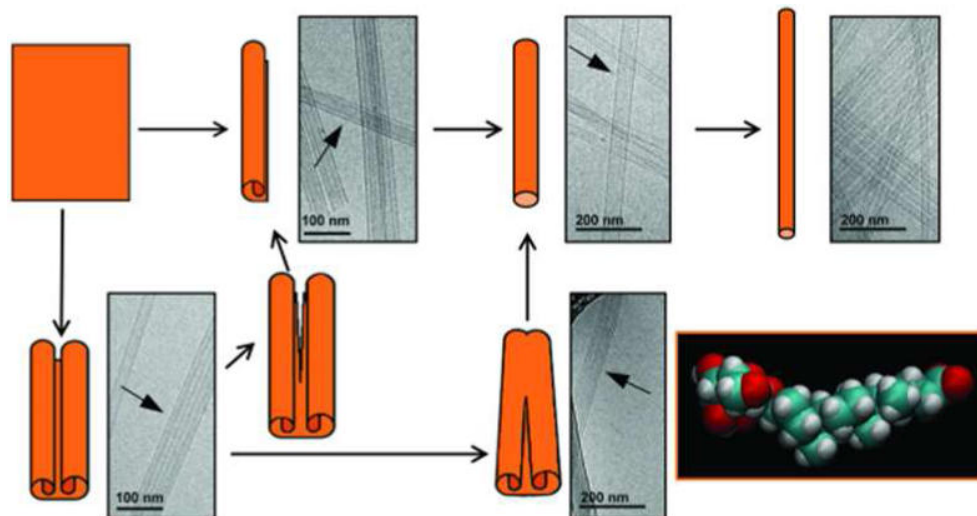


**Figure 2.7** Schematic representation for the kinetic process of nanotube formation from the sugar-substituted LCA derivative **5**. (Reprinted with permission from ref. 109. Copyright (2014) American Chemical Society.)

Maitra and coworkers<sup>111-113</sup> also made a series of phosphate derivatives of bile acids (**14-23**, Fig. 2.6), which formed micelles in basic solutions,<sup>111</sup> facilitating the solubilization of cholesterol.<sup>112</sup> Lowering the pH of the solutions gradually protonated the phosphoric acid groups, which led to the formation of hydrogels. The more hydrophilic gelators (**14** and **15**) formed hydrogels at pH 1.7-2.5, near the  $pK_{a1}$  (2.4) of the phosphoric acid group, while the more hydrophobic gelators (**22** and **23**) formed hydrogels at pH 7.0-7.5, near the  $pK_{a2}$  (8.1) of the phosphoric acid group.<sup>113</sup> Such results indicated that gelation occurs at specific HLB ranges when the system shows marginal solubility.

### 2.3.4 Cationic gelators

Basic functional groups such as primary, secondary or tertiary amines may be protonated and show improved solubility in acidic aqueous solutions. Quaternary amines are permanently cationic and exist as a water-soluble quaternary ammonium salt. Bile acid derivatives with such amino groups have the potential to form molecular hydrogels (Fig. 2.8).



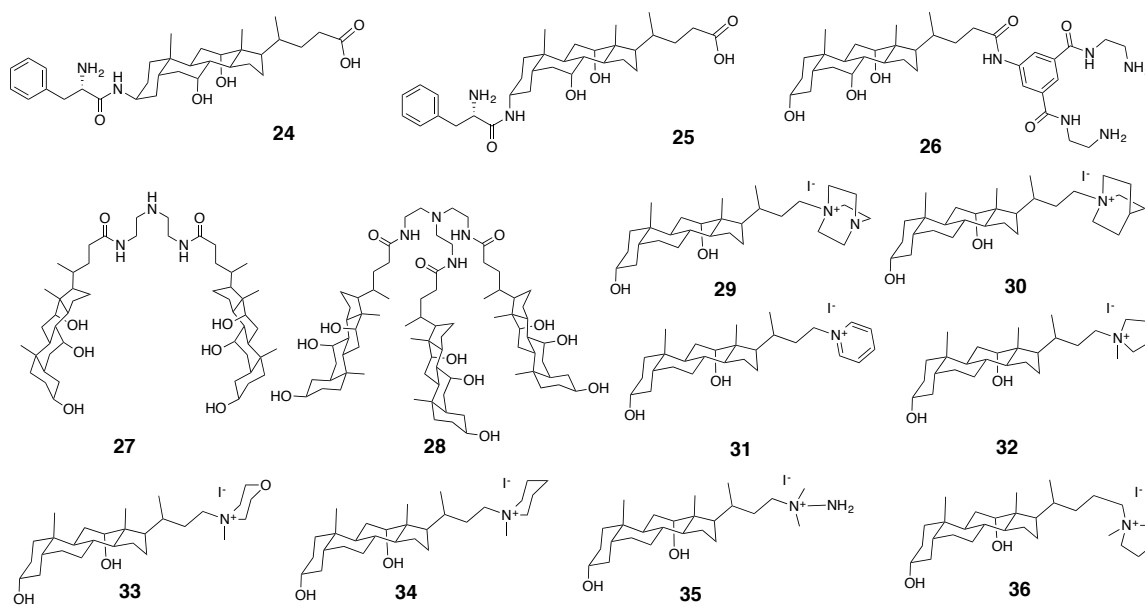


**Figure 2.8** The chemical structures of cationic molecular gelators derived from bile acids.

### 2.3.4.1 Bile acid derivatives with primary amines

Travaglini *et al.*<sup>114</sup> reported a bile acid-derived molecular hydrogelator synthesized by introducing an L-phenylalanine residue on a CA derivative through an amide bond at the 3- $\beta$  position (**24**, Fig 2.8), thus bearing both carboxylic acid and primary amine groups. It was insoluble in pure water but soluble in either basic or acidic aqueous solutions. At pH 10.0, with both carboxylic acid and amine groups protonated, the compound self-assembled to form globular micellar aggregates. At pH 1.1, where the compound is fully protonated and carries a net charge of +1, it self-assembled into long and extremely narrow nanotubes with inner and outer diameters of about 3 and 6 nm, respectively, which formed a hydrogel.<sup>114</sup> The molecular structure of **24** presented as a wedge and could aggregate to form monolayer nanotubes with a wall thickness of about 1.7 nm, close to the length of a single molecule ( $\sim$ 2.0 nm) (Fig. 2.9A). Its stereoisomer **25** also formed a hydrogel in acidic aqueous solution.<sup>115</sup> Compound **25** formed wedge-shaped face-to-face dimers, which interacted back-to-back with each other to form monolayer nanotubes with thickness around 1.7 nm. Parallel face-to-face dimers yielded narrower nanotubes with the same size as those from compound **24**, while antiparallel face-to-face dimers formed

wider nanotubes with larger cross-section diameters (16-19 nm), as shown in Fig. 2.9B. The self-assembly of **26** bearing two primary amine groups yielded a fibrillar network and formed hydrogels when the primary amine groups were protonated by HCl.<sup>116</sup> The mechanical properties of the hydrogels from **26** may be improved via interaction with a CA dicarboxylic acid derivative, as discussed in more detail further on.

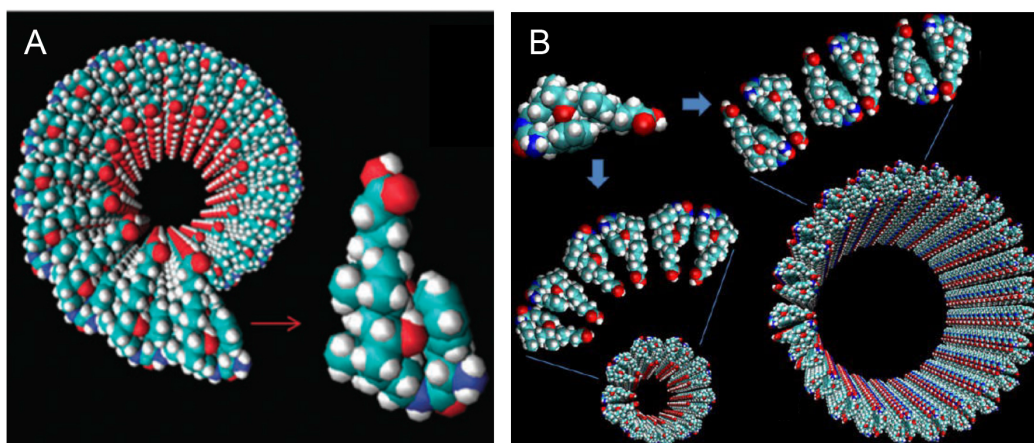


**Figure 2.9** Schematic representation of molecular arrangements of (A) nanotubes from wedge-shape **24**, and (B) narrow nanotubes by head-to-head arrangement (left) and wide nanotubes by head-to-tail arrangement (right) of compound **25**. (Reproduced and adapted with permission from ref. 114. Copyright (2012) Royal Society of Chemistry and from ref. 115. Copyright (2013) American Chemical Society.)

#### 2.3.4.2 Bile acid derivatives with secondary amines

Recently, we found that CA dimer **27** bearing a secondary amine and two amide groups may interact with a series of carboxylic acids in aqueous solutions to form hydrogels with 3-D fibrillar networks (Fig. 2.10A), and the gelation behavior and the mechanical properties of the hydrogel depend on the chemical structure of the carboxylic acid.<sup>117</sup> Monoacids with relatively longer alkyl chains formed stronger hydrogels through hydrophobic interactions, and diacids with additional hydroxyl groups also improved the mechanical properties of the hydrogels through hydrogen bonding with each other. Strong acids (such as trifluoroacetic acid) or acids that are too hydrophobic (such as pentanoic

acid and hexanoic acid) were not able to form hydrogels with the dimer. The driving forces for the gelation are protonation of the secondary amine of **27** and hydrogen bonding with the amide group. The molecular arrangement in the mixture leads to the gelation of the dimer in the presence of different organic acids (Fig. 2.10B). Protonation of the secondary amine improves the solubility of **27**, and the carboxylic acid forms hydrogen bonds with the amide group on **27**. This combination leads to a marginal solubility of the system, thereby forming a hydrogel.

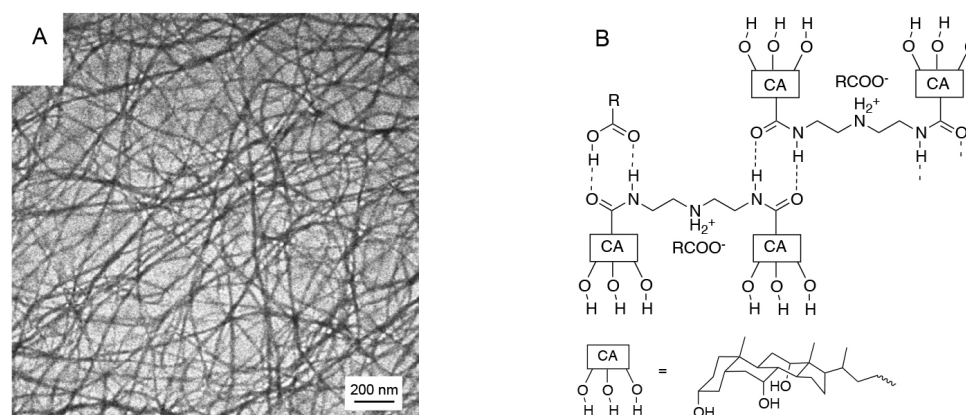


**Figure 2.10** Hydrogels made from **27** with various carboxylic acids. (A) 3-D fibrillar networks of the hydrogel from **27** with tartaric acid (both at 0.6 mM). (B) Schematic presentation of the interactions between **27** and carboxylic acids in hydrogels. (Adapted with permission from ref. 117. Copyright (2016) Royal Society of Chemistry.)

### 2.3.4.3 Bile acid derivatives with tertiary amines

Maitra and co-workers<sup>118-121</sup> reported CA trimer **28** with a tertiary amine as an efficient molecular hydrogelator. This trimer was insoluble in pure water. Protonation with HCl led to the formation of a weak and turbid hydrogel, which could transit to a transparent hydrogel by adding organic solvents such as acetone, ethanol, methanol, and DMSO. Transparent and thermally stable gels were obtained from **28** by interaction with acetic acid in aqueous solutions and the SAFINs in the hydrogels were observed by cryo-TEM (Fig. 2.11). The gelation efficiency of **28** and the thermo-stability of the resulting hydrogels decreased at higher concentrations of acetic acid.<sup>118</sup> The fibrous structure in the

hydrogels was used as a template to induce the formation of metal nanoparticles or nanotubes of metal oxide and sulfate.<sup>122-123</sup> Such a hydrogel may also be used as a reaction vessel to accommodate the photo-dimerization reaction of acenaphthylene.<sup>124</sup>

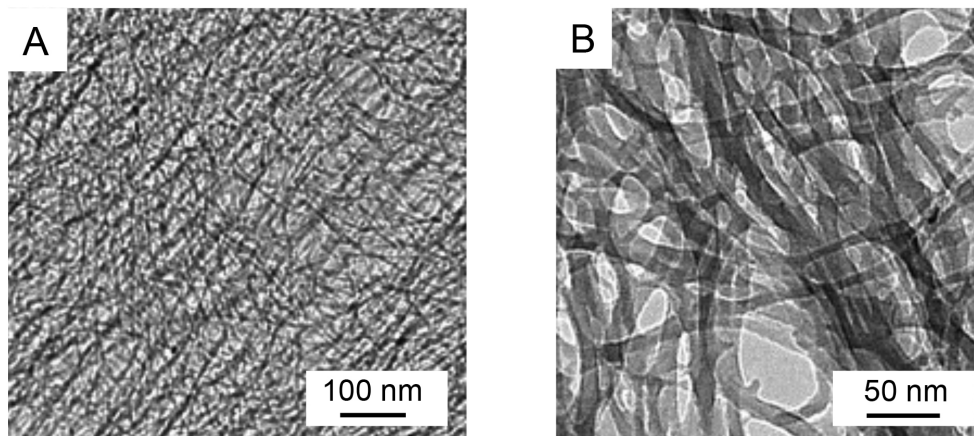


**Figure 2.11** Cryo-TEM image of the hydrogel from **28** (0.75 mM) in water with 20% acetic acid at different magnifications. (Adapted with permission from ref. 118. Copyright (2004) American Chemical Society.)

#### 2.3.4.4 Bile acid derivatives with quaternary ammoniums

Maitra and co-workers<sup>125-128</sup> also synthesized a series of bile acid-based quaternary ammonium iodide salts (**29-36** in Fig. 2.8) that formed hydrogels in pure water or aqueous solutions containing inorganic salt or organic solvents. Compounds **29**, **33**, **35** based on DCA formed hydrogels in pure water, while the **30**, **31**, **32**, **34**, and **36** formed hydrogels through the salting-out effect by addition of inorganic sodium salts such as NaCl, NaBr, and Na<sub>2</sub>SO<sub>4</sub>. The hydrogels formed by compounds **29**, **33**, **34** in NaCl aqueous solutions were found to show optical textures under a polarized optical microscope.<sup>126</sup> Compounds **30**, **32**, **34** formed hydrogels in the presence of organic solvents such as methanol, ethanol, DMF, and DMSO (up to 20%). They showed concentration-dependent aggregation behavior in aqueous solutions with 1 M NaCl, ranging from gels to microcrystals.<sup>128</sup> Compound **31** showed similar gelation behavior.<sup>125</sup> Various factors may affect their gelation behavior. For example, transparent hydrogels were obtained at lower

concentrations of both the gelator and NaCl, but became progressively translucent when the concentration of either increased. The amount of additives may also change the gelation ability of gelators. The minimum gelation concentration (MGC) of the gelators was lower with higher concentration of NaCl. However, gelation did not occur at salt concentrations higher than 4 M. On the other hand, adding organic solvents in the co-solvent system decreased the gelation ability (higher MGC). All these gelators are derivatives of DCA, and similar derivatives of CA and LCA were not able to form hydrogels,<sup>128</sup> indicating the structural importance in the gelation ability.

### 2.3.5 Neutral gelators

Introduction of hydrophilic neutral moieties onto the side chain of bile acids may improve the HLB and promote the formation of molecular hydrogels. A series of bile acid derivatives with neutral side chains are shown in Fig. 2.12.

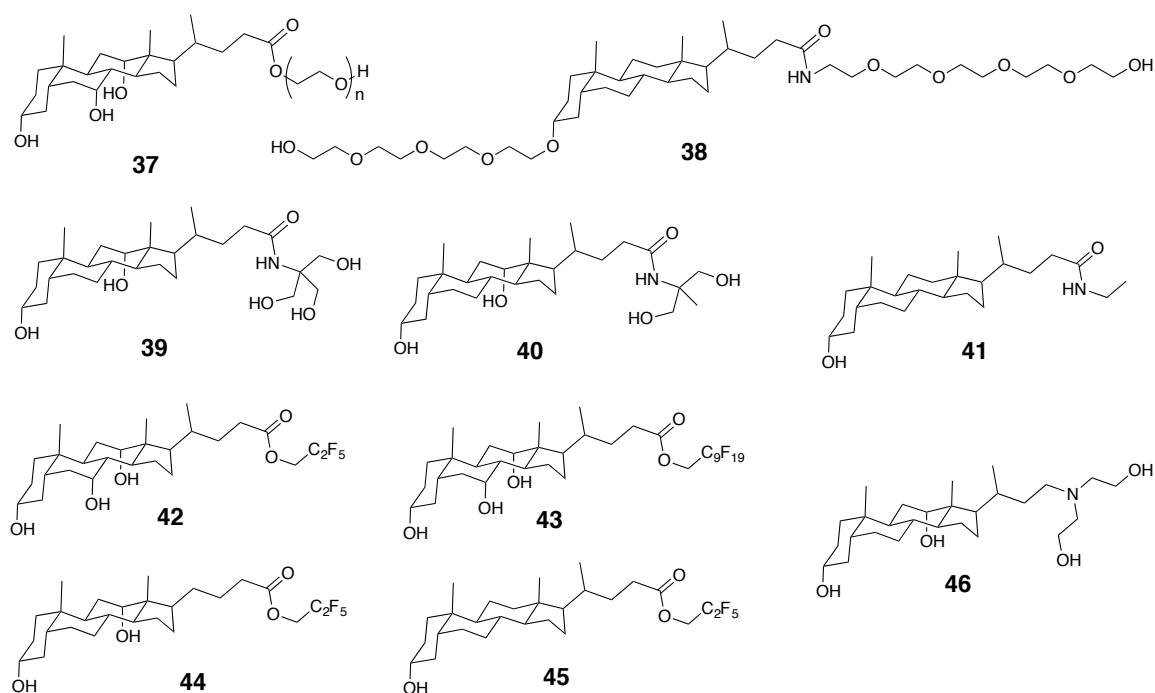


**Figure 2.12** The chemical structures of neutral molecular gelators derived from bile acids.

### 2.3.5.1 Hydrogels in neat water

Modification of bile acids with poly(ethylene glycol) (PEG) may improve their hydrophilicity and promote their self-assembly behavior in aqueous solutions. The hydrogelation of CA esters with PEGs of different lengths (**37**, Fig. 2.12) were studied,<sup>129-130</sup> and only CA esters with three or more ethylene glycol units formed hydrogels.<sup>129</sup> We have synthesized a compound based on LCA and tetra(ethylene glycol) (**38**, Fig. 2.12) via anionic polymerization. In aqueous solutions at high concentrations ( $\geq 10$  wt%), **38** formed cloudy hydrogels with hollow nanotubes (Fig. 2.13).<sup>131-132</sup> Such hydrogels show liquid crystalline behavior. The gelation behavior depended on the chemical structure of the bile acid derivatives, and no hydrogel was obtained from oligo(ethylene glycol) derivatives of CA or DCA.

### 2.3.5.2 Hydrogels in aqueous solutions with organic solvents

Two amide derivatives of DCA bearing hydroxyl groups (**39** and **40**, Fig. 2.12) were reported to be effective gelators in aqueous solutions with certain amounts of water-miscible organic solvents and yielded transparent, stable, and thermo-reversible gel-to-sol transition hydrogels.<sup>125, 133</sup> Head-to-tail molecular arrangement of both bile acid derivatives was found in the fibers from such hydrogels, which is similar to that in the single crystals obtained in non-gelling conditions. Aging of the hydrogels made from **39** and **40** yielded needlelike microcrystals eventually.<sup>133</sup> LCA-ethyl amide (**41**, Fig. 2.12) was reported to form hydrogels in mixtures of water and organic solvents such as acetone (90 vol%), acetonitrile (90 vol%), isopropanol (50 vol%), and methanol (30 vol%).<sup>134</sup> Compound **41** is also an effective organogelator in organic solvents such as benzene, ethyl acetate, and acetone.

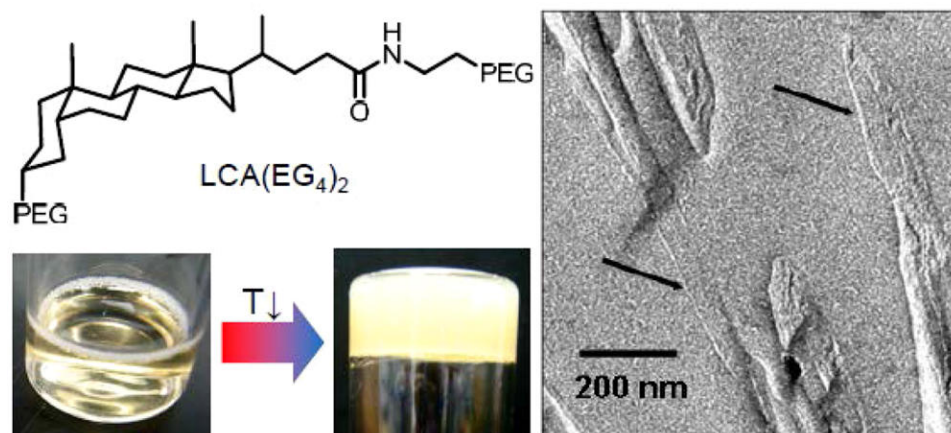


**Figure 2.13** Molecular hydrogels from the pegylated LCA derivative **38** and the fibrils morphology. (Reprinted with permission from ref. 132. Copyright (2013) American Chemical Society.)

Several bile acid esters with perfluoroalkyl side chains (**42-45**, Fig. 2.12) showed effective gelation abilities in aqueous solutions containing organic solvents such as DMSO and DMF.<sup>135</sup> The chemical structures affected the gelation abilities but no general rule could be established. Compounds **42**, **44**, **45** are fluoro-esters ( $C_2F_5$ ) of CA, DCA and LCA, respectively, and showed gelation ability in mixtures of water and organic solvents. Increasing the perfluoroalkyl chain length reduced their gelation abilities, but CA ester with a longer chain ( $C_9F_{19}$ , **43**) was able to form a hydrogel, whereas no gel was obtained from the other bile acids bearing the same group.<sup>135</sup> The ratio of water and organic solvents strongly affected the gelation behavior. For example, the CA ester **42** formed a hydrogel in a water/DMSO system with 50-67 vol% of DMSO, but more DMSO destroyed the gel and yielded a solution. In contrast, the LCA ester **45** formed a gel when DMSO was above 80 vol%, and the compound was insoluble at lower DMSO contents.<sup>135</sup>

Another DCA derivative with two hydroxyl groups and one tertiary amine (**46**, Fig. 2.12) formed hydrogels in aqueous solutions mixed with various organic solvents (DMF, DMSO, methanol, acetonitrile, *etc.*).<sup>136</sup> Hydrogels made of **46** are pH-sensitive and showed acid-instability in contrast to base-stability. The hydrogels transformed into solutions when the amino group was protonated by addition of acidic compounds such as

HI, whereas adding  $\text{NH}_3$  afterwards deprotonated the amino group again to form a hydrogel (Fig. 2.14).

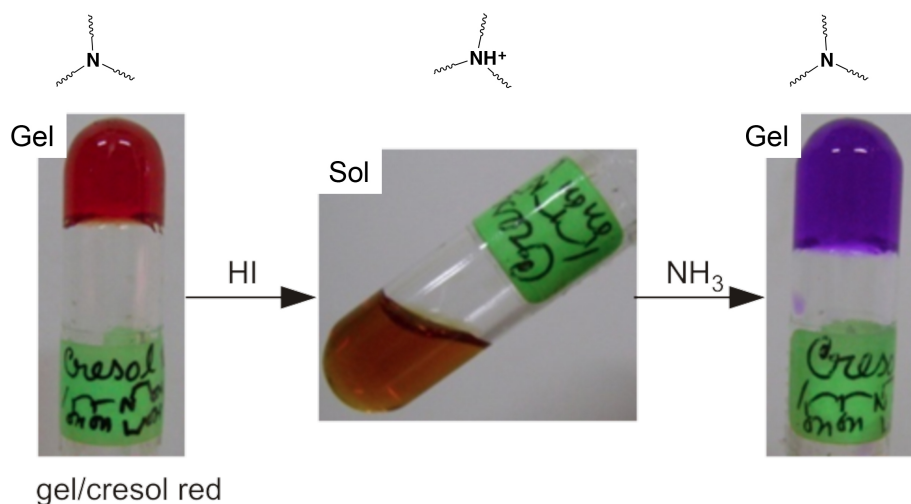


**Figure 2.14** pH-sensitivity of hydrogel from compound **46** in DMSO/ $\text{H}_2\text{O}$  (1/1 by volume). (Adapted with permission from ref. 136. Copyright 2011, Beilstein-Institut.)

### 2.3.6 Two-component hydrogels

The majority of studies on molecular gelators have been carried out with a single compound. Due to the serendipity for the formation of molecular gels, the design of new gelators with a specific range of properties is still a challenge. Therefore, a multi-component molecular gelation system could provide an alternative approach for designing gels by mixing two or more small molecules in specific solvents.<sup>137</sup>

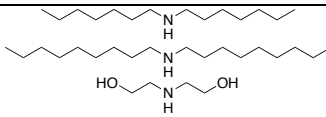
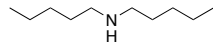
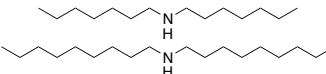
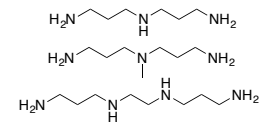
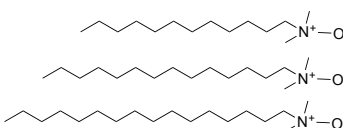
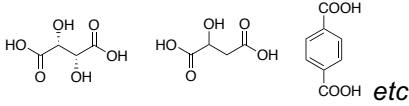
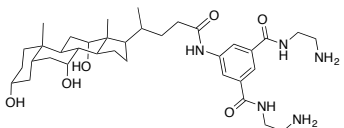
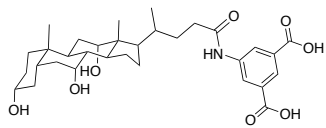
Bile acids have been reported to form two-component molecular hydrogels with certain basic compounds. Dastidar *et al.*<sup>138</sup> reported that some bile acids interacted with specific secondary amines (**47-49**, Table 2.1) to form organic salt and yield hydrogels in a mixture of water and DMSO (1:1, v/v). Gelation behavior of these salts depended on the chemical structure of both bile acids and the secondary amine. For example, CA and UDCA formed hydrogel with dinonylamine, whereas other bile acids did not. Pal *et al.*<sup>139</sup> also reported that LCA interacted with a series of primary diamines to yield hydrogels in water (**50**, Table 2.1), whereas no gelation was observed for other more hydrophilic bile acids such



as CA and DCA. The basicity and hydrogen bonding ability of the amines affected the gelation ability of LCA, and secondary amines or aromatic primary amines were not able to form hydrogels with LCA. The molecular structures of primary amines affected the mechanical properties of hydrogels of LCA. For example, 1,3-propanediamine yielded strong hydrogels with LCA, while 1,2-ethanediamine and 1,4-butanediamine only formed weak hydrogels with LCA under the same conditions. Rheological studies illustrated that the mechanical properties of the hydrogels may be tuned by controlling the ratio of amine to LCA. Higher amine content led to gels with lower values of  $G'$  and yield stress. Song *et al.*<sup>140-141</sup> illustrated the formation of two-component hydrogels from LCA and a series of basic alkylamine oxides (**51**, Table 2.1), which is driven by the balance of multiple hydrogen bonding and hydrophobic–hydrophilic interactions, as well as the steric effect of the LCA molecules. Xerogels prepared by removing the solvent of hydrogels were used to adsorb and remove organic dyes from aqueous solutions,<sup>140</sup> which may be useful in the purification of dye-contaminated water.

Aqueous solutions of bile salts have been used to dissolve and stabilize single-walled carbon nanotubes (SWCNTs).<sup>142-143</sup> However, NaDC at a high concentration (30 wt%) could interact with SWCNTs to form two-component hydrogels without changing pH (**52**, Table 2.1), while no hydrogel was observed from either single component under similar conditions.<sup>144</sup> NaDC may self-assemble to form nanofibers when the concentration is much higher than the CMC, and it also assembled on the surface of SWCNTs via hydrophobic interactions. The nanofibers and assembled SWCNTs interacted with each other to result in stable 3-D networks. Increasing the content of SWCNTs from 1 to 3 wt% increased the  $G'$  of the gel from 100 to  $10^5$  Pa. Such hydrogels showed excellent stretching capability and electrical conductivity, which may be used as conductive soft materials. Another study showed that the interactions between NaDC and graphene oxide (**52**, Table 2.1) yielded hydrogels with interesting dye absorbing capability.<sup>145</sup> A two-component hydrogel based on NaDC with various carboxylic acids (**53**, Table 2.1) such as L-tartaric acid, malic acid, and terephthalic acid was studied.<sup>146</sup> Increasing the concentration of acids could transit the transparent hydrogel to a turbid one. Crystallized nanospheres were formed in the nanofibers in transparent hydrogels after 7 days of equilibration.

**Table 2.1** Two-component hydrogels based on bile acids

Number	Component A	Component B	ref.
47	CA		138
48	DCA		138
49	UDCA		138
50	LCA	 <i>etc.</i>	139
51	LCA		140-141
52	NaDC	SWCNTs or graphene oxide	144-145
53	NaDC	 <i>etc.</i>	146
54			116

A two-component molecular hydrogelation system based on modified CA (**54**, Table 2.1) was developed by di Gregorio *et al.*<sup>116</sup> The CA derivative bearing two carboxylic acid groups (component B of **54**, Table 2.1) dissolved in water to form micelles, while that with diamine (component A of **54**, Table 2.1) self-assembled to form a weak hydrogel (the  $G'$  was less than 1 Pa at a concentration of 5 mM) with fibrous morphology in aqueous solutions. However, interaction between these compounds yielded a hydrogel with improved mechanical properties and  $G'$  higher than 1000 Pa when both species were at 2.5 mM. A stoichiometric 1:1 molar ratio mixture showed the best gelation efficiency,

whereas too much diamine or too much dicarboxylic acid deteriorated the mechanical properties of the hydrogels.

## 2.4. Polymeric supramolecular hydrogels based on bile derivatives

Polymers bearing bile acid moieties can form gels with good mechanical properties when chemically cross-linked.<sup>147-149</sup> A copolymer bearing CA and dopamine was also reported to interact with a synthetic nanosilicate to form a nanocomposite hydrogel.<sup>150</sup> The driving force is the adhesive interaction between the nanosilicate and the dopamine moieties on the surface of self-assembled micelles from the copolymer. Supramolecular interactions of bile acids also led to gel formation. For example, the addition of NaC reduced the sol-gel transition temperature of poly(N-isopropylacrylamide) (PNIPAM) upon heating,<sup>151</sup> due to the emulsifying effect of NaC. The sol-to-gel transition temperature was decreased from 32 to 29 °C in the presence of 16 mM NaC. Copolymers of NIPAM and bile acid-based monomers also formed thermo-reversible hydrogels, and these with higher content of bile acids showed lower sol-to-gel phase transition temperatures.<sup>152-154</sup> The copolymer of NIPAM and CA formed vesicles in aqueous solutions with diameters of a few micrometers, and the water molecules at the exterior of the vesicles served as the intermediate water bridges through hydrogen bonding to link the adjacent vesicles and to promote the formation of hydrogels.<sup>153</sup>

Host-guest interactions also showed to be effective to form hydrogels. Zhao and Stoddart<sup>155</sup> reported a polymeric two-component hydrogelation system from a DCA-modified  $\beta$ -cyclodextrin ( $\beta$ -CD) derivative and an azobenzene-branched poly(acrylic acid) copolymer. In the hydrogel, the *trans*-azobenzene units were accommodated in the hydrophobic cavities of  $\beta$ -CD while the DCA moieties were excluded. The *cis*-azobenzene, which was formed under the irradiation of UV light, could no longer be accommodated in the hydrophobic cavities of  $\beta$ -CD. Consequently, the complex was dissociated and the hydrogel was destroyed (Fig. 2.15A). Our group developed a supramolecular polymer hydrogel system based on CA and  $\beta$ -CD, with both attached as

pendant groups in separate copolymers with *N,N'*-dimethylacrylamide.<sup>156</sup> Both copolymers alone are soluble in water, while mixing their aqueous solutions induced the formation of hydrogels via the host-guest interactions between CA and  $\beta$ -CD (Fig. 2.15B). A rheological study indicated that the mechanical properties of the hydrogels could be altered with different ratios of the two pendants, and the gels showed the highest  $G'$  had a 1:1 molar ratio of CA to  $\beta$ -CD. Such hydrogels are thermo-reversible due to the physical interactions between two copolymers, and show shear-thickening behavior first and shear-thinning properties afterward when the applied shearing stress was raised. Moreover, the gelation systems showed interesting self-healing properties, where the sliced hydrogel recovered within less than 1 minute.<sup>156</sup>

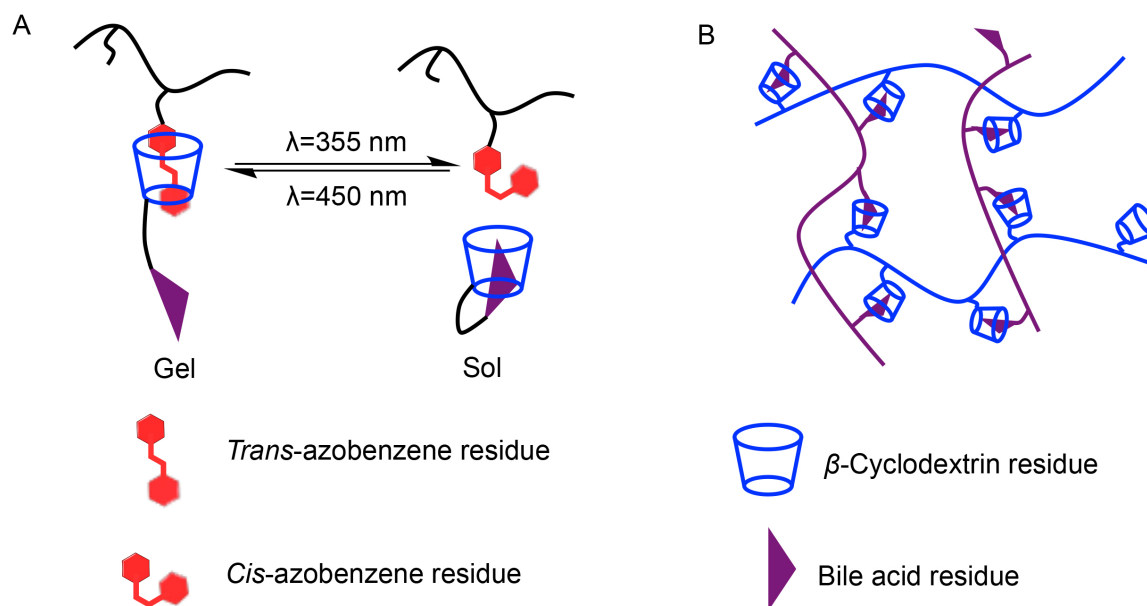


**Figure 2.15** Supramolecular hydrogels from polymers with bile acids. (A) Light responsive hydrogels from DCA- $\beta$ -CD and azobenzene-poly(acrylic acid). (B) Self-healable hydrogels from two polymer chains with CA and  $\beta$ -CD, respectively. (Adapted with permission from ref. 155. and 156. Copyright (2009, 2015) American Chemical Society.)

## 2.5. Conclusions

The unique facial amphiphilicity and biocompatibility of bile acids combined with their commercial availability and relative low cost make them useful and practical building blocks for preparing biomaterials. This review covers the development of supramolecular hydrogels based on bile acids, which may be used in areas such as drug delivery and nanotemplating. These studies mostly focused on the gelation abilities and gel properties. Designing new molecular gelators remains a challenge. Despite these efforts, a “general rule” for illustrating the relationship between the chemical structure and gelation ability has yet to be established, and most of the molecular gelators were reported to be found by serendipity or trial-and-error. In general, the right balance between hydrophobicity and hydrophilicity (HLB)<sup>53</sup> or marginal solubility in water<sup>117</sup> is a prerequisite for a compound to be a molecular hydrogelator. Although the theories of HLB and the packing parameter may potentially help to predict the formation of molecular hydrogels, both models have their limitations and still need to be improved and adapted for more general use. Insoluble compounds in water can be made to be *marginally soluble* by adjusting the pH of the media or the addition of miscible organic solvents. In contrast, soluble compounds can be made to be less soluble or marginal soluble with the help of salting-out effect or other means. The limited or marginal solubility of the species points to the favored direction for the formation of hydrogels. Such a rule may be applicable in the formation of organogels as well. Further understanding of the relationship between chemical structure and capability for the formation of hydrogels, including molecular hydrogels based on bile acids, is needed and will help in the design and synthesis of functional molecular gels targeted for biomedical applications.

## 2.6 Acknowledgements

Financial support from NSERC of Canada and FQRNT of Quebec is gratefully acknowledged. Meng Zhang thanks the Chinese Scholarship Council (CSC) for a scholarship.

## 2.7 References

1. R. G. Weiss; P. Terech. *Molecular Gels: Materials with Self-Assembled Fibrillar Networks*. Springer: Dordrecht, 2006.
2. G. Yu; X. Yan; C. Han; F. Huang. Characterization of Supramolecular Gels. *Chem. Soc. Rev.* **2013**, *42*, 6697-6722.
3. B. Escuder; J. F. Miravet. *Functional Molecular Gels*. Escuder, B.; Miravet, J. F. Eds.; Royal Society of Chemistry: Cambridge, 2014.
4. T. R. Hoare; D. S. Kohane. Hydrogels in Drug Delivery: Progress and Challenges. *Polymer* **2008**, *49*, 1993-2007.
5. P. K. Vemula; N. Wiradharma; J. A. Ankrum; O. R. Miranda; G. John; J. M. Karp. Prodrugs as Self-Assembled Hydrogels: A New Paradigm for Biomaterials. *Curr. Opin. Biotechnol.* **2013**, *24*, 1174-1182.
6. H. Storrie; M. O. Guler; S. N. Abu-Amara; T. Volberg; M. Rao; B. Geiger; S. I. Stupp. Supramolecular Crafting of Cell Adhesion. *Biomaterials* **2007**, *28*, 4608-4618.
7. C. Yang; D. Li; Z. Liu; G. Hong; J. Zhang; D. Kong; Z. Yang. Responsive Small Molecular Hydrogels Based on Adamantane-Peptides for Cell Culture. *J. Phys. Chem. B* **2012**, *116*, 633-638.
8. Z. Yang; H. Gu; Y. Zhang; L. Wang; B. Xu. Small Molecule Hydrogels Based on a Class of Antiinflammatory Agents. *Chem. Commun.* **2004**, 208-209.
9. D. Buenger; F. Topuz; J. Groll. Hydrogels in Sensing Applications. *Prog. Polym. Sci.* **2012**, *37*, 1678-1719.
10. S. Bhuniya; B. H. Kim. An Insulin-Sensing Sugar-Based Fluorescent Hydrogel. *Chem. Commun.* **2006**, 1842-1844.
11. A. Patwa; J. Labille; J. Y. Bottero; A. Thiery; P. Barthelemy. Decontamination of Nanoparticles from Aqueous Samples Using Supramolecular Gels. *Chem. Commun.* **2015**, *51*, 2547-2550.
12. G. Nystrom; M. P. Fernandez-Ronco; S. Bolisetty; M. Mazzotti; R. Mezzenga. Amyloid Templated Gold Aerogels. *Adv. Mater.* **2016**, *28*, 472-478.
13. N. M. Sangeetha; U. Maitra. Supramolecular Gels: Functions and Uses. *Chem. Soc. Rev.* **2005**, *34*, 821-836.

14. D. J. Abdallah; R. G. Weiss. Organogels and Low Molecular Mass Organic Gelators. *Adv. Mater.* **2000**, *12*, 1237-1247.
15. X. Du; J. Zhou; J. Shi; B. Xu. Supramolecular Hydrogelators and Hydrogels: From Soft Matter to Molecular Biomaterials. *Chem. Rev.* **2015**, *115*, 13165-13307.
16. P. Terech; R. G. Weiss. Low Molecular Mass Gelators of Organic Liquids and the Properties of Their Gels. *Chem. Rev.* **1997**, *97*, 3133-3160.
17. R. G. Weiss. The Past, Present, and Future of Molecular Gels. What Is the Status of the Field, and Where Is It Going? *J. Am. Chem. Soc.* **2014**, *136*, 7519-7530.
18. K. Araki; I. Yoshikawa. Nucleobase-Containing Gelators. *Top. Curr. Chem.* **2005**, *256*, 133-165.
19. A. Dasgupta; J. H. Mondal; D. Das. Peptide Hydrogels. *RSC Adv.* **2013**, *3*, 9117-9149.
20. S. Datta; S. Bhattacharya. Multifarious Facets of Sugar-Derived Molecular Gels: Molecular Features, Mechanisms of Self-Assembly and Emerging Applications. *Chem. Soc. Rev.* **2015**, *44*, 5596-5637.
21. M. Zinic; F. Vogtle; F. Fages. Cholesterol-Based Gelators. *Top. Curr. Chem.* **2005**, *256*, 39-76.
22. P. Babu; N. M. Sangeetha; U. Maitra. Supramolecular Chemistry of Bile Acid Derivatives: Formation of Gels. *Macromol. Symp.* **2006**, *241*, 60-67.
23. S. Mukhopadhyay; U. Maitra. Chemistry and Biology of Bile Acids. *Curr. Sci.* **2004**, *87*, 1666-1683.
24. J. Zhang; X. Zhu. Biomaterials Made of Bile Acids. *Sci. China Ser. B-Chem.* **2009**, *52*, 849-861.
25. J. Zhang; J. Luo; X. X. Zhu; M. J. Junk; D. Hinderberger. Molecular Pockets Derived from Cholic Acid as Chemosensors for Metal Ions. *Langmuir* **2010**, *26*, 2958-2962.
26. V. Janout; M. Lanier; S. L. Regen. Molecular Umbrellas. *J. Am. Chem. Soc.* **1996**, *118*, 1573-1574.
27. J. Luo; Y. Chen; X. X. Zhu. Invertible Amphiphilic Molecular Pockets Made of Cholic Acid. *Langmuir* **2009**, *25*, 10913-10917.
28. Y. Zhao; Z. Zhong. Oligomeric Cholates: Amphiphilic Foldamers with Nanometer-Sized Hydrophilic Cavities. *J. Am. Chem. Soc.* **2005**, *127*, 17894-17901.

29. Y. Zhao; H. Cho; L. Widanapathirana; S. Zhang. Conformationally Controlled Oligocholate Membrane Transporters: Learning through Water Play. *Acc. Chem. Res.* **2013**, *46*, 2763-2772.
30. M. A. Gauthier; Z. Zhang; X. X. Zhu. New Dental Composites Containing Multimethacrylate Derivatives of Bile Acids: A Comparative Study with Commercial Monomers. *ACS Appl. Mater. Interfaces* **2009**, *1*, 824-832.
31. M. A. Gauthier; P. Simard; Z. Zhang; X. X. Zhu. Bile Acids as Constituents for Dental Composites: In Vitro Cytotoxicity of (Meth)Acrylate and Other Ester Derivatives of Bile Acids. *J. R. Soc. Interface* **2007**, *4*, 1145-1150.
32. H. Svobodová; V. Nojonen; E. Kolehmainen; E. Sievanen. Recent Advances in Steroidal Supramolecular Gels. *RSC Adv.* **2012**, *2*, 4985-5007.
33. H. Zhang; J. Peng; K. Liu; Y. Fang. Supramolecular Gels of Cholic Acids and Their Derivatives. *Prog. Chem.* **2011**, *23*, 1591-1597.
34. C. Yan; M. E. Mackay; K. Czymmek; R. P. Nagarkar; J. P. Schneider; D. J. Pochan. Injectable Solid Peptide Hydrogel as a Cell Carrier: Effects of Shear Flow on Hydrogels and Cell Payload. *Langmuir* **2012**, *28*, 6076-6087.
35. W. T. Truong; L. Lewis; P. Thordarson, Biomedical Applications of Molecular Gels. In *Functional Molecular Gels*, Escuder, B.; Miravet, J. F., Eds. Royal Society of Chemistry: Cambridge, 2014; pp 157-194.
36. E. A. Appel; M. W. Tibbitt; M. J. Webber; B. A. Mattix; O. Veiseh; R. Langer. Self-Assembled Hydrogels Utilizing Polymer-Nanoparticle Interactions. *Nat. Commun.* **2015**, *6*, 6295.
37. L. Yu; J. Ding. Injectable Hydrogels as Unique Biomedical Materials. *Chem. Soc. Rev.* **2008**, *37*, 1473-1481.
38. A. Fini; A. Roda; R. Fugazza; B. Grigolo. Chemical Properties of Bile Acids: III. Bile Acid Structure and Solubility in Water. *J. Solution Chem.* **1985**, *14*, 595-603.
39. H. Amenitsch; H. Edlund; A. Khan; E. F. Marques; C. La Mesa. Bile Salts Form Lyotropic Liquid Crystals. *Colloids Surf. A Physicochem. Eng. Asp.* **2003**, *213*, 79-92.
40. S. Gouin; X. X. Zhu. Fluorescence and NMR Studies of the Effect of a Bile Acid Dimer on the Micellization of Bile Salts. *Langmuir* **1998**, *14*, 4025-4029.



41. A. Roda; A. F. Hofmann; K. J. Mysels. The Influence of Bile Salt Structure on Self-Association in Aqueous Solutions. *J. Biol. Chem.* **1983**, *258*, 6362-6370.
42. L. Galantini; M. C. di Gregorio; M. Gubitosi; L. Travaglini; J. V. Tato; A. Jover; F. Meijide; V. H. Soto Tellini; N. V. Pavel. Bile Salts and Derivatives: Rigid Unconventional Amphiphiles as Dispersants, Carriers and Superstructure Building Blocks. *Curr. Opin. Colloid Interface Sci.* **2015**, *20*, 170-182.
43. A. V. Verde; D. Frenkel. Simulation Study of Micelle Formation by Bile Salts. *Soft Matter* **2010**, *6*, 3815-3825.
44. K. Matsuoka; M. Suzuki; C. Honda; K. Endo; Y. Moroi. Micellization of Conjugated Chenodeoxy- and Ursodeoxycholates and Solubilization of Cholesterol into Their Micelles: Comparison with Other Four Conjugated Bile Salts Species. *Chem. Phys. Lipids* **2006**, *139*, 1-10.
45. A. Jover; F. Meijide; E. Rodríguez Núñez; J. Vázquez Tato. Aggregation Kinetics of Sodium Deoxycholate in Aqueous Solution. *Langmuir* **1998**, *14*, 4359-4363.
46. P. Schurtenberger; N. Mazer; W. Kaenzig. Static and Dynamic Light Scattering Studies of Micellar Growth and Interactions in Bile Salt Solutions. *J. Phys. Chem.* **1983**, *87*, 308-315.
47. D. Madenci; S. U. Egelhaaf. Self-Assembly in Aqueous Bile Salt Solutions. *Curr. Opin. Colloid Interface Sci.* **2010**, *15*, 109-115.
48. D. M. Small; S. A. Penkett; D. Chapman. Studies on Simple and Mixed Bile Salt Micelles by Nuclear Magnetic Resonance Spectroscopy. *Biochim. Biophys. Acta* **1969**, *176*, 178-189.
49. E. F. Marques; H. Edlund; C. La Mesa; A. Khan. Liquid Crystals and Phase Equilibria Binary Bile Salt-Water Systems. *Langmuir* **2000**, *16*, 5178-5186.
50. H. Edlund; A. Khan; C. La Mesa. Formation of a Liquid Crystalline Phase in the Water–Sodium Taurodeoxycholate System. *Langmuir* **1998**, *14*, 3691-3697.
51. K. Tamhane. Formation of Lyotropic Liquid Crystals Through the Self-Assembly of Bile acid Building Blocks. University of Central Florida, 2009.
52. K. Fan; L. Niu; J. Li; R. Feng; R. Qu; T. Liu; J. Song. Application of Solubility Theory in Bi-Component Hydrogels of Melamine with Di(2-ethylhexyl) Phosphoric Acid. *Soft Matter* **2013**, *9*, 3057.

53. L. A. Estroff; A. D. Hamilton. Water Gelation by Small Organic Molecules. *Chem. Rev.* **2004**, *104*, 1201-1218.
54. T. Kar; S. Debnath; D. Das; A. Shome; P. K. Das. Organogelation and Hydrogelation of Low-Molecular-Weight Amphiphilic Dipeptides: pH Responsiveness in Phase-Selective Gelation and Dye Removal. *Langmuir* **2009**, *25*, 8639-8648.
55. S. Dutta; T. Kar; D. Mandal; P. K. Das. Structure and Properties of Cholesterol-Based Hydrogelators with Varying Hydrophilic Terminals: Biocompatibility and Development of Antibacterial Soft Nanocomposites. *Langmuir* **2013**, *29*, 316-327.
56. W. C. Griffin. Classification of Surface-active agents by "HLB". *J. Cosmet. Sci.* **1949**, *1*, 311-326.
57. W. C. Griffin. Calculation of HLB values of Non-ionic surfactants. *J. Soc. Cosmet. Chem.* **1954**, *5*, 249-256.
58. J. T. Davies In *A Quantitative Kinetic Theory of Emulsion Type, I. Physical Chemistry of the Emulsifying Agent*, Gas/Liquid and Liquid/Liquid Interface. Proceedings of the International Congress of Surface Activity, 1957; pp 426-438.
59. J. N. Israelachvili; D. J. Mitchell; B. W. Ninham. Theory of Self-Assembly of Hydrocarbon Amphiphiles into Micelles and Bilayers. *J. Chem. Soc., Faraday Trans. 2* **1976**, *72*, 1525-1568.
60. J. N. Israelachvili. *Intermolecular and Surface Forces*. Academic Press: London, 1991.
61. V. V. Kumar. Complementary Molecular Shapes and Additivity of the Packing Parameter of Lipids. *Proc. Natl. Acad. Sci. U. S. A.* **1991**, *88*, 444-448.
62. R. Nagarajan. Molecular Packing Parameter and Surfactant Self-Assembly: The Neglected Role of the Surfactant Tail. *Langmuir* **2002**, *18*, 31-38.
63. Z. Chu; C. A. Dreiss; Y. Feng. Smart Wormlike Micelles. *Chem. Soc. Rev.* **2013**, *42*, 7174-7203.
64. M. Antonietti; S. Förster. Vesicles and Liposomes: A Self-Assembly Principle Beyond Lipids. *Adv. Mater.* **2003**, *15*, 1323-1333.
65. R. Oda, SAFIN Gels with Amphiphilic Molecules. In *Molecular Gels: Materials with Self-Assembled Fibrillar Networks*, Weiss, R. G.; Terech, P., Eds. Springer: Dordrecht, 2006; pp 577-612.

66. T. Kunitake; Y. Okahata; M. Shimomura; S. Yasunami; K. Takarabe. Formation of Stable Bilayer Assemblies in Water from Single-Chain Amphiphiles. Relationship between the Amphiphile Structure and the Aggregate Morphology. *J. Am. Chem. Soc.* **1981**, *103*, 5401-5413.
67. P. Terech; N. M. Sangeetha; S. Bhat; J.-J. Allegraud; E. Buhler. Ammonium Lithocholate Nanotubes: Stability and Copper Metallization. *Soft Matter* **2006**, *2*, 517-522.
68. P. Terech; S. Friol; N. Sangeetha; Y. Talmon; U. Maitra. Self-Assembled Nanoribbons and Nanotubes in Water: Energetic vs Entropic Networks. *Rheol. Acta* **2005**, *45*, 435-443.
69. B. Jean; L. Oss-Ronen; P. Terech; Y. Talmon. Monodisperse Bile-Salt Nanotubes in Water: Kinetics of Formation. *Adv. Mater.* **2005**, *17*, 728-731.
70. P. Terech; Y. Talmon. Aqueous Suspensions of Steroid Nanotubules: Structural and Rheological Characterizations. *Langmuir* **2002**, *18*, 7240-7244.
71. P. Terech; A. de Geyer; B. Struth; Y. Talmon. Self-Assembled Monodisperse Steroid Nanotubes in Water. *Adv. Mater.* **2002**, *14*, 495-498.
72. Y. Qiao; Y. Lin; Z. Yang; H. Chen; S. Zhang; Y. Yan; J. Huang. Unique Temperature-Dependent Supramolecular Self-Assembly: From Hierarchical 1D Nanostructures to Super Hydrogel. *J. Phys. Chem. B* **2010**, *114*, 11725-11730.
73. X. Zhan; K. Tamhane; T. Bera; J. Fang. Transcription of pH-Sensitive Supramolecular Assemblies into Silica: From Straight, Coiled, and Helical Tubes to Single and Double Fan-Like Bundles. *J. Mater. Chem.* **2011**, *21*, 13973.
74. X. Zhang; M. Mathew; A. J. Gesquiere; J. Fang. Fluorescent Composite Tubes with pH-Controlled Shapes. *J. Mater. Chem.* **2010**, *20*, 3716-3721.
75. X. Zhang; J. Fang. Assembly of Vesicles into Fractal and Prong Patterns on Substrates. *Soft Matter* **2010**, *6*, 2139-2142.
76. K. Tamhane; X. Zhang; J. Zou; J. Fang. Assembly and Disassembly of Tubular Spherulites. *Soft Matter* **2010**, *6*, 1224.
77. E. K. Hobbie; J. A. Fagan; M. L. Becker; S. D. Hudson; N. Fakhri; M. Pasquali. Self-Assembly of Ordered Nanowires in Biological Suspensions of Single-Wall Carbon Nanotubes. *ACS Nano* **2009**, *3*, 189-196.

78. Y. V. Zastavker; N. Asherie; A. Lomakin; J. Pande; J. M. Donovan; J. M. Schnur; G. B. Benedek. Self-Assembly of Helical Ribbons. *Proc. Natl. Acad. Sci. U. S. A.* **1999**, *96*, 7883-7887.
79. D. S. Chung; G. B. Benedek; F. M. Konikoff; J. M. Donovan. Elastic Free-Energy of Anisotropic Helical Ribbons as Metastable Intermediates in the Crystallization of Cholesterol. *Proc. Natl. Acad. Sci. U. S. A.* **1993**, *90*, 11341-11345.
80. S. B. Schryver. Some Investigations on the Phenomena of "Clot" Formations. Part I.-On the Clotting of Milk. *Proc. R. Soc. B* **1913**, *86*, 460-481.
81. S. B. Schryver. Investigations Dealing with the Phenomena of "Clot" Formations. Part II.-The Formation of a Gel from Cholate Solutions having Many Properties Analogous to those of Cell Membranes. *Proc. R. Soc. B* **1914**, *87*, 366-374.
82. S. B. Schryver. Investigations Dealing with the Phenomena of Clot Formations. Part III.--Further Investigations of the Cholate Gel. *Proc. R. Soc. B* **1916**, *89*, 176-183.
83. A. Chakrabarty; U. Maitra; A. D. Das. Metal Cholate Hydrogels: Versatile Supramolecular Systems for Nanoparticle Embedded Soft Hybrid Materials. *J. Mater. Chem.* **2012**, *22*, 18268-18274.
84. Y. Qiao; Y. Lin; Y. Wang; Z. Yang; J. Liu; J. Zhou; Y. Yan; J. Huang. Metal-Driven Hierarchical Self-Assembled One-Dimensional Nanohelices. *Nano Lett.* **2009**, *9*, 4500-4504.
85. J. Shen; Y. Chen; J. Huang; J. Chen; C. Zhao; Y. Zheng; T. Yu; Y. Yang; H. Zhang. Supramolecular Hydrogels for Creating Gold and Silver Nanoparticles in Situ. *Soft Matter* **2013**, *9*, 2017-2023.
86. S. Banerjee; R. Kandanelli; S. Bhowmik; U. Maitra. Self-Organization of Multiple Components in a Steroidal Hydrogel Matrix: Design, Construction and Studies on Novel Tunable Luminescent Gels and Xerogels. *Soft Matter* **2011**, *7*, 8207-8215.
87. S. Bhowmik; S. Banerjee; U. Maitra. A Self-Assembled, Luminescent Europium Cholate Hydrogel: A Novel Approach Towards Lanthanide Sensitization. *Chem. Commun.* **2010**, *46*, 8642-8644.
88. Y. Wang; X. Xin; W. Li; C. Jia; L. Wang; J. Shen; G. Xu. Studies on the Gel Behavior and Luminescence Properties of Biological Surfactant Sodium Deoxycholate/Rare-Earth Salts Mixed Systems. *J. Colloid Interface Sci.* **2014**, *431*, 82-89.

89. R. Laishram; S. Bhowmik; U. Maitra. White Light Emitting Soft Materials from Off-the-Shelf Ingredients. *J. Mater. Chem. C* **2015**, *3*, 5885-5889.
90. V. Noponen; K. Toikkanen; E. Kalenius; R. Kuosmanen; H. Salo; E. Sievanen. Stimuli-Responsive Bile Acid-Based Metallogels Forming in Aqueous Media. *Steroids* **2015**, *97*, 54-61.
91. M. Dukh; D. Šaman; J. Kroulík; I. Černý; V. Pouzar; V. Král; P. Drašar. Metal Coordination as a Tool for Controlling the Self-Assembling and Gelation Properties of Novel Type Cholic Amide–Phenanthroline Gelating Agent. *Tetrahedron* **2003**, *59*, 4069-4076.
92. M. Maity; U. Maitra. An Easily Prepared Palladium-Hydrogel Nanocomposite Catalyst for C–C Coupling Reactions. *J. Mater. Chem. A* **2014**, *2*, 18952-18958.
93. J. S. Shen; Y. L. Chen; Q. P. Wang; T. Yu; X. Y. Huang; Y. Yang; H. W. Zhang. In Situ Synthesis of Red Emissive Copper Nanoclusters in Supramolecular Hydrogels. *J. Mater. Chem. C* **2013**, *1*, 2092-2096.
94. J.-S. Shen; Y.-L. Chen; Q.-P. Wang; T. Yu; X.-Y. Huang; Y. Yang; H.-W. Zhang. In Situ Synthesis of Red Emissive Copper Nanoclusters in Supramolecular Hydrogels. *J. Mater. Chem. C* **2013**, *1*, 2092-2096.
95. H. Sobotka; N. Czechowiczka. The Gelation of Bile Salt Solutions. *J. Colloid Sci.* **1958**, *13*, 188-191.
96. A. Jover; F. Mejjide; E. R. Nunez; J. V. Tato. Dynamic Rheology of Sodium Deoxycholate Gels. *Langmuir* **2002**, *18*, 987-991.
97. A. Jover; F. Mejjide; E. R. Nunez; J. V. Tato; M. Mosquera; F. R. Prieto. Unusual Pyrene Excimer Formation During Sodium Deoxycholate Gelation. *Langmuir* **1996**, *12*, 1789-1793.
98. D. M. Blow; A. Rich. Studies on the Formation of Helical Deoxycholate Complexes. *J. Am. Chem. Soc.* **1960**, *82*, 3566-3571.
99. A. Rich; D. M. Blow. Formation of a Helical Steroid Complex. *Nature* **1958**, *182*, 423-426.
100. Y. Zhang; X. Xin; J. Shen; W. Tang; Y. Ren; L. Wang. Biodegradable, Multiple Stimuli-Responsive Sodium Deoxycholate–Amino Acids–NaCl Mixed Systems for Dye Delivery. *RSC Adv.* **2014**, *4*, 62262-62271.

101. X. Sun; X. Xin; N. Tang; L. Guo; L. Wang; G. Xu. Manipulation of the Gel Behavior of Biological Surfactant Sodium Deoxycholate by Amino Acids. *J. Phys. Chem. B* **2014**, *118*, 824-832.
102. X. Sun; Z. Du; E. Li; X. Xin; N. Tang; L. Wang; J. Yuan. Rheological Properties of the Gels of Biological Surfactant Sodium Deoxycholate/Amino Acids/Halide Salts Systems. *Colloids Surf. A Physicochem. Eng. Asp.* **2014**, *457*, 345-353.
103. K. E. McNeel; S. Das; N. Siraj; Negulescu, II; I. M. Warner. Sodium Deoxycholate Hydrogels: Effects of Modifications on Gelation, Drug Release, and Nanotemplating. *J. Phys. Chem. B* **2015**, *119*, 8651-8659.
104. S. Das; S. L. de Rooy; A. N. Jordan; L. Chandler; Negulescu, II; B. El-Zahab; I. M. Warner. Tunable Size and Spectral Properties of Fluorescent NanoGUMBOS in Modified Sodium Deoxycholate Hydrogels. *Langmuir* **2012**, *28*, 757-765.
105. C. Valenta; E. Nowack; A. Bernkop-Schnurch. Deoxycholate-Hydrogels: Novel Drug Carrier Systems for Topical Use. *Int. J. Pharm.* **1999**, *185*, 103-111.
106. W. Liang; J. R. Guman-Sepulveda; S. He; A. Dogariu; J. Y. Fang. Microrheology and Release Behaviors of Self-Assembled Steroid Hydrogels. *J. Mater. Sci. Chem. Eng.* **2015**, *03*, 6-15.
107. V. H. Soto Tellini; A. Jover; F. Meijide; J. V. Tato; L. Galantini; N. V. Pavel. Supramolecular Structures Generated by a p-Tert-Butylphenyl-Amide Derivative of Cholic Acid: From Vesicles to Molecular Tubes. *Adv. Mater.* **2007**, *19*, 1752-1756.
108. L. Galantini; C. Leggio; A. Jover; F. Meijide; N. V. Pavel; V. H. Soto Tellini; J. V. Tato; R. Di Leonardo; G. Ruocco. Kinetics of Formation of Supramolecular Tubules of a Sodium Cholate Derivative. *Soft Matter* **2009**, *5*, 3018.
109. M. Gubitosi; L. Travaglini; A. D'Annibale; N. V. Pavel; J. Vazquez Tato; M. Obiols-Rabasa; S. Sennato; U. Olsson; K. Schillen; L. Galantini. Sugar-Bile Acid-Based Bolaamphiphiles: From Scrolls to Monodisperse Single-Walled Tubules. *Langmuir* **2014**, *30*, 6358-6366.
110. M. Maity; V. S. Sajisha; U. Maitra. Hydrogelation of Bile Acid–Peptide Conjugates and in Situ Synthesis of Silver and Gold Nanoparticles in the Hydrogel Matrix. *RSC Adv.* **2015**, *5*, 90712-90719.

111. U. Maitra; P. Babu. First Synthesis of Phosphonobile Acids and Preliminary Studies on Their Aggregation Properties. *Steroids* **2003**, *68*, 459-463.
112. P. Babu; U. Maitra. Synthesis and in Vitro Cholesterol Dissolution by 23- and 24-Phosphonobile Acids. *Steroids* **2005**, *70*, 681-689.
113. P. Babu; D. Chopra; T. N. Row; U. Maitra. Micellar Aggregates and Hydrogels from Phosphonobile Salts. *Org. Biomol. Chem.* **2005**, *3*, 3695-3700.
114. L. Travaglini; A. D'Annibale; K. Schillen; U. Olsson; S. Sennato; N. V. Pavel; L. Galantini. Amino Acid-Bile Acid Based Molecules: Extremely Narrow Surfactant Nanotubes Formed by a Phenylalanine-Substituted Cholic Acid. *Chem. Commun.* **2012**, *48*, 12011-12013.
115. L. Travaglini; A. D'Annibale; M. C. di Gregorio; K. Schillen; U. Olsson; S. Sennato; N. V. Pavel; L. Galantini. Between Peptides and Bile Acids: Self-Assembly of Phenylalanine Substituted Cholic Acids. *J. Phys. Chem. B* **2013**, *117*, 9248-9257.
116. M. C. di Gregorio; N. V. Pavel; J. Miragaya; A. Jover; F. Meijide; J. Vazquez Tato; V. H. Tellini; L. Galantini. Catanionic Gels Based on Cholic Acid Derivatives. *Langmuir* **2013**, *29*, 12342-12351.
117. M. Zhang; K. C. Waldron; X. X. Zhu. Formation of Molecular Hydrogels from a Bile Acid Derivative and Selected Carboxylic Acids. *RSC Adv.* **2016**, *6*, 35436-35440.
118. S. Mukhopadhyay; U. Maitra; I. Ira; G. Krishnamoorthy; J. Schmidt; Y. Talmon. Structure and Dynamics of a Molecular Hydrogel Derived from a Tripodal Cholamide. *J. Am. Chem. Soc.* **2004**, *126*, 15905-15914.
119. P. Terech; U. Maitra. Structural and Rheological Properties of Aqueous Viscoelastic Solutions and Gels of Tripodal Cholamide-Based Self-Assembled Supramolecules. *J. Phys. Chem. B* **2008**, *112*, 13483-13492.
120. U. Maitra; S. Mukhopadhyay; A. Sarkar; P. Rao; S. S. Indi. Hydrophobic Pockets in a Nonpolymeric Aqueous Gel: Observation of Such a Gelation Process by Color Change. *Angew. Chem. Int. Ed. Engl.* **2001**, *40*, 2281-2283.
121. S. Mukhopadhyay; Ira; G. Krishnamoorthy; U. Maitra. Dynamics of Bound Dyes in a Nonpolymeric Aqueous Gel Derived from a Tripodal Bile Salt. *J. Phys. Chem. B* **2003**, *107*, 2189-2192.

122. S. Bhat; U. Maitra. Nanoparticle-Gel Hybrid Material Designed with Bile Acid Analogues. *Chem. Mater.* **2006**, *18*, 4224-4226.
123. G. Gundiah; S. Mukhopadhyay; U. G. Tumkurkar; A. Govindaraj; U. Maitra; C. N. R. Rao. Hydrogel Route to Nanotubes of Metal Oxides and Sulfates. *J. Mater. Chem.* **2003**, *13*, 2118-2122.
124. S. Bhat; U. Maitra. Hydrogels as Reaction Vessels: Acenaphthylene Dimerization in Hydrogels Derived from Bile Acid Analogues. *Molecules* **2007**, *12*, 2181-2189.
125. N. M. Sangeetha; R. Balasubramanian; U. Maitra; S. Ghosh; A. R. Raju. Novel Cationic and Neutral Analogues of Bile Acids: Synthesis and Preliminary Study of Their Aggregation Properties. *Langmuir* **2002**, *18*, 7154-7157.
126. N. M. Sangeetha; S. Bhat; A. R. Choudhury; U. Maitra; P. Terech. Properties of Hydrogels Derived from Cationic Analogues of Bile Acid: Remarkably Distinct Flowing Characteristics. *J. Phys. Chem. B* **2004**, *108*, 16056-16063.
127. P. Terech; N. M. Sangeetha; B. Deme; U. Maitra. Self-Assembled Networks of Ribbons in Molecular Hydrogels of Cationic Deoxycholic Acid Analogues. *J. Phys. Chem. B* **2005**, *109*, 12270-12276.
128. S. Bhat; U. Maitra. Low Molecular Mass Cationic Gelators Derived from Deoxycholic Acid: Remarkable Gelation of Aqueous Solvents. *Tetrahedron* **2007**, *63*, 7309-7320.
129. X. Wang; Y. Lu; Y. Duan; L. Meng; C. Li. Helical Crystals with a Sixfold Screw Axis. *Adv. Mater.* **2008**, *20*, 462-465.
130. J. Zhang; X. Wang; B. Zhao; C. Li. Facile Synthesis of Narrowly Dispersed Silver Nanoparticles in Hydrogel. *Chem. Lett.* **2006**, *35*, 40-41.
131. S. Strandman; F. Le Devedec; X. X. Zhu. Thermosensitivity of Bile Acid-Based Oligo(Ethylene Glycol) Stars in Aqueous Solutions. *Macromol. Rapid Commun.* **2011**, *32*, 1185-1189.
132. S. Strandman; F. Le Devedec; X. X. Zhu. Self-Assembly of Bile Acid-PEG Conjugates in Aqueous Solutions. *J. Phys. Chem. B* **2013**, *117*, 252-258.
133. P. Terech; N. M. Sangeetha; U. Maitra. Molecular Hydrogels from Bile Acid Analogues with Neutral Side Chains: Network Architectures and Viscoelastic Properties.



Junction Zones, Spherulites, and Crystallites: Phenomenological Aspects of the Gel Metastability. *J. Phys. Chem. B* **2006**, *110*, 15224-15233.

134. R. Kuosmanen; R. Puttreddy; R. M. Willman; I. Aijalainen; A. Galandakova; J. Ulrichova; H. Salo; K. Rissanen; E. Sievanen. Biocompatible Hydrogelators Based on Bile Acid Ethyl Amides. *Steroids* **2016**, *108*, 7-16.

135. S. Banerjee; V. M. Vidya; A. J. Savyasachi; U. Maitra. Perfluoroalkyl Bile Esters: A New Class of Efficient Gelators of Organic and Aqueous–Organic Media. *J. Mater. Chem.* **2011**, *21*, 14693.

136. U. Maitra; A. Chakrabarty. Protonation and Deprotonation Induced Organo/Hydrogelation: Bile Acid Derived Gelators Containing a Basic Side Chain. *Beilstein J. Org. Chem.* **2011**, *7*, 304-309.

137. J. Raeburn; D. J. Adams. Multicomponent Low Molecular Weight Gelators. *Chem. Commun.* **2015**, *51*, 5170-5180.

138. P. Dastidar; S. Okabe; K. Nakano; K. Iida; M. Miyata; N. Tohnai; M. Shibayama. Facile Syntheses of a Class of Supramolecular Gelator Following a Combinatorial Library Approach: Dynamic Light Scattering and Small-Angle Neutron Scattering Studies. *Chem. Mater.* **2005**, *17*, 741-748.

139. A. Pal; H. Basit; S. Sen; V. K. Aswal; S. Bhattacharya. Structure and Properties of Two Component Hydrogels Comprising Lithocholic Acid and Organic Amines. *J. Mater. Chem.* **2009**, *19*, 4325-4334.

140. S. Song; L. Feng; A. Song; J. Hao. Room-Temperature Super Hydrogel as Dye Adsorption Agent. *J. Phys. Chem. B* **2012**, *116*, 12850-12856.

141. S. Song; R. Dong; D. Wang; A. Song; J. Hao. Temperature Regulated Supramolecular Structures Via Modifying the Balance of Multiple Non-Covalent Interactions. *Soft Matter* **2013**, *9*, 4209-4218.

142. W. Wenseleers; I. I. Vlasov; E. Goovaerts; E. D. Obraztsova; A. S. Lobach; A. Bouwen. Efficient Isolation and Solubilization of Pristine Single-Walled Nanotubes in Bile Salt Micelles. *Adv. Funct. Mater.* **2004**, *14*, 1105-1112.

143. S. Lin; D. Blankshtein. Role of the Bile Salt Surfactant Sodium Cholate in Enhancing the Aqueous Dispersion Stability of Single-Walled Carbon Nanotubes: A Molecular Dynamics Simulation Study. *J. Phys. Chem. B* **2010**, *114*, 15616-15625.

144. Z. Tan; S. Ohara; M. Naito; H. Abe. Supramolecular Hydrogel of Bile Salts Triggered by Single-Walled Carbon Nanotubes. *Adv. Mater.* **2011**, *23*, 4053-4057.
145. L. Wang; X. Xin; M. Yang; X. Ma; J. Shen; Z. Song; S. Yuan. Effects of Graphene Oxide and Salinity on Sodium Deoxycholate Hydrogels and Their Applications in Dye Absorption. *Colloids Surf., A* **2015**, *483*, 112-120.
146. G. Li; Y. Hu; J. Sui; A. Song; J. Hao. Hydrogelation and Crystallization of Sodium Deoxycholate Controlled by Organic Acids. *Langmuir* **2016**, *32*, 1502-1509.
147. J.-Q. Hao; H. Li; H.-G. Woo. Synthesis and Characterization of Cholic Acid-Containing Biodegradable Hydrogels by Photoinduced Copolymerization. *J. Appl. Polym. Sci.* **2009**, *112*, 2976-2980.
148. X. Gu; J. D. Jennings; J. Snarr; V. Chaudhary; J. E. Pollard; P. B. Savage. Optimization of Ceragenins for Prevention of Bacterial Colonization of Hydrogel Contact Lenses. *Invest. Ophthalmol. Vis. Sci.* **2013**, *54*, 6217-6223.
149. C. C. Li; G. J. Wang; H. Y. Gao; M. L. Zhai; J. Q. Li. Temperature-, pH-, and Ion-Stimulus- Responsive Swelling Behaviors of Poly( dimethylaminoethyl methacrylate) Gel Containing Cholic Acid. *J. Appl. Polym. Sci.* **2014**, *131*, 39998.
150. Y.-G. Jia; X. X. Zhu. Nanocomposite Hydrogels of LAPONITE® Mixed with Polymers Bearing Dopamine and Cholic Acid Pendants. *RSC Adv.* **2016**, *6*, 23033-23037.
151. A. C. Kumar; H. Erothu; H. B. Bohidar; A. K. Mishra. Bile-Salt-Induced Aggregation of Poly(N-Isopropylacrylamide) and Lowering of the Lower Critical Solution Temperature in Aqueous Solutions. *J. Phys. Chem. B* **2011**, *115*, 433-439.
152. Z. Zhang; J. Liu; Q. Luo; J. Zhang; J. Xu; X. X. Zhu. Construction of a Tunable Metallohydrolase Center on an Invertible Molecular Pocket. *Org. Biomol. Chem.* **2011**, *9*, 8220-8223.
153. X. D. Wang; Y. Q. Duan; C. X. Li; Y. Lu. Synthesis, Self-Assembly, and Formation of Polymer Vesicle Hydrogels of Thermoresponsive Copolymers. *J. Mater. Sci.* **2015**, *50*, 3541-3548.
154. X. X. Zhu; D. Avocce; H. Y. Liu; A. Benrebouh. Copolymers of N-Alkylacrylamides as Thermosensitive Hydrogels. *Macromol. Symp.* **2004**, *207*, 187-192.
155. Y. L. Zhao; J. F. Stoddart. Azobenzene-Based Light-Responsive Hydrogel System. *Langmuir* **2009**, *25*, 8442-8446.

156. Y.-G. Jia; X. X. Zhu. Self-Healing Supramolecular Hydrogel Made of Polymers Bearing Cholic Acid and  $\beta$ -Cyclodextrin Pendants. *Chem. Mater.* **2015**, 27, 387-393.

## Chapter 3

# Formation of molecular hydrogels from a bile acid derivative and selected carboxylic acids\*

### Abstract

Bile acids are natural compounds that can be made into dimers by covalently linking two of them through diethylenetriamine. A cholic acid dimer of this kind is synthesized and is found to form thermally reversible hydrogels with selected carboxylic acids through combined hydrogen bonding and ionic interactions. The gelation and viscoelastic properties of the hydrogels may be varied by judicious choice of the carboxylic mono- and diacids. The total organic content (the dimer and carboxylic acid) represents about 2% or less by weight in the ternary mixture. The molecular arrangement between the dimer and carboxylic acid is proposed to illustrate the formation mechanism of the hydrogels. The marginal solubility of the dimer-acid mixtures seems to be the deciding factor in obtaining the hydrogels.

### 3.1 Introduction

Molecular gels are an important class of soft materials that may be potentially used for drug delivery, tissue engineering, and sensing.<sup>1-3</sup> In molecular gels, solvents are immobilized by a small amount (typically < 2 wt%) of low molecular weight gelators

---

\*Published as a communication: M. Zhang; K. C. Waldron; X. X. Zhu. *RSC Adv.* **2016**, *6*, 35436-35440.

Contributions of author other than supervisors

Meng Zhang: Experimental design and conduction, data analysis, manuscript writing.

(LMWGs).<sup>4</sup> The small molecules self-assemble to form fibrils and 3-dimensional networks facilitated by supramolecular interactions such as hydrogen bonding, hydrophobic interaction,  $\pi$ - $\pi$  stacking, electrostatic attraction, and charge transfer interactions between the gelators and solvents.<sup>5</sup> Such gels often show advantages of biodegradability and diversity of functionality due to noncovalent interactions and precisely controlled structures.<sup>6</sup> No general rule based on molecular structure seems to exist to predict the gelation behavior, and many LMWGs have been discovered by serendipity.<sup>7-9</sup>

Bile acids are natural compounds found in humans and most animals. In their salt form or after suitable chemical modification, they may form hydrogels by self-assembly.<sup>10-17</sup> For example, sodium cholate may interact with metal cations ( $\text{Cu}^{2+}$ ,  $\text{Zn}^{2+}$ ,  $\text{Co}^{2+}$ ,  $\text{Ag}^+$ , trivalent lanthanides, *etc.*) to form hydrogels.<sup>18-21</sup> A cholic acid-based trimer was reported to form a hydrogel in the presence of up to 20% of acetic acid in aqueous solutions,<sup>22-24</sup> while strong inorganic acid such as HCl may not favor the gelation of the trimer. The necessity of the acids and the interactions between the trimer and acetic acid during the gelation remain unclear. In our work, we discovered that an otherwise insoluble cholic acid-based dimer linked through amide groups and bearing a secondary amine (Fig. 3.1) forms a hydrogel in the presence of certain carboxylic acids. The properties of the hydrogels appear to depend on the structure of the acids. Therefore, investigation of their gelation behaviors may lead to a better understanding of these molecular hydrogels.

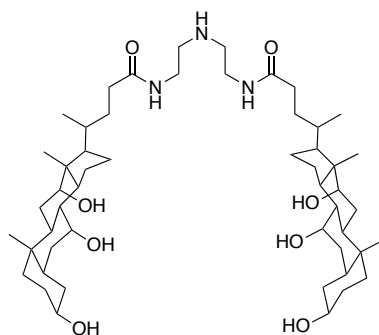


**Figure 3.1** Molecular structure of the dimer based on cholic acid.

## 3.2 Results and discussions

The dimer based on cholic acid (Fig. 3.1) was synthesized according to a literature procedure with a simple two-step synthesis and a high yield (Scheme 3.S1), and it was previously reported to manifest interesting selective antifungal activities.<sup>25</sup> We have found that the dimer has limited solubility in water, even in the presence of HCl, but may be solubilized in the presence of certain amounts of selected carboxylic acids to form hydrogels (Chart 3.1A). Carboxylic acids that are either too strong or too hydrophobic do not favour the formation of hydrogels (Chart 3.1B, Fig. 3.S1A and B), which we discuss in more detail further on. In these experiments, hydrogels formed only when the carboxylic acid groups are in excess of the secondary amine groups of the cholic acid dimers. The dimer cannot be dissolved in water at a [dimer]/[-COOH] ratio of 1:1 and a cloudy liquid formed, but a transparent hydrogel was obtained at a [dimer]/[-COOH] ratio of 1:2 (see Fig. 3.S1C and D). Therefore, we fixed the concentration of the monoprotic acids at 40 mM and that of diprotic acids at 20 mM, keeping the ratio of [dimer]/[-COOH] at 1:2.

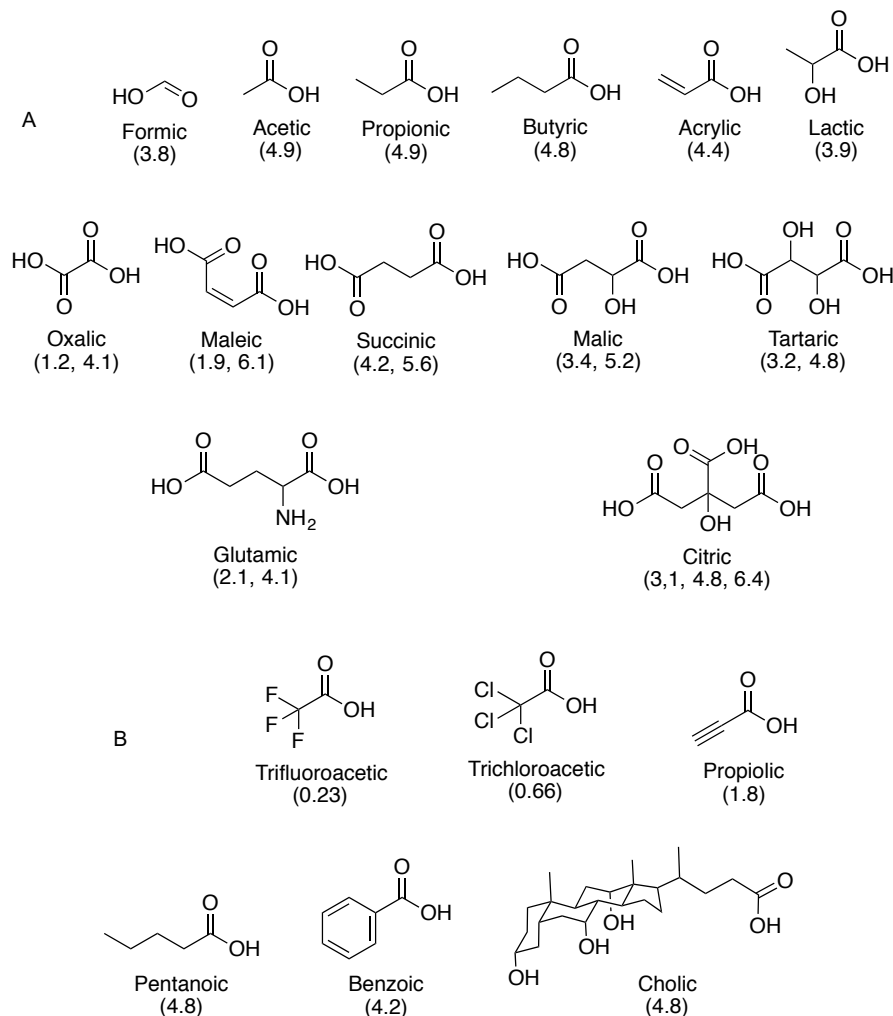


**Chart 3.1** The structure of various carboxylic acids tested for hydrogelation with the dimer: (A) acids that can form a hydrogel; (B) acids that cannot form a hydrogel. The values in brackets indicate the  $pK_a$  of the carboxylic acid groups.

Rheological studies may provide useful information related to the structure in gels. The mixture of 20 mM dimer and 40 mM acetic acid in water was studied as an example. Both  $G'$  and  $G''$  increased during the gelation process (Fig. 3.S2A), reaching a plateau after 10 minutes. Neither  $G'$  nor  $G''$  showed obvious change under a small oscillation stress (Fig. 3.S2B), demonstrating the stability of the 3-D networks in the hydrogel. A further increase in stress ( $> 20$  Pa) caused a yielding process and flow of the hydrogel due to disintegration of the 3-D fibrillar networks. The moduli ( $G'$ ,  $G''$ ) of the hydrogel were found to depend

on the frequency of stress oscillation (Fig. 3.S2C).  $G'$  remained larger than  $G''$ , although both increased with increasing frequency.  $G''$  increased at a faster rate than  $G'$  and a crossover point would be expected at a higher frequency, e.g., between 100 and 1000 Hz, which is beyond the detection limit. Both  $G'$  and  $G''$  decreased with increasing temperature, and their crossover point was observed at around 58 °C (Fig. 3.S2D), indicating a gel-sol transition. Further rheological tests illustrated that a deviation of the ratio of [dimer]/[-COOH] from 1:2 resulted in weaker hydrogels (lower  $G'$  values and lower gel-sol transition temperatures, as shown in Fig. 3.S3).

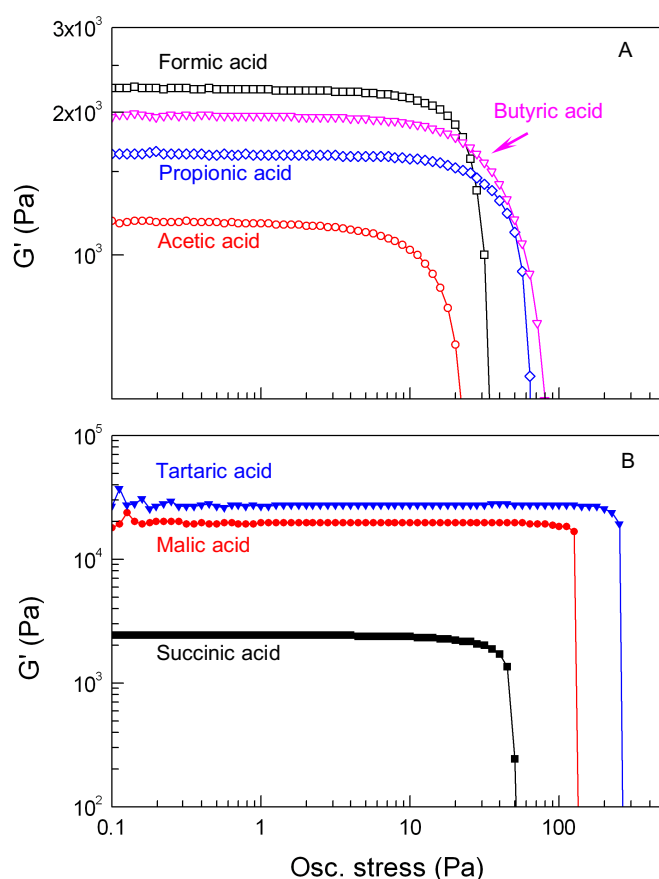


**Figure 3.2** Oscillatory stress sweep experiments of the hydrogel formed from the dimer (20 mM) and (A) monoprotic acids (40 mM) and (B) diprotic acids (20 mM). [-COOH] = 40 mM.



The minimal gelation concentration (MGC) of the dimer was found to be dependent on the chemical structure of the carboxylic acids used in the hydrogel. Among the monoprotic acids tested at a concentration of 40 mM, the lowest MGC of the dimer was 5.5 mM obtained with formic acid and with butyric acid. In comparison, lower MGC values were obtained with 20 mM diprotic acids where the presence of more hydroxyl groups leads to even lower MGC values (Table 3.S1). The dimer may form hydrogels at a lower concentration when the content of the carboxylic acid decreases, which is similar to the gelation behavior of a cholic acid trimer with acetic acid.<sup>23</sup>

The mechanical properties of the hydrogels were also found to be related to the structure of the carboxylic acid. Whereas the dimer can form gels in the presence of all four monoacids having 1-4 carbon atoms (Fig. 3.2A), a longer alkyl chain on the acid results in better mechanical properties of the gel, likely due to enhanced hydrophobic interaction between the alkyl chains of the carboxylic acid.<sup>26</sup> Formic acid can form multiple hydrogen bonds,<sup>27</sup> thus improving the interactions between acid molecules that are complexed with the dimer. Therefore, the hydrogel made with formic acid showed the highest modulus among all the hydrogels in the monoacid series (Fig. 3.2A). In contrast, the hydrogels formed by the diacids have higher  $G'$  than those formed by the monoacids (Fig. 3.2B).

The diacids in Figure 3.2B all have 4 carbon atoms but different numbers of hydroxyl groups. The presence of additional hydroxyl groups led to better mechanical properties of the gels. For example,  $G'$  increased by an order of magnitude when tartaric acid replaced succinic acid, implying that extra hydroxyl groups improve the interactions between gelator molecules in acid-dimer complexes to yield stronger self-assembled fibrillar networks (SAFINs) in the hydrogels.

The transmission electron microscopy (TEM) images (Fig. 3.3) show the existence of well-developed intertwined SAFINs in the acid-dimer hydrogels. Different morphologies were observed for hydrogels obtained with different carboxylic acids: interactions with acetic acid yielded mostly straight fibers of 20-40 nm in diameter (Fig. 3.3A) whereas more flexible and uniform-sized fibers of around 20 nm in diameter were observed when

tartaric acid was used (Fig. 3.3C). Similar morphologies were also observed by AFM (Fig. 3.S4). Such morphology differences may explain the different gelation capabilities of the dimer with the different acids: Thin, flexible, and highly entangled nanofibers may accompany systems with better gelation capabilities.<sup>28</sup> The self-assembled fibers had lengths of micrometers, and the 3-D network immobilizes water molecules such that the solution thickens to form a hydrogel. The concentration used for Fig. 3.3C corresponds to the lowest MGC of the dimer. The complex consisting of one dimer molecule and one tartaric acid molecule may immobilize more than  $9 \times 10^4$  water molecules, which indicates the good gelation capability of the dimer.

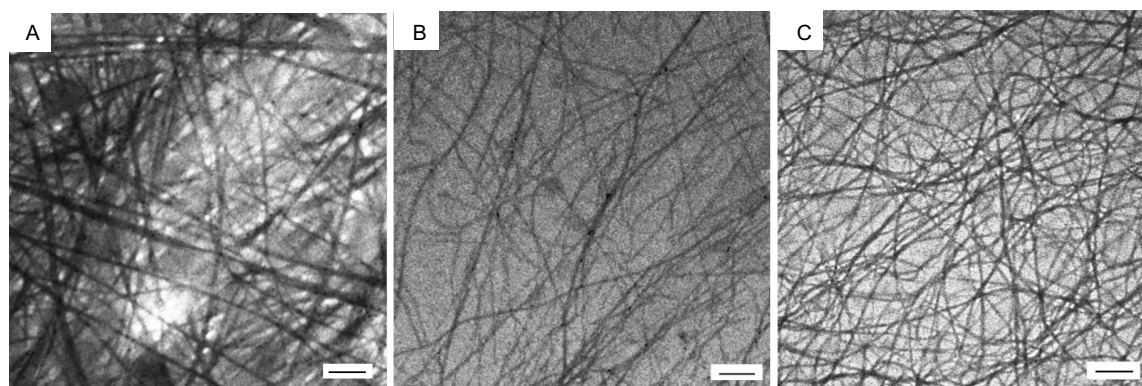


**Figure 3.3** TEM images of the fibrillar network in hydrogels formed by (A) 6 mM dimer and 12 mM acetic acid; (B) 1.2 mM dimer and 1.2 mM succinic acid; and (C) 0.6 mM dimer and 0.6 mM tartaric acid. (Black scale bar = 200 nm).

The  $^1\text{H}$  NMR spectrum of acetic acid-dimer hydrogel in  $\text{D}_2\text{O}$  varied with temperature (Fig. 3.S6). The proton peaks from the dimer were broad and unresolved at room temperature but distinguishable when temperature was higher than  $45^\circ\text{C}$ , indicating the increased mobility of the dimer due to the gel-sol transition process. However, the acetic acid peak in the  $^1\text{H}$  NMR spectrum of the hydrogel was visible throughout the temperature range, and its integration values relative to the internal standard did not change with temperature. Therefore, acetic acid and the dimer in the hydrogel may exist in regions with different mobility.

FT-IR spectroscopy was used to study the physical interactions in the molecular hydrogels. The FT-IR spectrum of the aerogel formed from the dimer and succinic acid is similar to that of the dimer alone, except for the new peaks from the carboxylic acid groups on succinic acid (Fig. 3.S7). In Fig. 3.4A, the second derivative analysis of the dimer FT-IR spectrum shows the amide I band (C=O stretching) split into two peaks, 1651 and 1627  $\text{cm}^{-1}$ , and the amide II band (complex of C-N stretching and N-H bending) at 1545  $\text{cm}^{-1}$ . After gelation with succinic acid, only a single peak for the amide I band appears at 1650  $\text{cm}^{-1}$ , while the amide II band shows a slight shift to 1549  $\text{cm}^{-1}$  (Fig. 3.4B). These results indicate that the environment of the amide groups changes upon gelation.

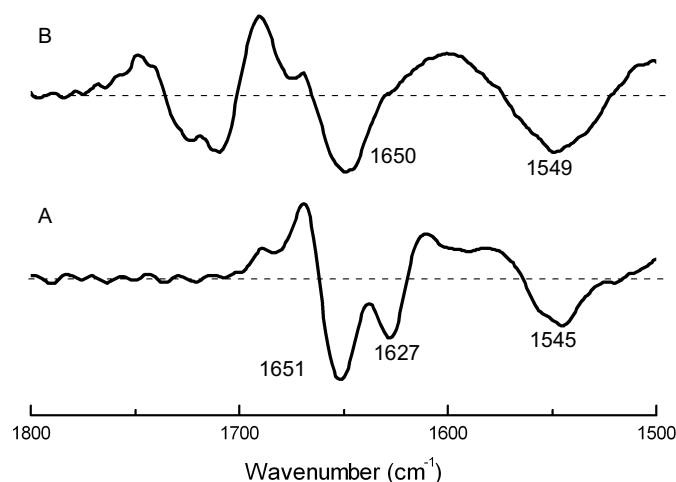


**Figure 3.4** Second derivative of the FT-IR spectra of (A) the dimer; (B) the aerogel of dimer-succinic acid (20 mM-20 mM).

The split peaks of the dimer's amide I band (1651 and 1627  $\text{cm}^{-1}$ , Fig. 3.4A) are similar to those reported for the amide group of poly(*N*-isopropylacrylamide) in a hydrogel,<sup>29</sup> indicating the formation of amide-amide and amide-hydroxyl hydrogen bonds, respectively, in the dimer alone with a proposed molecular arrangement schematically shown in Fig. 3.5A. The disappearance of the peak at 1627  $\text{cm}^{-1}$  and the shift of the amide II band (Fig. 3.4B) in the acid-dimer aerogel indicates the disruption of the amide-hydroxyl hydrogen bonds of the dimer and the formation of new hydrogen bonds during gelation, where cholic acid hydroxyl groups are replaced by the carboxylic acid groups

(Fig. 3.5B) due to the better H-acceptor ability of the carbonyl oxygen, and the better H-donor ability of the carboxylic acid hydrogen.<sup>30</sup> Formation of the amide-carboxylic acid complex may also help to solubilize the dimer in aqueous solutions upon heating, whereas the cooling process leads to the self-assembly of the dimer to form SAFINs and thus a hydrogel.

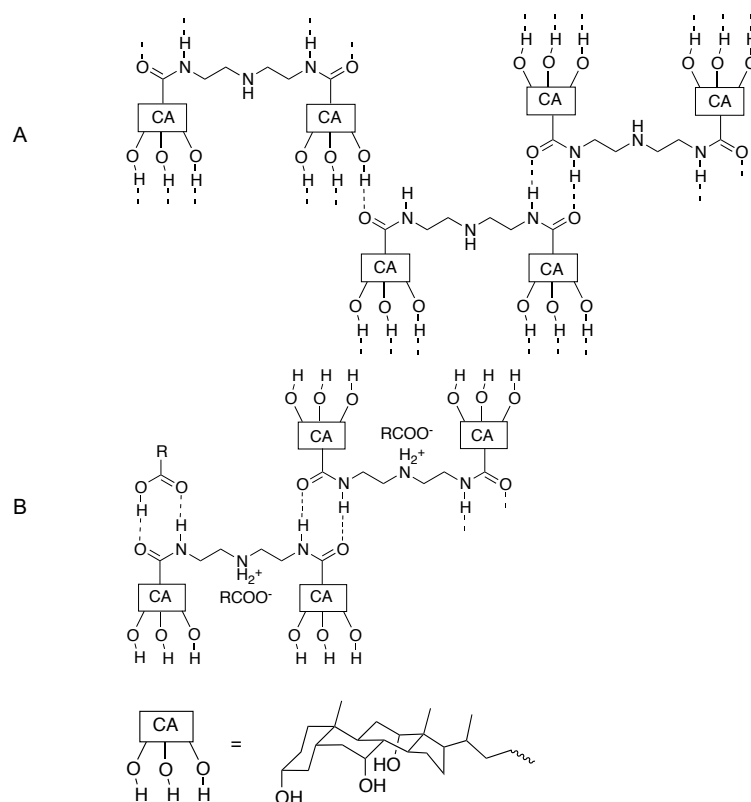


**Figure 3.5** The schematic representation of the hydrogen bonds (A) between the dimers; and (B) between the dimer and carboxylic acid after gelation in water.

For the formation of hydrogels with the dimer, the general requirements of the carboxylic acids are: (1) they should be soluble enough in water to interact with the dimer and form complexes that stabilize the dimer and induce formation of a fibrillar network under suitable conditions; (2) they should be able to protonate the dimer's secondary amine group to increase its polarity, which is feasible since the acids have  $pK_a$  lower than 5.0 (Chart 3.1) and aliphatic secondary amines have a  $pK_b$  value of around 3.0,<sup>31</sup> which

should be the case for the dimer; (3) they should be able to form hydrogen bonds with the dimer's amide groups to dissociate interactions between the dimer molecules. Strong carboxylic acids with low  $pK_a$ , such as trifluoroacetic acid, are mostly deprotonated in water, hindering the formation of hydrogen bonds with the amide group on the dimer as proposed in Fig. 3.5B.<sup>32</sup>

### 3.3 Conclusions

In summary, the dimer based on cholic acid interacts with weak and hydrophilic carboxylic acids in water to form transparent hydrogels. It is interesting to note that the total organic contents of cholic acid dimer and the carboxylic acid represent about 2% or less by weight in the mixture. The added carboxylic acid protonates the secondary amine group on the dimer making an otherwise insoluble dimer now marginally soluble in water. Note that no hydrogels are formed with carboxylic acids that are either strong electrolytes or too hydrophobic. The marginal solubility of the gelator seems to be the key in the formation of hydrogels. The formation and rearrangement of hydrogen bonds in the system lead to a stable 3-D fibrillar network in water to yield a hydrogel. All the hydrogels made from the dimer show thermo-reversible gel-sol transitions. Their mechanical properties and morphology vary with the chemical structure of the carboxylic acids used. Monoacids with longer alkyl chains form stronger gels due to hydrophobic interactions; diacids with hydroxyl groups also improve the mechanical properties, owing to the formation of multiple hydrogen bonds. This proves also the case for formic acid due to its greater hydrogen bond formation capabilities. The good gelation ability of the dimer in addition to its biocompatibility may make such hydrogels useful for a variety of biomedical applications. Moreover, a general rule for the gelation ability of the dimer with various carboxylic acids is now established. This may be useful in designing new functional molecular hydrogels and in predicting the gelation behavior of the dimer with acids and other acidic biomolecules of natural origin. In addition, the reported antifungal activities of the dimer may be retained in the hydrogels formed, making them useful in bio-related applications.

### 3.4 Acknowledgements

Financial support from NSERC of Canada, FQRNT of Quebec, and the Canada Research Chair program is gratefully acknowledged. Meng Zhang thanks the Chinese Scholarship Council (CSC) for a scholarship.

### 3.5 Supporting information

#### 3.5.1 Experimental part

*Materials and method* Cholic acid, N-hydroxysuccinimide (NHS), dicyclohexylcarbodiimide (DCC), diethylenetriamine, and all organic acids were purchased from Sigma-Aldrich (Oakville, ON, Canada) and used without further purification. Anhydrous tetrahydrofuran (THF), acetonitrile (ACN), and dimethylformamide (DMF) were redistilled from a solvent purification system from Glass Contour (Nashua, NH, United States). All the hydrogel samples were prepared with fresh Milli-Q water. For the test of gelation, stock solutions of different carboxylic acids were prepared in Milli-Q water and diluted to the desired concentration. To this solution, a known amount of the cholic acid dimer was added to reach a dimer concentration of 20 mM. The mixture was heated and sonicated and then cooled gradually to room temperature and left to stand for several hours. The samples were periodically verified for signs of gelation by inversion of vials. For the minimal gelation concentration (MGC) tests, the solutions of different carboxylic acids were fixed at 40 mM carboxylic acid groups (i.e., diprotic acids prepared at 20 mM). A series of samples of the dimer with concentrations differing by 0.5 mM were prepared by dissolving the dimer in the acid solutions through heating and sonication. The samples were equilibrated at room temperature and checked for the formation of hydrogels after 48 hours. The lowest concentration of the dimer for the formation of a stable hydrogel by vial-inversion was taken as the MGC.

*<sup>1</sup>H NMR spectroscopy.* The hydrogel sample was made in D<sub>2</sub>O with 20 mM of the dimer and 40 mM acetic acid, and a trace amount of trioxane was added as an internal standard. The sample was heated first to obtain a homogeneous solution and then transferred to an NMR tube immediately. The hydrogel formed inside the tube at room temperature and was equilibrated for at least 24 hours. The <sup>1</sup>H NMR spectra at different temperatures were recorded on a Bruker AV400 spectrometer operating at 400 MHz.

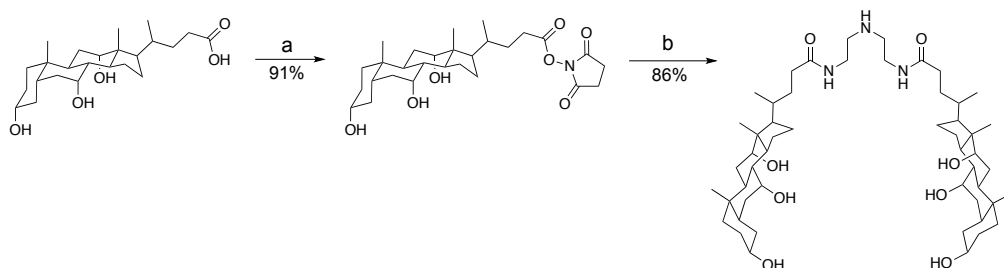
*FT-IR spectroscopy.* A Nicolet 6700 FT-IR spectrometer with an attenuated total reflection (ATR) accessory was used to record the FT-IR spectra. The hydrogel samples with the desired concentrations of the dimer and the acids in H<sub>2</sub>O were freeze-dried to obtain aerogels for which an FT-IR spectrum was recorded by collecting 128 scans at a resolution of 2 cm<sup>-1</sup>.

*Transmission electron microscopy (TEM).* Three µl of the hydrogel samples of the dimer prepared with different carboxylic acids were placed on carbon-coated copper grids (300 mesh, Carbon Type-B, Ted Pella, Inc.) at room temperature. After equilibration for 1 min., excess sample was removed by a filter paper and the remaining sample was dried under vacuum to obtain a thin film on the grid. Samples were observed on FEI Tecnai 12 TEM at 120 kV, equipped with AMT XR80C CCD camera system.

*Rheology.* The rheological study of the hydrogel samples was done on a TA-AR 2000 rheometer, using a cone-geometry with 40 mm diameter. All measurements were performed with a fixed gap of 55 µm between the geometry and the plate. The hydrogel samples were melted to obtain a homogeneous solution. Aliquots of the solution were transferred to the center of the rheometer plate and a very small oscillatory stress of 0.1 Pa was applied to record the storage moduli (G') and loss moduli (G'') until a plateau was observed. Oscillatory frequency sweep experiments of the equilibrated hydrogel were performed in the linear viscoelastic region at 25 °C, with a constant stress of 0.1 Pa, for a scale from 0.01 to 100 Hz. Oscillatory stress sweep experiments were performed at 25 °C, with a constant frequency of 1 Hz. Oscillatory temperature sweep experiments were performed in the range of 20-70 °C at 1 Hz with a oscillatory stress of 0.1 Pa.

### 3.5.2 Supporting data

**Scheme 3.S1** Synthesis of the dimer<sup>a</sup>



<sup>a</sup> Reaction conditions: (a) NHS/DCC in THF/ACN, 18 h, room temperature; (b) Diethylenetriamine in DMF, 2 h, 60 °C.

**Table 3.S1** The acids tested and the minimum gelation concentrations of the cholic acid dimer

Carboxylic acids, [-COOH] = 40 mM	Chemical structure	pK <sub>a</sub>	Dimer MGC <sup>a</sup>	
			(mM)	(wt%)
Formic acid		3.8	5.5	0.49
Acetic acid		4.9	8.0	0.71
Propionic acid		4.9	6.5	0.58
Butyric acid		4.8	5.5	0.49
Succinic acid		4.2, 5.6	4.0	0.35
Malic acid		3.4, 5.2	3.0	0.27
Tartaric acid		3.2, 4.8	1.5	0.13

<sup>a</sup> Estimated minimum gelation concentration (MGC) of the dimer in the presence of the carboxylic acids (monoacids at 40 mM and diacids at 20 mM).



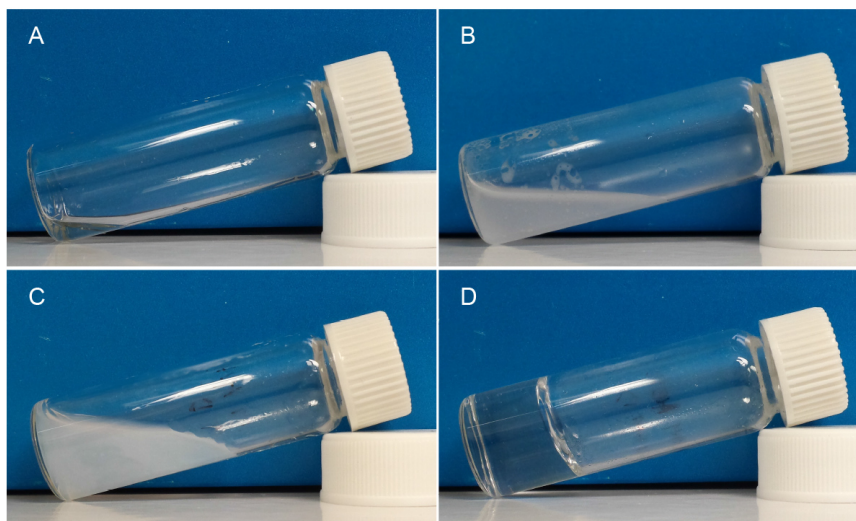


**Figure 3.S1** Behavior of the dimer in the presence of certain carboxylic acids: (A) Homogeneous solution obtained from the dimer and trifluoroacetic acid; (B) Precipitation, which occurred after the addition of water into the mixture of the dimer and trifluoroacetic acid; (C) Viscous and cloudy liquid obtained from an aqueous solution of acetic acid and the dimer (both at 20 mM); (D) Transparent and stable hydrogel obtained from an aqueous solution of acetic acid (40 mM) and the dimer (20 mM).

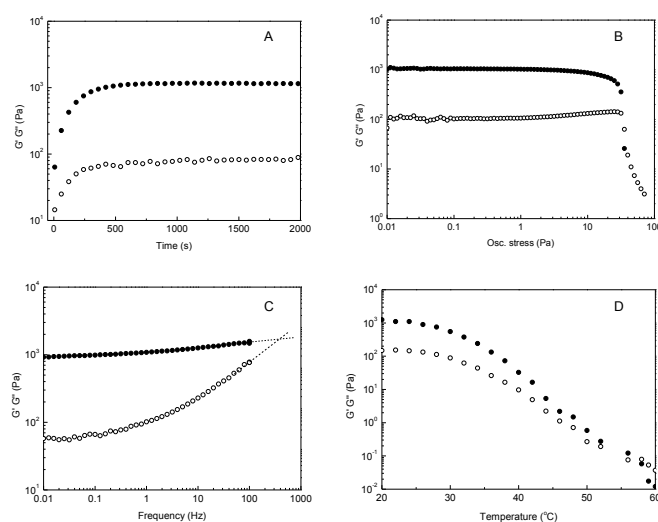


**Figure 3.S2** Viscoelastic properties of the dimer-acid hydrogel (20 mM dimer-40 mM acetic acid) in water: (A) Gelation over time; (B) Oscillatory stress sweep; (C) Frequency sweep; (D) Oscillatory temperature sweep.  $G'$  (closed circles),  $G''$  (open circles).

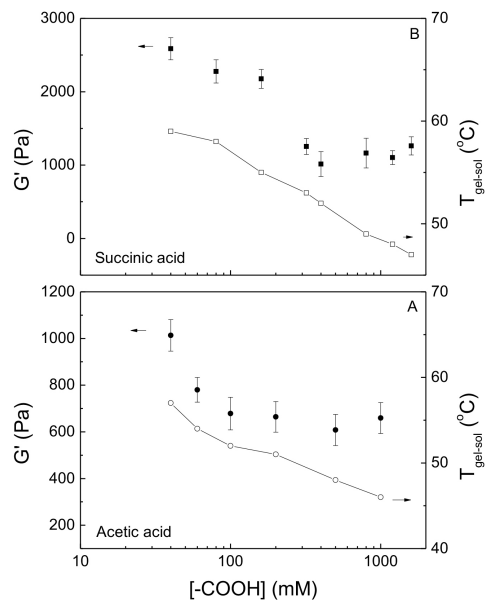


**Figure 3.S3** Viscoelastic properties of the hydrogels formed by the cholic acid dimer (20 mM) and various concentration of (A) Acetic acid. (B) Succinic acid.  $T_{\text{gel-sol}}$ : gel-sol transition temperature.

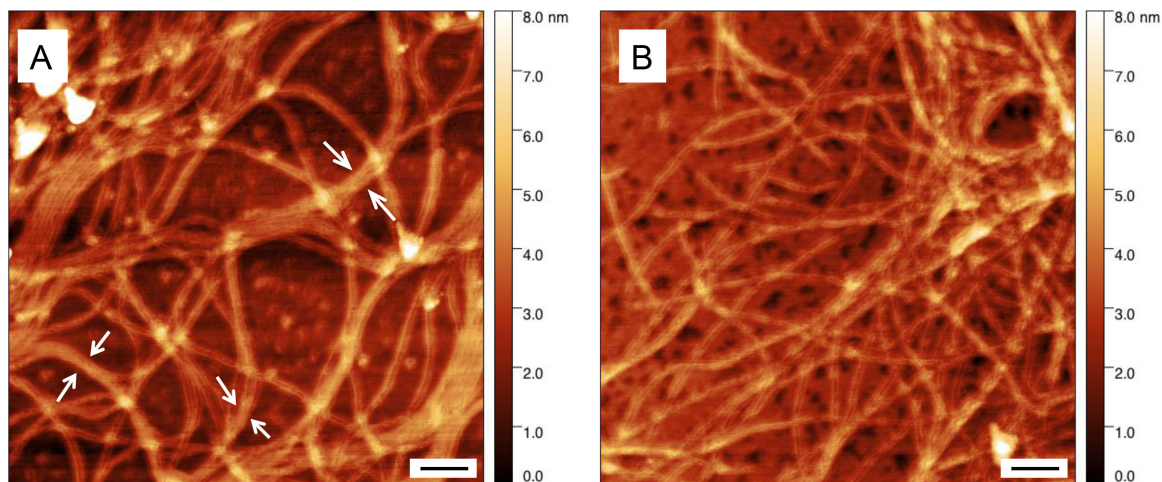


**Figure 3.S4** AFM images (black scale bar = 200 nm) of the fibrillar network in hydrogels formed by (A) 6 mM dimer and 12 mM acetic acid (the white arrows indicate entwined nanofibers), and (B) 0.6 mM dimer and 0.6 mM tartaric acid.

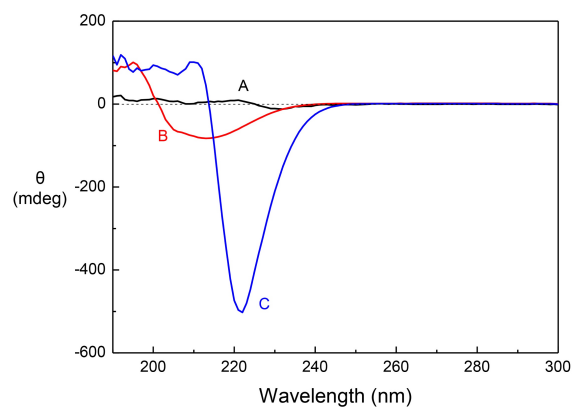


**Figure 3.S5** The CD spectra of the hydrogel samples formed with (A) 6 mM dimer and 12 mM acetic acid; (B) 0.6 mM dimer and 0.6 mM tartaric acid; and (C) 6 mM dimer and 6 mM tartaric acid.

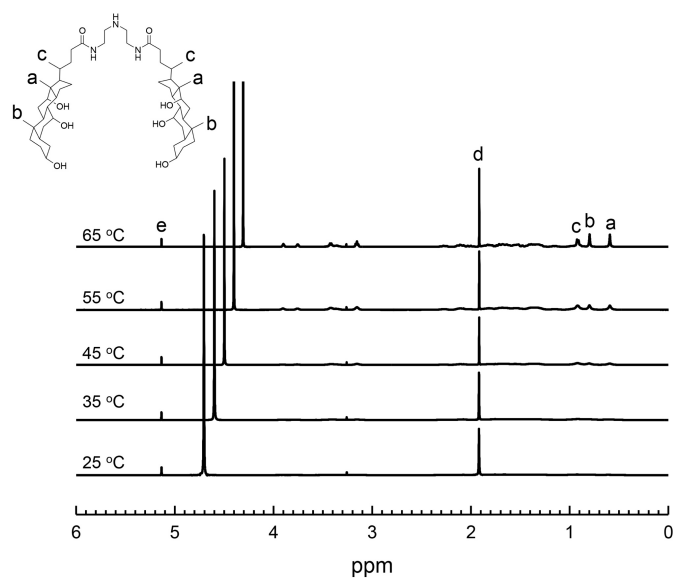


**Figure 3.S6**  $^1\text{H}$  NMR spectra of hydrogel of acetic acid-dimer (40 mM-20 mM) in  $\text{D}_2\text{O}$  at different temperatures. Peaks a, b, and c indicate the protons at methyl groups on the cholic acid dimer, peak d is from protons of the methyl group on acetic acid, peak e is from protons of trioxane added as an internal standard, the peaks at about 4.7 that varies with temperature are water solvent residual signals.

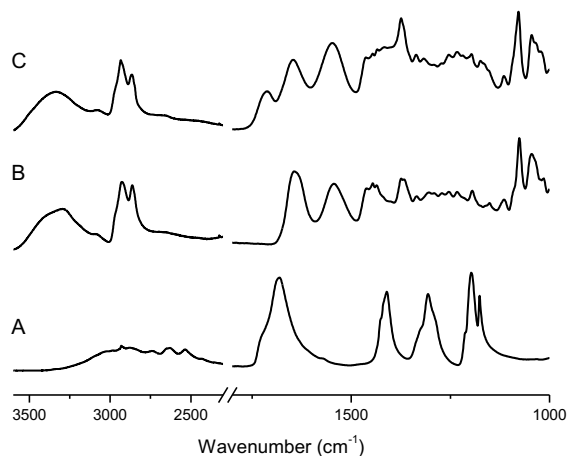


**Figure 3.S7** FT-IR spectra of (A) succinic acid; (B) the dimer; (C) aerogel of succinic acid-dimer (20 mM-20 mM).

### 3.6 References

1. R. G. Weiss; P. Terech. *Molecular Gels: Materials with Self-Assembled Fibrillar Networks*. Springer: Dordrecht, 2006.
2. B. Escuder; J. F. Miravet. *Functional Molecular Gels*. Escuder, B.; Miravet, J. F. Eds.; Royal Society of Chemistry: Cambridge, 2014.
3. A. Dasgupta; J. H. Mondal; D. Das. Peptide hydrogels. *RSC Adv.* **2013**, *3*, 9117-9149.
4. P. Terech; R. G. Weiss. Low Molecular Mass Gelators of Organic Liquids and the Properties of Their Gels. *Chem. Rev.* **1997**, *97*, 3133-3160.
5. M. O. Piepenbrock; G. O. Lloyd; N. Clarke; J. W. Steed. Metal- and Anion-Binding Supramolecular Gels. *Chem. Rev.* **2010**, *110*, 1960-2004.
6. L. A. Estroff; A. D. Hamilton. Water Gelation by Small Organic Molecules. *Chem. Rev.* **2004**, *104*, 1201-1218.
7. R. G. Weiss. The Past, Present, and Future of Molecular Gels. What Is the Status of the Field, and Where Is It Going? *J. Am. Chem. Soc.* **2014**, *136*, 7519-7530.
8. J. Raeburn; D. J. Adams. Multicomponent Low Molecular Weight Gelators. *Chem. Commun.* **2015**, *51*, 5170-5180.

9. X. Du; J. Zhou; J. Shi; B. Xu. Supramolecular Hydrogelators and Hydrogels: From Soft Matter to Molecular Biomaterials. *Chem. Rev.* **2015**, *115*, 13165-13307.
10. S. Strandman; F. Le Devedec; X. X. Zhu. Self-Assembly of Bile Acid-PEG Conjugates in Aqueous Solutions. *J. Phys. Chem. B* **2013**, *117*, 252-258.
11. H. Svobodová; V. Noponen; E. Kolehmainen; E. Sievanen. Recent Advances in Steroidal Supramolecular Gels. *RSC Adv.* **2012**, *2*, 4985-5007.
12. Y. L. Zhao; J. F. Stoddart. Azobenzene-Based Light-Responsive Hydrogel System. *Langmuir* **2009**, *25*, 8442-8446.
13. V. H. Soto Tellini; A. Jover; F. Meijide; J. V. Tato; L. Galantini; N. V. Pavel. Supramolecular Structures Generated by a p-Tert-Butylphenyl-Amide Derivative of Cholic Acid: From Vesicles to Molecular Tubes. *Adv. Mater.* **2007**, *19*, 1752-1756.
14. L. Galantini; C. Leggio; A. Jover; F. Meijide; N. V. Pavel; V. H. Soto Tellini; J. V. Tato; R. Di Leonardo; G. Ruocco. Kinetics of Formation of Supramolecular Tubules of a Sodium Cholate Derivative. *Soft Matter* **2009**, *5*, 3018.
15. M. Gubitosi; L. Travaglini; A. D'Annibale; N. V. Pavel; J. Vazquez Tato; M. Obiols-Rabasa; S. Sennato; U. Olsson; K. Schillen; L. Galantini. Sugar-Bile Acid-Based Bolaamphiphiles: From Scrolls to Monodisperse Single-Walled Tubules. *Langmuir* **2014**, *30*, 6358-6366.
16. Y. Zhang; X. Xin; J. Shen; W. Tang; Y. Ren; L. Wang. Biodegradable, Multiple Stimuli-Responsive Sodium Deoxycholate–Amino Acids–NaCl Mixed Systems for Dye Delivery. *RSC Adv.* **2014**, *4*, 62262-62271.
17. M. Maity; V. S. Sajisha; U. Maitra. Hydrogelation of Bile Acid–Peptide Conjugates and in Situ Synthesis of Silver and Gold Nanoparticles in the Hydrogel Matrix. *RSC Adv.* **2015**, *5*, 90712-90719.
18. A. Chakrabarty; U. Maitra; A. D. Das. Metal Cholate Hydrogels: Versatile Supramolecular Systems for Nanoparticle Embedded Soft Hybrid Materials. *J. Mater. Chem.* **2012**, *22*, 18268-18274.
19. R. Kandaneli; A. Sarkar; U. Maitra. Tb(3+) Sensitization in a Deoxycholate Organogel Matrix, and Selective Quenching of Luminescence by an Aromatic Nitro Derivative. *Dalton Trans.* **2013**, *42*, 15381-15386.

20. Y. Qiao; Y. Lin; Z. Yang; H. Chen; S. Zhang; Y. Yan; J. Huang. Unique Temperature-Dependent Supramolecular Self-Assembly: From Hierarchical 1D Nanostructures to Super Hydrogel. *J. Phys. Chem. B* **2010**, *114*, 11725-11730.
21. S. Bhowmik; S. Banerjee; U. Maitra. A Self-Assembled, Luminescent Europium Cholate Hydrogel: A Novel Approach Towards Lanthanide Sensitization. *Chem. Commun.* **2010**, *46*, 8642-8644.
22. U. Maitra; S. Mukhopadhyay; A. Sarkar; P. Rao; S. S. Indi. Hydrophobic Pockets in a Nonpolymeric Aqueous Gel: Observation of Such a Gelation Process by Color Change. *Angew. Chem. Int. Ed. Engl.* **2001**, *40*, 2281-2283.
23. S. Mukhopadhyay; U. Maitra; I. Ira; G. Krishnamoorthy; J. Schmidt; Y. Talmon. Structure and Dynamics of a Molecular Hydrogel Derived from a Tripodal Cholamide. *J. Am. Chem. Soc.* **2004**, *126*, 15905-15914.
24. P. Terech; U. Maitra. Structural and Rheological Properties of Aqueous Viscoelastic Solutions and Gels of Tripodal Cholamide-Based Self-Assembled Supramolecules. *J. Phys. Chem. B* **2008**, *112*, 13483-13492.
25. D. B. Salunke; B. G. Hazra; V. S. Pore; M. K. Bhat; P. B. Nahar; M. V. Deshpande. New Steroidal Dimers With Antifungal and Antiproliferative Activity. *J. Med. Chem.* **2004**, *47*, 1591-1594.
26. V. J. Nebot; J. Armengol; J. Smets; S. F. Prieto; B. Escuder; J. F. Miravet. Molecular Hydrogels from Bolaform Amino Acid Derivatives: A Structure-Properties Study Based on the Thermodynamics of Gel Solubilization. *Chem. Eur. J.* **2012**, *18*, 4063-4072.
27. L. Senthilkumar; T. K. Ghanty; S. K. Ghosh; P. Kolandaivel. Hydrogen Bonding in Substituted Formic Acid Dimers. *J. Phys. Chem. A* **2006**, *110*, 12623-12638.
28. G. Zhu; J. S. Dordick. Solvent Effect on Organogel Formation by Low Molecular Weight Molecules. *Chem. Mater.* **2006**, *18*, 5988-5995.
29. Y. Hirashima; H. Sato; A. Suzuki. ATR-FTIR Spectroscopic Study on Hydrogen Bonding of Poly(N-isopropylacrylamide-co-sodium acrylate) Gel. *Macromolecules* **2005**, *38*, 9280-9286.
30. L. F. Pacios. *Hydrogen Bonding: New Insights*. Grabowski, S. J. Eds.; Springer: Dordrecht, 2006.

31. S. Zhang. A Reliable and Efficient First Principles-Based Method for Predicting pKa Values. 4. Organic Bases. *J. Comput. Chem.* **2012**, *33*, 2469-2482.
32. C. D. Blundell; P. L. Deangelis; A. Almond. Hyaluronan: The Absence of Amide-Carboxylate Hydrogen Bonds and the Chain Conformation in Aqueous Solution are Incompatible with Stable Secondary and Tertiary Structure Models. *Biochem. J.* **2006**, *396*, 487-498.

## Chapter 4

### Self-assembly of a bile acid derivative in aqueous solutions:

#### From nanofibers to nematic hydrogels\*

##### Abstract

A mixture of a cholic acid dimer with a secondary amine group and formic acid at a molar ratio of 1/1 is regarded as an organic salt and it self-assembles in aqueous solutions to form monodisperse nanofibers. The nanofibers are separated at low concentrations of the mixture but entangle with each other at high concentrations to form well-dispersed and randomly-arranged 3-D fibrous networks. Above the minimum gelation concentration of the dimer, the fibrous network is strong enough to gelate the aqueous solutions to form a hydrogel. Hydrogels obtained from the dimer salt at a lower concentration are isotropic and show dark field under polarized microscope, whereas they become anisotropic (i.e. nematic hydrogels) upon increasing the dimer salt concentration or under physical stirring. The parallel arrangement of nanofibers from randomly-directed fibrous networks may be responsible for the formation of such nematic hydrogels.

##### 4.1 Introduction

Molecular gels may exist as self-assembled fibrillar networks (SAFINs) due to the interaction of low-molecular-weight gelators and specific solvents.<sup>1</sup> The fibers have

---

\*Published as an article: M. Zhang; C. Fives; K. C. Waldron; X. X. Zhu. *Langmuir* **2017**, 10.1021/acs.langmuir.6b04033

Contributions of author other than supervisors

Meng Zhang: Experimental design and conduction, data analysis, manuscript writing.

Colin Fives: Rheological measurements and optical microscopic observation of hydrogels.



diameters of nanometers and lengths in excess of micrometers, and can entangle with each other to yield stable 3-D networks, which immobilize the solvent via surface tension.<sup>2</sup> Molecular gels are mostly isotropic with well-dispersed and randomly-directed nanofibers, whereas some of them have been reported to behave as lyotropic liquid crystals, thus the so-called “nematic gels”.<sup>3-6</sup> Such nematic molecular gels may be useful in applications such as tissue engineering, cell culture and mechano-optical sensing.<sup>6-7</sup>

Bile acids are natural compounds that exist in large quantities in the gallbladder of humans and most animals, acting as emulsifiers to promote the digestion and absorption of lipids and fat-soluble vitamins.<sup>8</sup> Their sodium salts were reported to form micelles or lyotropic liquid crystals in aqueous solutions depending on their concentrations,<sup>9</sup> and sodium lithocholate, the most hydrophobic bile acid sodium salt, was reported to form monodispersed nanotubes with ordered arrangement.<sup>10-14</sup> A series of bile acid derivatives have been shown to gelate in either organic solvents or aqueous solutions,<sup>15-19</sup> yielding organogels or hydrogels, some of which behaved as liquid crystals and showed optical textures when observed by a polarized optical microscope.<sup>20-21</sup> The mechanism for such liquid crystalline behavior of gels based on bile acids, however, remains unclear to date.

Previous work in our group showed that a cholic acid dimer with a diethylenetriamine linker can interact with various carboxylic acids by the protonation of the secondary amine group of the dimer and hydrogen bonding with the amide group to yield hydrogels.<sup>22</sup> We found that some of these hydrogels show iridescent optical textures under crossed polarized films when a relatively high concentration of the gelator is present. Inspired by this discovery, we studied the concentration-dependent self-assembling behavior of a mixture of the same dimer and formic acid at a molar ratio of 1/1. Formic acid is selected for its simplicity in all the carboxylic acids tested. The acid-base interaction between the carboxylic acid group and the secondary amine group on the dimer forms an organic salt. We discuss both the optical and mechanical properties of the hydrogels, which are observed to depend on the concentration of the dimer salt. The study of the hydrogels based on this organic salt will lead to a better understanding of the molecular hydrogelation system.

## 4.2 Experimental section

*Materials and methods.* All the chemicals were purchased from Sigma-Aldrich and used without further purification. The samples were prepared with fresh Milli-Q water. The calculated amount of the cholic acid dimer and formic acid were dissolved in water under heating to obtain a solution with desired concentrations of the dimer salt. The hot solution was cooled down and equilibrated at room temperature for several hours. The samples were examined for signs of gelation by inversion of vials.

*Fluorescence spectroscopy.* Pyrene was dissolved in acetone and diluted with water to obtain a stock solution of 0.3  $\mu\text{M}$ , which was used throughout the fluorescence measurements. A stock solution of the dimer/formic acid salt having a concentration of 1.0 mM was prepared in the pyrene stock solution and diluted afterward with the pyrene stock solution to the desired concentrations. The samples were equilibrated at room temperature for 24 hours before use. The emission fluorescence spectra of pyrene were recorded at room temperature on a Cary Eclipse fluorescence spectrophotometer (Agilent Technologies) with an excitation wavelength at 335 nm. The slit widths of excitation and emission were both at 2.5 nm. The intensity ratio of the third over the first emission band ( $I_3/I_1$ ) was measured to monitor the relative hydrophobicity of the environment around pyrene.<sup>23</sup>

*Rheology.* The rheological tests of the hydrogel samples were carried out on an AR 2000 rheometer (TA Instruments) with a cone geometry of 40 mm diameter, and a fixed gap of 55  $\mu\text{m}$  between the geometry and the plate was used during the measurements. The hydrogel samples were “melted” in a water bath at 60 °C, and aliquots of the hot solutions were put in the center of the rheometer plate and allowed to cool to re-form the hydrogel. The storage modulus ( $G'$ ) and loss modulus ( $G''$ ) were measured at 25 °C with a very small oscillatory stress of 0.05 Pa and an oscillatory frequency of 1 Hz until a plateau was reached. The oscillatory stress sweep test was conducted afterward at 25 °C with a constant oscillatory frequency of 1 Hz. Both  $G'$  and  $G''$  remained constant when the oscillatory stress was small but started to decrease at higher values of stress. The oscillatory stress causing a 10% decrease in  $G'$  was regarded as the yielding stress.<sup>24</sup>

Measurements of both moduli and yielding stress ( $\delta^*$ ) were repeated three times to obtain the average value and error. Oscillatory temperature sweep experiments were performed in the range of 20-70 °C at 1 Hz with an oscillatory stress of 0.5 Pa.

*Transmission electronic microscopy (TEM).* The hydrogel samples were drop-casted on carbon-coated copper grids (300 mesh, Carbon Type-B, Ted Pella, Inc.) at room temperature and dried under vacuum. Samples were observed on FEI Tecnai 12 TEM at 80 kV, equipped with AMT XR80C CCD camera system.

*Polarized optical microscopy (POM).* Hydrogel samples were melted and the resultant hot solution was transferred into the 1 mm quartz cells and cooled down at room temperature to re-form the hydrogels. The hydrogels were observed under an Axioskop polarized optical microscope (Zeiss).

*Small-angle X ray scattering (SAXS).* The hot solutions with desired concentration of the dimer salt were transferred into glass capillaries (1.5 mm diameter, Cedarlane) and equilibrated at room temperature to re-form the hydrogel. The glass capillaries were then fixed inside a vacuum chamber of a Nanostar X-ray instrument (Bruker) with a Vantec 2000 2-D detector and a 50 kV 0.6 mA generator, at a sample-to-detector distance of 107.25 cm. The SAXS measurements were carried out using a scanning time of 2 h at room temperature on a pressure below 0.2 mbar. Both the scattering images and curves were obtained by solvent subtraction.

### **4.3 Results and discussion**

We recently reported that a cholic acid dimer linked via a secondary amine tether formed hydrogels with selected carboxylic acids by the protonation and hydrogen bonding of its secondary amine and amide groups.<sup>22</sup> The mechanical strength of the hydrogels strongly depends on the chemical structure of the acids and the acid/dimer molar ratio. Acids that can interact with each other by hydrogen bonding and hydrophobic interactions through the side chains yielded stronger hydrogels with the dimer, and a hydrogel was

obtained only when the  $[-\text{COOH}]/[\text{dimer}]$  ratio was equal or higher than 2, whereas too much acid weakened the hydrogels.<sup>22</sup> Exceptionally, formic acid was able to form a hydrogel with the dimer at a molar ratio of 1/1 because the carboxylic acid group and formyl group are able to participate in hydrogen-bonding with the amide groups on the dimer, in addition to the protonation of the secondary amine group. To study the concentration-dependent properties of the hydrogels without variation of the acid/dimer ratio, the cholic acid dimer and formic acid was mixed at a molar ratio of 1/1 in aqueous solutions to yield an organic salt and its self-assembling behavior is shown by the images in Fig. 1. The optical and mechanical properties of the hydrogel depend strongly on the concentration of the dimer salt, as discussed in more details further on.

The formic acid/dimer salt was produced in water to form transparent solutions at low concentrations. A stable transparent hydrogel was obtained when the concentration of the dimer salt was higher than 8 mM, which is the minimum gelation concentration (MGC). Hydrogels with the dimer salt slightly higher than the MGC were isotropic. For example, a hydrogel with 14 mM dimer salt showed extinction when observed by both POM and crossed polarized films (Fig. 1B). Such a hydrogel may be disrupted to yield a viscous liquid after agitation, which behaves as a liquid crystal showing colorful textures between crossed polarized films (Fig. 1C). Such textures indicate the existence of ordered aggregates upon agitation, which can weaken the gels.<sup>10</sup> When the dimer salt concentration reaches 15 mM, the hydrogel samples show optical textures when observed under POM, and gels with even higher dimer salt concentration show brighter textures (Figs. 1D to F). When a hydrogel at a dimer concentration of 25 mM was equilibrated at 45 °C ( $T_{\text{gel-sol}}$  of the hydrogel with 25 mM dimer salt is about 55 °C) for 20 minutes, the nematic hydrogel changed to an isotropic one.

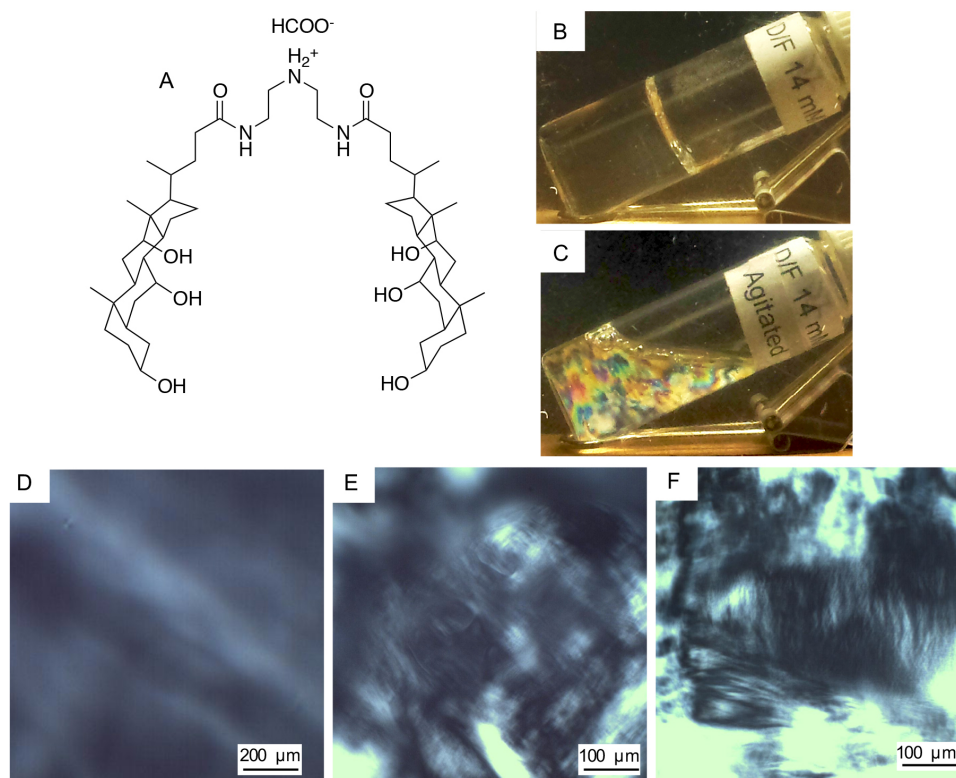


**Figure 4.1** (A) The chemical structure of the formic acid/cholic acid dimer salt. The hydrogel made from 14 mM the dimer salt observed between the crossed polarized film (B) before and (C) after agitation. The POM images of hydrogels having the dimer salt at concentrations of (D) 15 mM, (E) 20 mM, and (F) 25 mM.

Fluorescence spectroscopy is effective in the study of the formation of assemblies. Pyrene was used as a probe to study the self-assembling behavior of the organic salt in aqueous solutions. The intensity ratio of the third ( $I_3$ ) over the first ( $I_1$ ) emission peaks is sensitive to the environment in which the nonpolar pyrene molecules are located, where a higher  $I_3/I_1$  ratio indicates the probes is in a more hydrophobic environment.<sup>25-26</sup> At low concentrations of the dimer salt, the value of the  $I_3/I_1$  ratio in pyrene fluorescence spectra did not show an obvious change and remained similar to that in pure water (Fig. 2), indicating that the dimer salt was soluble in water as free molecules. The value of  $I_3/I_1$  only started to rise when the dimer salt concentration was higher than 60  $\mu\text{M}$ , which is regarded as the first critical aggregation concentration ( $\text{CAC}_1$ ). This concentration is much

lower than the critical micellar concentration (CMC) of sodium cholate (> 10 mM) due to the greater hydrophobicity of the dimer salt.<sup>27</sup> A second abrupt increment of the  $I_3/I_1$  ratio was observed when the concentration of the dimer salt reached 300  $\mu\text{M}$  ( $\text{CAC}_2$ ), indicating a secondary aggregation in the solution. All the pyrene molecules appear to exist as single molecules in the dimer salt solutions because no excimer peak indicative overlapped pyrenes was observed in the fluorescence spectra of the pyrene, which is different from other reported gelation systems based on bile acids.<sup>28-29</sup>

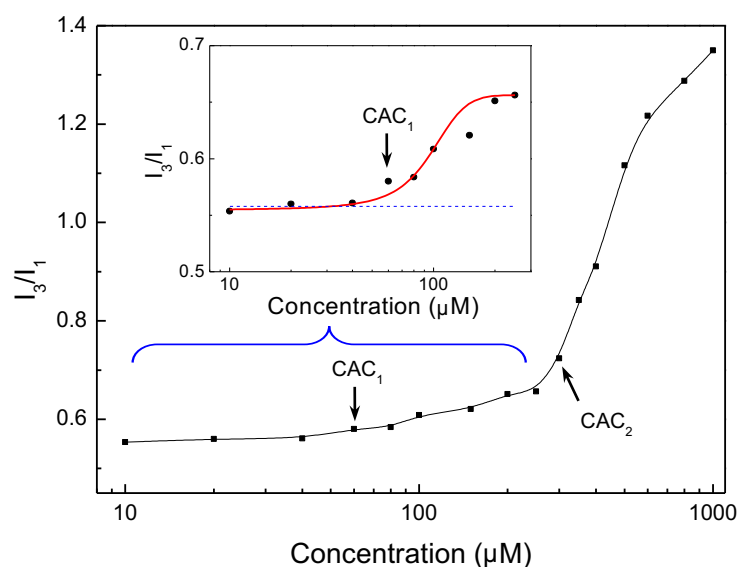


**Figure 4.2** Variation of the  $I_3/I_1$  ratio of pyrene fluorescence spectra as a function of the dimer salt concentration. The lines have been drawn as visual guides.

Rheological measurements indicate that higher concentrations of the dimer salt in water yielded hydrogels with better mechanical properties (Fig. 3). The gel-sol transition temperature ( $T_{\text{gel-sol}}$ ) increases from 49 to 57  $^{\circ}\text{C}$  when the concentrations of the dimer salt was varied from 10 to 35 mM (Fig. 3A). The enthalpy change of the gel-sol transition may be calculated by plotting the concentration against the reciprocal of  $T_{\text{gel-sol}}$  in the form of an equation developed by Eldridge and Ferry:<sup>30-32</sup>

$$\ln(C) = \frac{\Delta H}{RT_{gel-sol}} + k \quad (1)$$

where  $C$  is the concentration of the gelator,  $\Delta H$  is the enthalpy change associated with the formation of fibrous network,  $R$  is the gas constant, and  $k$  is a constant. The estimated value of  $\Delta H$  from Fig. 3A is about -139 kJ/mol.

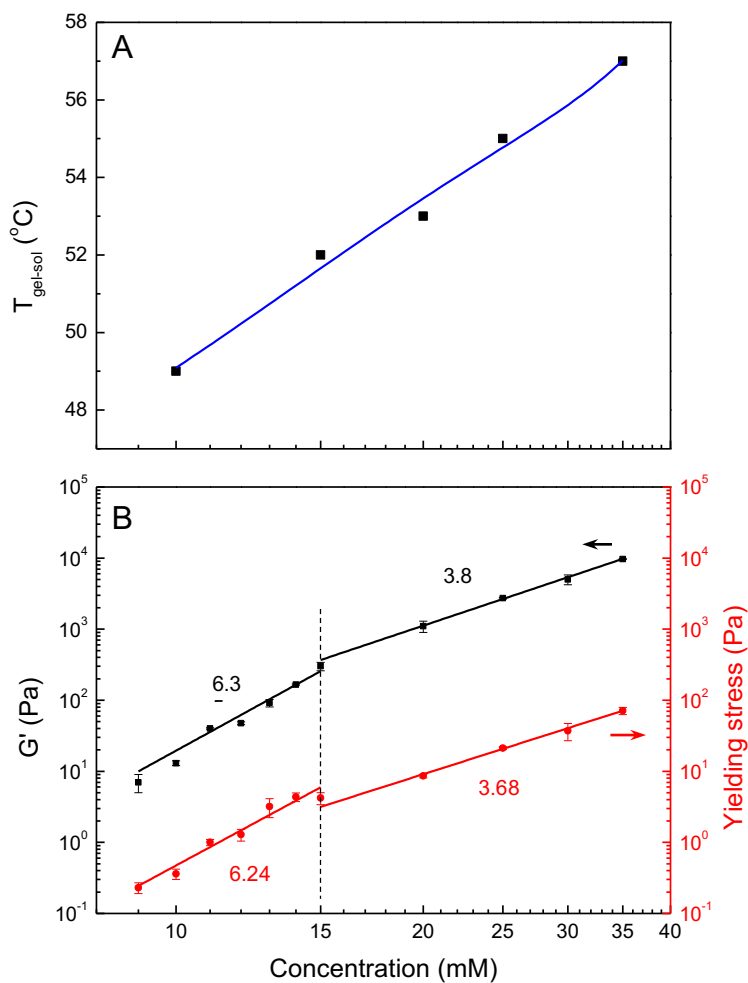


**Figure 4.3** Rheological properties of hydrogels at various concentrations of the dimer salt. (A) Gel-sol transition temperature, the blue line was drawn as a visual guide. (B) Storage modulus and yielding stress, the black and red lines were obtained from linear fitting with slope values marked besides the segments.

The properties of the entangled worm-like micelles (or nanofibers), such as storage modulus ( $G'$ ), static viscosity and self-diffusion coefficient, are strongly dependent on the concentration of the surfactant and follow scaling laws in the form of power increment (*ex.*  $G' = kC^n$ ) where the exponent values vary in different systems.<sup>33</sup> Fig. 3B shows the relationship between the value of  $G'$  of the hydrogel and concentrations of the dimer salt, and the value of  $G'$  increased for about 1000 times when the concentration of the dimer salt increased from 9 to 35 mM. The  $G'$  values follow scaling laws in the concentration ranges with different values of the scaling exponent, ranging from about 6.4 between 9 and 15 mM to about 3.9 at higher concentrations (15-35 mM, Fig. 3B). Plotting curves of the yield stress ( $\delta^*$ ) of these hydrogels with concentration also showed similar exponent values (6.2 and 3.7, respectively).

Certain molecular hydrogels based on bile acids have been studied as colloidal gels involving floc-like elements,<sup>20, 34</sup> and their mechanical properties (such as  $G'$ ) followed scaling laws with the gelator concentrations where the exponent values depended on the relative strength of interactions between and within the flocs. Two regimes can be defined: the “weak-link regime”, where the mechanical properties of the gels are determined by the inter-floc interactions, and the “strong-link regime”, where the mechanical properties are determined by the intra-floc interactions.<sup>20,34</sup> In the weak-link regime, the values of  $G'$  and  $\delta^*$  may be predicted by the following expression:<sup>35-36</sup>

$$G', \delta^* \propto C^{1/(3-d_f)} \quad (2)$$

where  $C$  is the gelator concentration and  $d_f$  is the fractal dimension of the flocs, which reflects how the mass of the colloidal material within a floc scales with the floc size. The exponent values of  $G'$  and  $\delta^*$  with the concentration in the “strong-link regime”, however, are not consistent with each other, the value of  $G'$  increases with the concentration while that of  $\delta^*$  show a decrease at high gelator concentration.<sup>35</sup> The similarity of the scaling exponent value between the  $G'$  and  $\delta^*$  (Fig. 3B) with the dimer salt concentration may indicate that this particular hydrogelation system is in the “weak-link regime”, which means that the mechanical strength of the hydrogels is mainly determined by the interactions between nanofibers via junction points.



The transmission electron microscopy (TEM) images show the morphology of the self-assemblies of the dimer salt in aqueous solutions at various concentrations (Fig. 4). Monodispersed and isolated nanofibers with diameters about 20 nm start to be observed at a dimer salt concentration of 60  $\mu\text{M}$  (Fig. 4A), corresponding to  $\text{CAC}_1$  shown in Fig. 2. Nanofibers become more abundant at higher dimer concentrations and tend to intertwine with each other to yield a network, as shown by the arrows in Fig. 4B, corresponding to the beginning of the second aggregation concentration ( $\text{CAC}_2$ ) at 0.5 mM. The intertwined nanofibers may provide a more hydrophobic environment to accommodate the nonpolar pyrene molecules, leading to an increase of  $I_3/I_1$  on fluorescence spectra as seen in Fig. 2. With lower density of the fibers, the mixture remains as a solution and becomes a transparent hydrogel only when the concentration of the dimer salt reached the minimum gelation concentration of 8 mM, where higher density of the fibrillar networks can be observed (Fig. 4D).

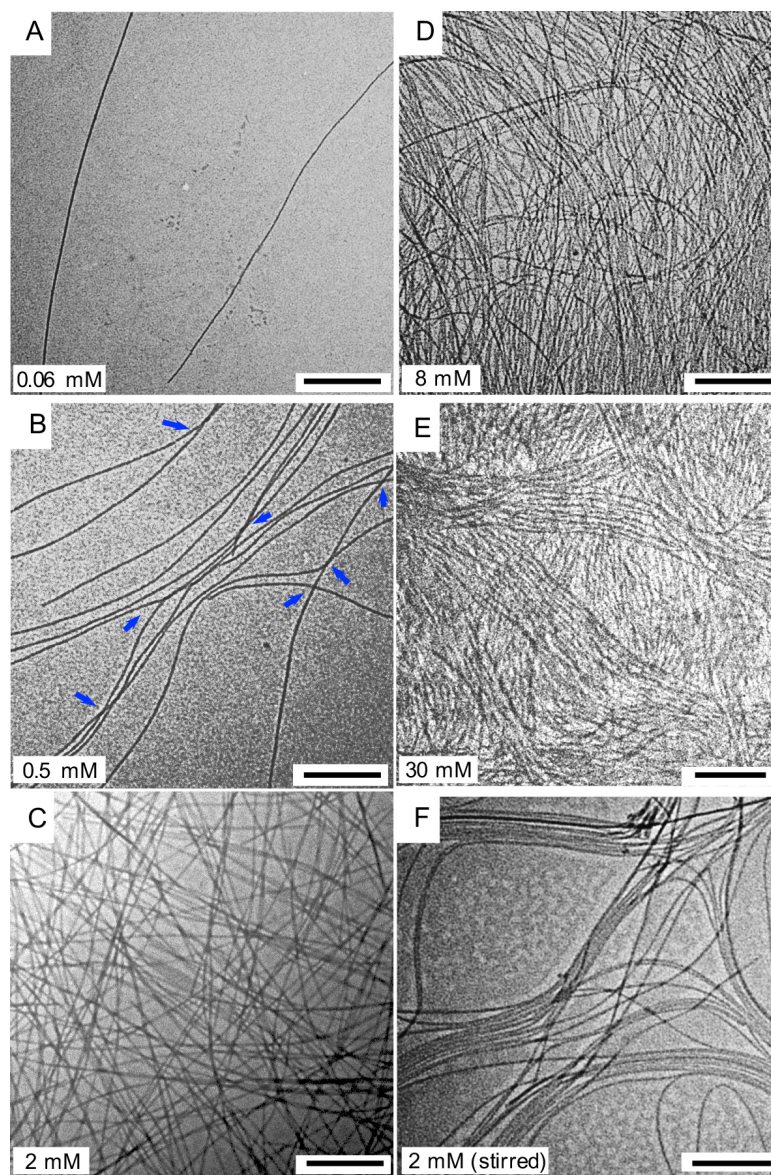


**Figure 4.4** TEM images of self-assemblies of the dimer salt in water upon equilibration at concentrations of (A) 0.06 mM (sol), (B) 0.5 mM (sol), (C) 2 mM (sol), (D) 8 mM (gel), (E) 30 mM (nematic gel), and (F) 2 mM after stirring for 30 min (sol). (Black scale bar = 500 nm).

The nanofibers in the aqueous solutions can form ordered secondary aggregates via parallel arrangement under certain conditions. For example, increasing the concentration of the dimer salt induced the ordered arrangement of the nanofibers. In a nematic hydrogel

with dimer salt concentration of 30 mM, parallel arranged nanofibers were observed by TEM (Fig. 4E). Alternatively, physical stirring of a solution of the dimer salt at 2 mM for 30 min induced alignment of the nanofibers (Fig. 4F). The stirring applies a shear force to the nanofibers so they may be aligned with the direction of the flow. Ordered nanofibers are similar to the polymer chains in a polymer crystal,<sup>37</sup> and may be responsible for the liquid crystalline properties of hydrogels when the concentration of the dimer salt is above 15 mM or the salt solution is stirred (Figs. 1D to F).<sup>4,5</sup> Such parallel fibrous arrangements can also reduce the density of the junction points between nanofibers, which is the determining factor for the elasticity of hydrogels. Therefore, a hydrogel having such ordered structures may be weaker than one having randomly directed fibrillar networks at the same concentration.<sup>10</sup> For example, agitation of a stable isotropic hydrogel leads to the formation of a nematic fluid (Figs. 1C and F). Formation of such aligned fibrous aggregates may also be responsible for the lower scaling exponent values of both  $G'$  and  $\delta^*$  for the nematic hydrogels than that from isotropic gels at low concentrations. The aligned aggregates in nematic gels may increase the degree of anisotropy and reduce the value of the fractal dimension from a randomly distributed fibrous network,<sup>38-39</sup> which subsequently yield lower scaling exponent values in Fig. 3 according to equation 2 (the estimated values of  $d_f$  from the scaling exponents in Fig. 3B are about 2.84 and 2.73 for the concentration ranges of 9-15 and 15-35 mM, respectively).

Small-angle X-ray scattering (SAXS) experiment was conducted to characterize the hydrogels based on the dimer salt. When the test capillary tube was placed in the instrument vertically, the 2-D SAXS pattern of a hydrogel sample with 30 mM dimer salt showed a strongly anisotropic pattern of two intense spots lying along the horizontal equatorial line (Fig. 5A). Such an image indicates that the nanofibers in the hydrogel are highly oriented with an elongational axis parallel to the capillary axis, which confirms the observation of ordered aggregates by TEM (Fig. 4E). The SAXS diffractogram in Fig. 5B shows the relationship between the intensity ( $\log I$ ) and the scattering vector ( $\log Q$ ), where  $Q$  is equal to  $(4\pi/\lambda) \sin\theta$ . Theoretically, the intensity of the SAXS diffractogram ( $I$ ) for a solid nanofiber with a diameter of  $D$  may be modeled by the following expression:<sup>10,40</sup>

$$I \propto \left[ \frac{J_1(QD/2)}{QD/2} \right]^2 \quad (3)$$

where  $J_1(QD/2)$  is the Bessel function of the first kind. However, a peak mismatch was found between the experimental spectrum and the theoretical modeling curve of the nanofibers for  $D = 20$  nm (Fig. 5B, red line, where the diameter value was estimated from Fig. 4A), whereas a modeling curve of nanofibers with  $D = 28$  nm shows the same peak as the experimental spectrum (Fig. 5B, blue line). This is about 8 nm thicker than the fibers observed by TEM since the sample in the SAXS measurements remained hydrated while that for the TEM experiments was dried. The difference of 8 nm represents most probably the thickness of the water layer between two parallel and adjacent fiber segments.

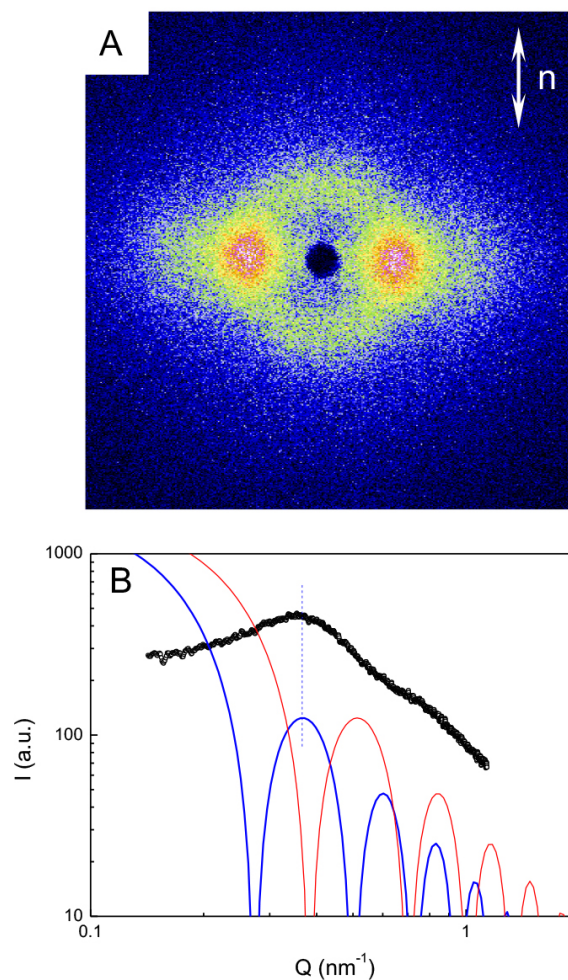


**Figure 4.5** SAXS result of a nematic hydrogel sample with 30 mM dimer salt. (A) 2-D SAXS pattern image. The white arrow indicates the director  $n$  of the nematic hydrogel. (B) SAXS diffractogram of the hydrogel (black open circles), theoretical fitting curve of for nanofibers of 20 nm diameter (red line), and theoretical fitting curve for 28 nm nanofibers (blue line).

#### 4.4 Conclusions

Gelation can be regarded as an intermediate transient state for a solution to crystallize when the solute molecules are more ordered, or to precipitate when the solute molecules are disordered. The nematic hydrogels obtained in this study exemplify the final state of the system with ordered fine structures/morphologies observed microscopically. In

summary, an organic salt based on the cholic acid dimer and formic acid can self-assemble in aqueous solutions to form nanofibers above its CAC of 60  $\mu\text{M}$ . The isolated nanofibers entangle with each other at concentrations above the CAC. When the concentration of the dimer salt reaches the minimum gelation concentration, the 3-D network of entangled nanofibers is strong enough to immobilize the aqueous solution and form a stable hydrogel. The randomly directed fibrous network then transits to ordered aggregates with aligned nanofibers upon the stirring of the hydrogel or at high salt concentrations. The aligned nanofibers cause changes in both the optical and mechanical properties of hydrogels, and make them behave as liquid crystals, although showing weaker mechanical strength of the hydrogels or lower scaling exponent value with concentrations. Such hydrogels are sensitive to a change in their environment change and may find use in areas such as drug delivery and cell culture.<sup>7</sup> Formic acid has been studied in detail here, but such a behavior is more general and was also observed for the cholic acid dimer salts with other carboxylic acids, such as acetic acid, succinic acid and tartaric acid.

## 4.5 Acknowledgments

Financial support from NSERC of Canada and FQRNT of Quebec is gratefully acknowledged. We thank Prof. C. Geraldine Bazuin for helpful discussion and Ms. Francine Belanger for her help with SAXS measurements. Meng Zhang thanks the Chinese Scholarship Council (CSC) for a scholarship.

## 4.6 References

1. R. G. Weiss; P. Terech. *Molecular Gels: Materials with Self-Assembled Fibrillar Networks*. Springer: Dordrecht, 2006.
2. L. A. Estroff; A. D. Hamilton. Water Gelation by Small Organic Molecules. *Chem. Rev.* **2004**, *104*, 1201-1218.

3. J. Campbell; M. Kuzma; M. M. Labes. A Nonaqueous Lyotropic Nematic Gel. *Mol. Cryst. Liq. Cryst.* **1983**, *95*, 45-50.
4. J. H. Ryu; M. Lee. Transformation of Isotropic Fluid to Nematic Gel Triggered by Dynamic Bridging of Supramolecular Nanocylinders. *J. Am. Chem. Soc.* **2005**, *127*, 14170-14171.
5. Z. Huang; H. Lee; E. Lee; S. K. Kang; J. M. Nam; M. Lee. Responsive Nematic Gels from the Self-Assembly of Aqueous Nanofibres. *Nat. Commun.* **2011**, *2*, 459.
6. S. Zhang; M. A. Greenfield; A. Mata; L. C. Palmer; R. Bitton; J. R. Mantei; C. Aparicio; M. O. de la Cruz; S. I. Stupp. A Self-Assembly Pathway to Aligned Monodomain Gels. *Nat. Mater.* **2010**, *9*, 594-601.
7. Z. L. Wu; J. P. Gong. Hydrogels with Self-Assembling Ordered Structures and Their Functions. *NPG Asia Mater.* **2011**, *3*, 57-64.
8. B. Staels; V. A. Fonseca. Bile Acids and Metabolic Regulation: Mechanisms and Clinical Responses to Bile Acid Sequestration. *Diabetes Care* **2009**, *32 Suppl 2*, S237-245.
9. H. Amenitsch; H. Edlund; A. Khan; E. F. Marques; C. La Mesa. Bile Salts Form Lyotropic Liquid Crystals. *Colloids Surf. A Physicochem. Eng. Asp.* **2003**, *213*, 79-92.
10. P. Terech; A. de Geyer; B. Struth; Y. Talmon. Self-Assembled Monodisperse Steroid Nanotubes in Water. *Adv. Mater.* **2002**, *14*, 495-498.
11. P. Terech; Y. Talmon. Aqueous Suspensions of Steroid Nanotubules: Structural and Rheological Characterizations. *Langmuir* **2002**, *18*, 7240-7244.
12. B. Jean; L. Oss-Ronen; P. Terech; Y. Talmon. Monodisperse Bile-Salt Nanotubes in Water: Kinetics of Formation. *Adv. Mater.* **2005**, *17*, 728-731.
13. P. Terech; S. Friol; N. Sangeetha; Y. Talmon; U. Maitra. Self-Assembled Nanoribbons and Nanotubes in Water: Energetic vs Entropic Networks. *Rheol. Acta* **2005**, *45*, 435-443.
14. P. Terech; N. M. Sangeetha; S. Bhat; J.-J. Allegraud; E. Buhler. Ammonium Lithocholate Nanotubes: Stability and Copper Metallization. *Soft Matter* **2006**, *2*, 517-522.
15. H. Svobodová; V. Noponen; E. Kolehmainen; E. Sievanen. Recent Advances in Steroidal Supramolecular Gels. *RSC Adv.* **2012**, *2*, 4985-5007.

16. S. Bhat; U. Maitra. Nanoparticle-Gel Hybrid Material Designed with Bile Acid Analogues. *Chem. Mater.* **2006**, *18*, 4224-4226.
17. P. Dastidar; S. Okabe; K. Nakano; K. Iida; M. Miyata; N. Tohnai; M. Shibayama. Facile Syntheses of a Class of Supramolecular Gelator Following a Combinatorial Library Approach: Dynamic Light Scattering and Small-Angle Neutron Scattering Studies. *Chem. Mater.* **2005**, *17*, 741-748.
18. M. Zhang; S. Strandman; K. C. Waldron; X. X. Zhu. Supramolecular Hydrogelation with Bile Acid Derivatives: Structures, Properties and Applications. *J. Mater. Chem. B* **2016**, *4*, 7506-7520.
19. L. Galantini; M. C. di Gregorio; M. Gubitosi; L. Travaglini; J. V. Tato; A. Jover; F. Meijide; V. H. Soto Tellini; N. V. Pavel. Bile Salts and Derivatives: Rigid Unconventional Amphiphiles as Dispersants, Carriers and Superstructure Building Blocks. *Curr. Opin. Colloid Interface Sci.* **2015**, *20*, 170-182.
20. N. M. Sangeetha; S. Bhat; A. R. Choudhury; U. Maitra; P. Terech. Properties of Hydrogels Derived from Cationic Analogues of Bile Acid: Remarkably Distinct Flowing Characteristics. *J. Phys. Chem. B* **2004**, *108*, 16056-16063.
21. A. Chakrabarty; U. Maitra. Organogels from Dimeric Bile Acid Esters: In Situ Formation of Gold Nanoparticles. *J. Phys. Chem. B* **2013**, *117*, 8039-8046.
22. M. Zhang; K. C. Waldron; X. X. Zhu. Formation of Molecular Hydrogels from a Bile Acid Derivative and Selected Carboxylic Acids. *RSC Adv.* **2016**, *6*, 35436-35440.
23. K. Kalyanasundaram; J. K. Thomas. Environmental Effects on Vibronic Band Intensities in Pyrene Monomer Fluorescence and Their Application in Studies of Micellar Systems. *J. Am. Chem. Soc.* **1977**, *99*, 2039-2044.
24. T. G. Mezger. *The Rheology Handbook: For Users of Rotational and Oscillatory Rheometers*. Vincentz Network GmbH & Co KG: 2006.
25. Y. L. Chen; J. T. Luo; X. X. Zhu. Fluorescence Study of Inclusion Complexes between Star-Shaped Cholic Acid Derivatives and Polycyclic Aromatic Fluorescent Probes and The Size Effects of Host and Guest Molecules. *J. Phys. Chem. B* **2008**, *112*, 3402-3409.
26. J. Luo; Y. Chen; X. X. Zhu. Invertible Amphiphilic Molecular Pockets Made of Cholic Acid. *Langmuir* **2009**, *25*, 10913-10917.



27. S. Gouin; X. X. Zhu. Fluorescence and NMR Studies of the Effect of a Bile Acid Dimer on the Micellization of Bile Salts. *Langmuir* **1998**, *14*, 4025-4029.
28. S. Mukhopadhyay; U. Maitra; I. Ira; G. Krishnamoorthy; J. Schmidt; Y. Talmon. Structure and Dynamics of a Molecular Hydrogel Derived from a Tripodal Cholamide. *J. Am. Chem. Soc.* **2004**, *126*, 15905-15914.
29. A. Jover; F. Mejjide; E. R. Nunez; J. V. Tato; M. Mosquera; F. R. Prieto. Unusual Pyrene Excimer Formation During Sodium Deoxycholate Gelation. *Langmuir* **1996**, *12*, 1789-1793.
30. J. E. Eldridge; J. D. Ferry. Studies of the Cross-linking Process in Gelatin Gels. III. Dependence of Melting Point on Concentration and Molecular Weight. *J. Phys. Chem.* **1954**, *58*, 992-995.
31. S. R. Raghavan; B. H. Cipriano, Gel Formation: Phase Diagrams Using Tabletop Rheology and Calorimetry. In *Molecular Gels: Materials with Self-Assembled Fibrillar Networks*, Weiss, R. G.; Terech, P., Eds. Springer: Dordrecht, 2006; p 251.
32. M. Laupheimer; N. Preisig; C. Stubenrauch. The Molecular Organogel n-Decane/12-Hydroxyoctadecanoic Acid: Sol–Gel Transition, Rheology, and Microstructure. *Colloids Surf. A Physicochem. Eng. Asp.* **2015**, *469*, 315-325.
33. J.-F. Berret, Rheology of Wormlike Micelles: Equilibrium Properties and Shear Banding Transitions. In *Molecular Gels: Materials with Self-Assembled Fibrillar Networks*, Weiss, R. G.; Terech, P., Eds. Springer: Dordrecht, 2006.
34. P. Terech; U. Maitra. Structural and Rheological Properties of Aqueous Viscoelastic Solutions and Gels of Tripodal Cholamide-Based Self-Assembled Supramolecules. *J. Phys. Chem. B* **2008**, *112*, 13483-13492.
35. M. O. Piepenbrock; G. O. Lloyd; N. Clarke; J. W. Steed. Metal- and Anion-Binding Supramolecular Gels. *Chem. Rev.* **2010**, *110*, 1960-2004.
36. H. Wu; M. Morbidelli. A Model Relating Structure of Colloidal Gels to Their Elastic Properties. *Langmuir* **2001**, *17*, 1030-1036.
37. L. C. Sawyer; D. T. Grubb; G. F. Meyers. *Polymer Microscopy*. Springer: New York, 2008.

38. A. Takahashi; R. Kita; T. Shinozaki; K. Kubota; M. Kaibara. Real Space Observation of Three-Dimensional Network Structure of Hydrated Fibrin Gel. *Colloid Polym. Sci.* **2003**, *281*, 832-838.
39. D. A. Lidar; O. Biham; D. Avnir. Limited Range Fractality of Randomly Adsorbed Rods. *J. Chem. Phys.* **1997**, *106*, 10359.
40. L. Travaglini; A. D'Annibale; K. Schillen; U. Olsson; S. Sennato; N. V. Pavel; L. Galantini. Amino Acid-Bile Acid Based Molecules: Extremely Narrow Surfactant Nanotubes Formed by a Phenylalanine-Substituted Cholic Acid. *Chem. Commun.* **2012**, *48*, 12011-12013.

## Chapter 5

# Supramolecular hydrogels formed by CO<sub>2</sub> and bile salts in water\*

### Abstract

Bubbling carbon dioxide (CO<sub>2</sub>) into aqueous solutions of bile salts such as sodium deoxycholate caused a gelation of the solution, forming a hydrogel made of entirely natural biological molecules and providing a convenient storage reservoir of CO<sub>2</sub> in water. The carboxylate group of the bile salt becomes protonated in the aqueous solutions to make the bile acid only marginally soluble in water, which induces the formation of a hydrogel with nanofibrous structures. Such hydrogels show reversible gel-sol transition by purging CO<sub>2</sub> and N<sub>2</sub> alternatively. The mechanical properties of the hydrogels may be varied by the amounts of CO<sub>2</sub> in the media, reaching a peak value of the storage modulus of the hydrogel. Bubbling CO<sub>2</sub> initially yielded a transparent hydrogel which upon continued purging became mechanically stronger but finally rather opaque. The hydrogels may be mechanically strengthened by the addition of inorganic salts such as NaCl.

### 5.1 Introduction

Bile acids are natural compounds in the body of humans and most animals and help in the digestion of fats and fat-soluble nutrients. Though amphiphilic in nature, bile acids are generally hydrophobic and their solubility in water is limited.<sup>1</sup> In their salt form,

---

\*M. Zhang and X. X. Zhu. Submitted for publication as a communication in *Angew. Chem. Int. Ed.*

Contributions of author other than supervisor

Meng Zhang: Experimental design and conduction, data analysis, manuscript writing.

however, they are quite soluble in water to form micelles or lyotropic liquid crystals depending on their concentration.<sup>2</sup>

CO<sub>2</sub> is a common and nontoxic gas and has gained much attention due to its environmental importance and its potential applications. It may be bound to polymers bearing primary or secondary amine in non-aqueous solutions to form carbamates, making polymer chains cross-linked to yield organogels that may be useful in paint surface cleaning.<sup>3-4</sup> Organogels may be obtained by the binding of CO<sub>2</sub> to primary or secondary amines bearing relatively long alkyl chains in organic solvents such as ethanol, DMSO, and silicon oil.<sup>5-6</sup> CO<sub>2</sub> is slightly soluble in water and its acidity helps to protonate functional groups such as carboxylates and amines, changing the hydrophobicity of certain pH-responsive polymers and their aggregation behaviors in aqueous solutions,<sup>7-11</sup> and may induce gel-sol phase transition in such polymers.<sup>12</sup>

Several low-molecular-weight compounds with long alkyl chains bearing amine group were reported to interact with CO<sub>2</sub> to form supramolecular hydrogels with worm-like micelles (nanofibers) in aqueous solutions.<sup>13-15</sup> The hydrogels were quite weak with a complex modulus lower than 10 Pa (at 2 wt% of gelators), which may restrict their applications. In this work, we found that bubbling CO<sub>2</sub> into the aqueous solutions of bile salts such as NaDC yielded hydrogels with varying mechanical strengths. The appearance and mechanical properties of the hydrogels were found to depend strongly on the amount of CO<sub>2</sub> introduced.

## 5.2 Results and discussions

We have tested several bile salts for their gelation behavior in water with CO<sub>2</sub>. The ease of gelation is found to depend on the relative hydrophilicity of the bile salt. Sodium cholate (NaC), the most hydrophilic one, does not form a hydrogel even after purging with CO<sub>2</sub> (Fig. 5.S1A). The most hydrophobic bile salt, sodium lithocholate (NaLC, Fig. 5.1A), however, already forms a hydrogel when its concentration in water is sufficiently high (3 wt%, Fig. 5.S1E). At a lower concentration (2 wt%, Fig. 5.S1D), a bluish viscous

solution is obtained, which turns into an opaque hydrogel upon purging with CO<sub>2</sub> (Fig. 5.S1C), and the gelation is thermally irreversible. NaDC and sodium chenodeoxycholate (NaCDC) (Fig. 5.1A) are intermediate in terms of hydrophilicity among the bile acids and may be dissolved in water to form transparent solutions, which can then turn into hydrogels upon bubbling of CO<sub>2</sub> (Figs. 5.1B and 5.S1B). A hydrogel based on sodium deoxycholate (NaDC) can be obtained within several minutes after bubbling CO<sub>2</sub>, while the formation of a stable hydrogel by NaCDC requires a longer equilibration time (more than 24 h). Therefore, NaDC is taken as a convenient example to study the hydrogels based on bile salts and CO<sub>2</sub>, due to its advantages such as fast gelation and thermo-reversibility. Bubbling CO<sub>2</sub> into the aqueous solutions of NaDC yields a weak transparent hydrogel initially (at 1 or 2 s, Fig. 5.1C), and then an opaque hydrogel when purged longer with CO<sub>2</sub> (at ca. 5 s, Fig. 5.1D). These transparent and opaque hydrogels may both transit back to transparent solutions by heating and by bubbling N<sub>2</sub>. The sol-gel transition process is reversible and repeatable (Fig. 5.1).

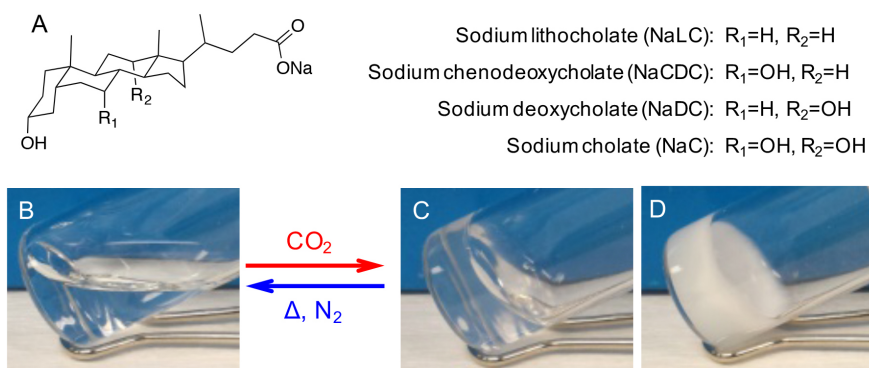


**Figure 5.1** (A) The chemical structure of NaLC, NaCDC, NaDC, and NaC. (B) An aqueous solution of 2 wt% NaDC. (C) A transparent hydrogel with 2 wt% NaDC by bubbling CO<sub>2</sub> for 2 s, (D) An opaque hydrogel with 2 wt% NaDC by bubbling CO<sub>2</sub> for 5 s.

Bile salts form micelles in aqueous solutions above the critical micelle concentration (CMC), which may vary with the temperature,<sup>16</sup> ionic strength,<sup>17</sup> and the presence of additives such as a dimeric bile salt.<sup>18</sup> Pyrene may be used as a fluorescent probe to study

the micellization of lipids by monitoring the changes of the intensity ratio of the third to the first peak ( $I_3/I_1$ ) of its fluorescence spectrum.<sup>19</sup> A two-step increment of the  $I_3/I_1$  ratio (Fig. 5.S2) indicates the formation of primary and secondary micelles at concentrations of approximately 3 and 5 mM, respectively<sup>16,20</sup>.

The morphological transition of NaDC in aqueous solutions with various amounts of  $\text{CO}_2$  was studied by transmission electron microscope (TEM). NaDC (at 10 mM) forms non-spherical micelles in aqueous solutions with an average diameter of about 10 nm (Fig. 5.2A), which are the secondary micelles of NaDC with aggregation numbers of 10-100.<sup>21</sup> When the concentration of  $\text{CO}_2$  reaches 4 mM in the solution, NaDC self-assembles to form nanofibers with diameters about 10-20 nm (Fig. 5.2B), and a transparent hydrogel is obtained. When the concentration of  $\text{CO}_2$  further increases to 40 mM, the hydrogel becomes opaque, and a mixture of thin nanofibers and thicker nano-shreds is obtained (Fig. 5.2C).

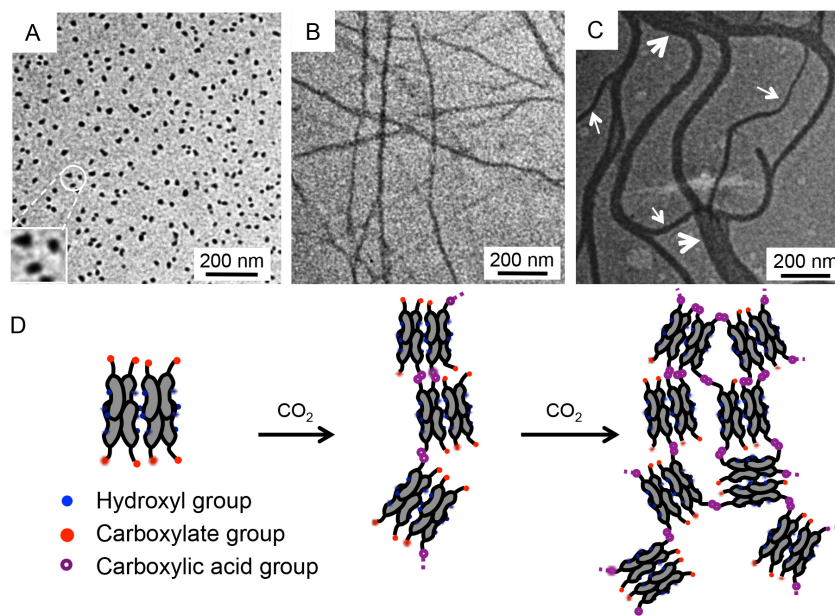


**Figure 5.2** TEM images of (A) aqueous solution with 10 mM NaDC, (B) transparent hydrogel with 10 mM NaDC and 4 mM  $\text{CO}_2$ , and (C) opaque hydrogel with 10 mM NaDC and 40 mM  $\text{CO}_2$ . (D) Schematic representation of the mechanism for the formation of hydrogels from aqueous solutions of NaDC and further aggregation with increasing contents of  $\text{CO}_2$ .

It is known that the carboxylate and hydroxyl groups of bile salts face the aqueous environment to stabilize the micelles, and the hydroxyl groups on the surface of micelles may interact with each other to yield secondary micelles.<sup>22</sup> When CO<sub>2</sub> is introduced into the aqueous solutions containing NaDC micelles, the carboxylate groups may be protonated. The micelles may be linked through hydrogen bonding between the protonated carboxylate groups, yielding nanofibers with a diameter in the same range of the size of the NaDC micelles (Fig. 5.2B), and leading to the formation of transparent hydrogels. With increasing content of CO<sub>2</sub>, more of the carboxylate groups become protonated, facilitating the formation of more hydrogen bonds between the nanofibers, yielding thicker nano-shreds (opaque gels). The process is illustrated in Fig. 5.2D.

The mechanical properties of the hydrogels depend on the content of CO<sub>2</sub> in the solutions. At a low concentration of CO<sub>2</sub> (8 mM), the NaDC solution (23 mM, 1 wt%) remains transparent without the formation of a hydrogel. Increasing the concentration of CO<sub>2</sub> to 12 mM, a weak transparent hydrogel with a storage modulus (G') of 16 Pa is obtained, but turns more opaque and stronger (G' about 46 Pa) when the concentration of CO<sub>2</sub> reaches 40 mM. Beyond this point, the hydrogel becomes more turbid and weaker (Fig. 5.3A), which may be caused by the formation of thicker nano-shreds (Fig. 5.2C) that may reduce the homogeneity and the density of the junction points in the 3-D network.<sup>23</sup> The initial gels are rather weak like most of the hydrogels based on NaDC,<sup>24-25</sup> but the gelation process increases the amount of CO<sub>2</sub> absorbed in the aqueous mixture and further stabilizes the dissolved CO<sub>2</sub>. This is in agreement with the observation that aqueous solutions of NaDC formed hydrogels when the pH value of the solution is reduced to around 7,<sup>26-29</sup> and further decrease in pH causes the weakening of the hydrogels or precipitation.<sup>24,28</sup>

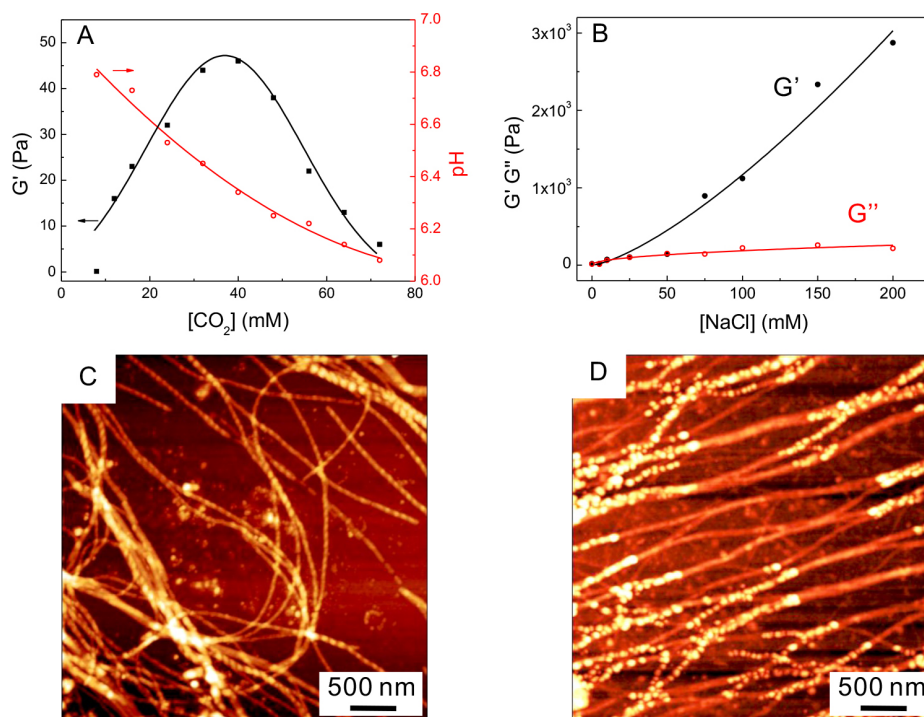


**Figure 5.3** Mechanical properties and morphology of hydrogels obtained from NaDC (23 mM) and CO<sub>2</sub>. (A) The variations of G' and pH value of the system with the concentration of CO<sub>2</sub>. (B) Variation of G' and G'' of the hydrogel at 40 mM CO<sub>2</sub> with the addition of NaCl in the mixture. The lines are drawn as visual guides. AFM images of hydrogels (C) with 40 mM CO<sub>2</sub> and (D) with 40 mM CO<sub>2</sub> and 200 mM NaCl.

The mechanical strengths of the hydrogels of NaDC and CO<sub>2</sub> may be improved by the addition of inorganic salts such as NaCl, due to the salting-out effect (Fig. 5.3B). In a hydrogel with 23 mM NaDC and 40 mM CO<sub>2</sub>, the storage and loss moduli G' and G'' are low and similar in value when the concentration of NaCl is low (<50 mM). When the concentration of NaCl is higher (>75 mM), the G' of hydrogel increases significantly to about 3000 Pa when NaCl concentration reaches 200 mM, while the G'' value does not show any significant change. These hydrogels are among the toughest gels with storage moduli much higher than those of the NaDC hydrogels formed in phosphate buffer solutions (~1000 Pa for a gel with 174 mM NaDC, > 7 times more concentrated than the solutions used in the present work) or formed by the addition of HCl (~3 Pa for a gel with 100 mM NaDC) and organic acids (~600 Pa for a gel with a mixture of 200 mM NaDC



and 20 mM L-tartaric acid).<sup>24, 29-30</sup> Higher concentrations of NaCl beyond 300 mM caused the formation of white precipitates.

The atomic-force microscope (AFM) images show the morphology variations of the hydrogels induced by salting-out effect (Figs. 5.3C and D). The image of the turbid hydrogel with 23 mM NaDC and 40 mM CO<sub>2</sub> shows a mixture of fine nanofibers and thicker nano-shred (Fig. 5.3C), which is consistent with the TEM image of the opaque hydrogels (Fig. 5.2C). Upon the addition of NaCl, the transparent hydrogel shows a network of well-dispersed nanofibers with diameters of about 60-100 nm without any thick nano-shred (Fig. 5.3D). The addition of NaCl into the solution of NaDC and CO<sub>2</sub> interferes the formation of large aggregates during the gelation process. The hydrophobic interaction between NaDC molecules may be enhanced by the salting-out effect of NaCl,<sup>31</sup> leading to the formation of stronger nanofibers, and thus hydrogels of improved mechanical strength and higher transparency.

The FT-IR spectrum of deoxycholic acid (DCA) shows two peaks at 1715 and 1698 cm<sup>-1</sup> (Fig. 5.4A), related to the C=O stretching vibration of free and hydrogen-bonded carboxylic acid groups, respectively. The sharp peak at 3550 cm<sup>-1</sup> confirms the existence of free carboxylic acid groups. These bands are absent in the spectrum of NaDC. Instead, NaDC shows a different band at 1555 cm<sup>-1</sup> (Fig. 5.4B), which is related to the C=O stretching vibration of the carboxylate group. The hydrogels were then freeze-dried to obtain aerogels, which showed both peaks of the carboxylate and hydrogen-bonded carboxylic acid, and the intensity of the latter peak increased with increasing content of CO<sub>2</sub> in the gel (Figs. 5.4C-F). The change in the IR spectra indicates the gradual protonation of the carboxylate groups by interacting with CO<sub>2</sub> and hydrogen-bonding. The hydrogen bonding of the carboxylic acid groups may be crucial to the formation of the hydrogels.

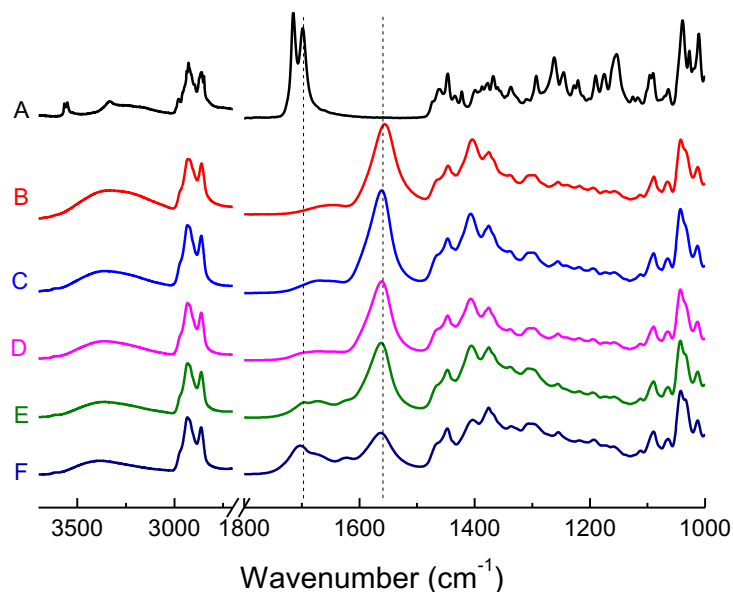


**Figure 5.4** FT-IR spectra of (A) DCA; (B) NaDC; and the freeze-dried aerogels of 23 mM NaDC with CO<sub>2</sub> at a concentration of (C) 16 mM, (D) 24 mM, (E) 48 mM, and (F) 64 mM.

### 5.3 Conclusions

In summary, bubbling CO<sub>2</sub> into the aqueous solutions of selected bile salts such as NaDC and NaCDC led to the formation of hydrogels. The gels are generally weak but provide an interesting way to absorb and maintain CO<sub>2</sub> in water. The otherwise water-soluble bile salts such as NaDC may be protonated by CO<sub>2</sub> to make it only marginally soluble to yield a hydrogel. The hydrogen bonding and the formation of nanofibers are the key factors in the gelation process. Larger amounts of CO<sub>2</sub> increase the degree of protonation of the carboxylate groups and the density of hydrogen bonds, leading to the bundling of the fibers into thicker nano-shreds, so that the hydrogels become opaque. The mechanical properties of the hydrogels may be enhanced by the addition of an inorganic salt such as NaCl via the salting-out effect. The fact that both bile salts and CO<sub>2</sub> are natural

biological compounds should make such hydrogels biocompatible and potentially useful in biomedical applications such as cell culture, tissue engineering and drug delivery.

## 5.4 Acknowledgements

Financial support from NSERC of Canada and FQRNT of Quebec is gratefully acknowledged. We thank Mr. Hu Zhu for his help with AFM measurements. Meng Zhang thanks the Chinese Scholarship Council (CSC) for a scholarship.

## 5.5 Supporting information

### 5.5.1 Experimental section

*Materials and method* Sodium deoxycholate (NaDC), sodium chenodeoxycholate (NaCDC) sodium cholate (NaC), lithocholic acid (LCA), and sodium chloride were purchased from Sigma-Aldrich and used without further purification. CO<sub>2</sub> was purchased from Praxair. All the samples were prepared with fresh Milli-Q water.

Sodium lithocholate (NaLC) was obtained by dissolving LCA in aqueous solution with equimolar of NaOH under heating. CO<sub>2</sub> was introduced into aqueous solutions of NaDC, NaCDC, NaC, and NaLC by bubbling for a few seconds, and the mixtures were subsequently equilibrated at room temperature to check the formation of hydrogels.

The solubility of CO<sub>2</sub> in pure water at 0 °C under ambient pressure was reported to be about 80 mM.<sup>32</sup> CO<sub>2</sub> was purged into degassed Milli-Q water in an ice bath for at least 1 hour to obtain a saturated CO<sub>2</sub> solution. Purging of CO<sub>2</sub> was continued until the solution was used.<sup>33</sup> The saturated CO<sub>2</sub> solution was diluted to desired concentrations and used to induce the hydrogelation of bile salts.

The pH value of the hydrogels from NaDC was measured by Benchtop pH Meter (SPER Scientific). Freshly prepared aqueous solutions with calculated amount of NaDC

and CO<sub>2</sub> was stirred for 30 s before the pH was measured. The solution was sealed and the pH value was recorded when a stable solution or hydrogel was obtained.

*Fluorescence.* Pyrene was used as a fluorescence probe to study the aggregation behavior of NaDC. Its fluorescence spectrum is sensitive to the hydrophobicity of their environment, and the value of I<sub>3</sub>/I<sub>1</sub> increases when pyrene enters the hydrophobic core of the micelles from a polar environment. The stock solution of pyrene was freshly prepared in acetone and diluted with Milli-Q water to a concentration of 0.3 μM, which was then used in the fluorescence measurements. NaDC was dissolved in the pyrene stock solution to reach a concentration of 10 mM, which was diluted afterward with the stock solution of pyrene to desired concentrations. The samples were equilibrated at room temperature for 24 hours before use. The fluorescence emission spectra of pyrene were recorded at room temperature on a Cary Eclipse fluorescence spectrophotometer (Agilent Technologies) with an excitation wavelength of 335 nm. The slit widths of excitation and emission were both at 2.5 nm.

*Rheology.* The rheological measurements of the hydrogel samples were done at 20 °C on an AR 2000 rheometer (TA Instruments) with a steel cone-geometry of 40 mm diameter, and a fixed gap of 55 μm between the plate and the cone. The solutions with desired concentration of NaDC, CO<sub>2</sub>, and NaCl were prepared and stirred for 30 s with a magnetic stirring bar, and aliquots of the solutions were transferred immediately to the center of rheometer plate. A very small oscillatory strain of 0.1% was applied to record the storage moduli (G') and loss moduli (G'') until a plateau was reached.

*Transmission electron microscopy (TEM).* Three μl of the samples of NaDC aqueous solutions with or without CO<sub>2</sub> were drop-coated on carbon-coated copper grids (300 mesh, Carbon Type-B, Ted Pella, Inc.) at room temperature. The excess of the samples was removed by a filter paper to obtain a thin film on the surface of the copper grid, which was dried under vacuum. Samples were observed on FEI Tecnai 12 TEM at 80 kV, equipped with AMT XR80C CCD camera system.

*Atomic-force microscopy (AFM).* The hydrogel samples were drop-coated on the silicon wafers (University Wafer) at ambient conditions and dried under vacuum. AFM

images were recorded in tapping mode AFM using a Multimode microscope controlled by a Nanoscope V controller (Bruker) at room temperature. Gwyddion 2.30 software was used to process the AFM images.

*FT-IR spectroscopy.* Hydrogels of NaDC induced by CO<sub>2</sub> in Milli-Q water were freeze-dried to obtain aerogels to record the FT-IR spectra. A Nicolet 6700 attenuated total reflection (ATR) FT-IR spectrometer (Thermo Fisher Scientific) was used and the spectra were recorded by collecting 128 scans at a resolution of 2 cm<sup>-1</sup>.

### 5.5.2 Supporting data

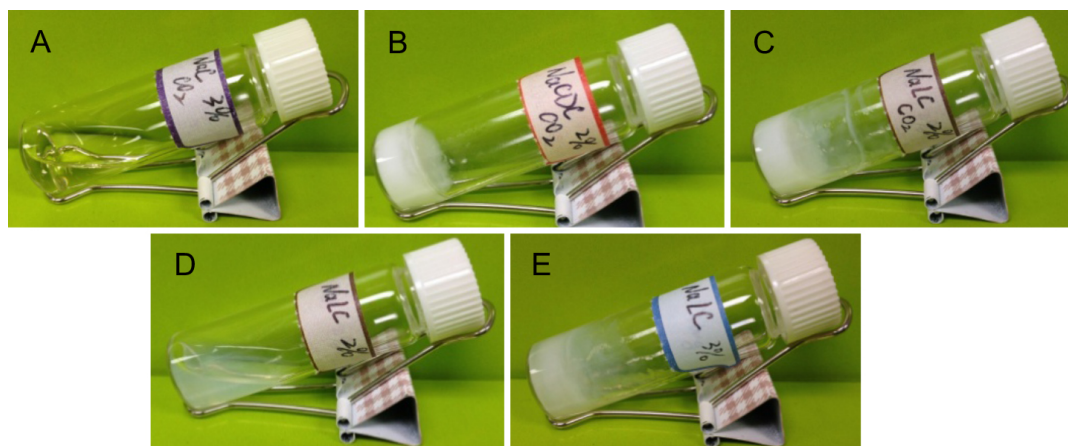


**Figure 5.S1** (A) An aqueous solution of NaC (3 wt%), (B) A hydrogel with 2 wt% NaCDC in water, (C) A hydrogel with 2 wt% NaLC in water. A, B and C were all purged with CO<sub>2</sub>. (D) A bluish viscous solution with 2 wt% NaLC in water, (E) A bluish stable hydrogel with 3 wt% NaLC. D and E were not purged with CO<sub>2</sub>.

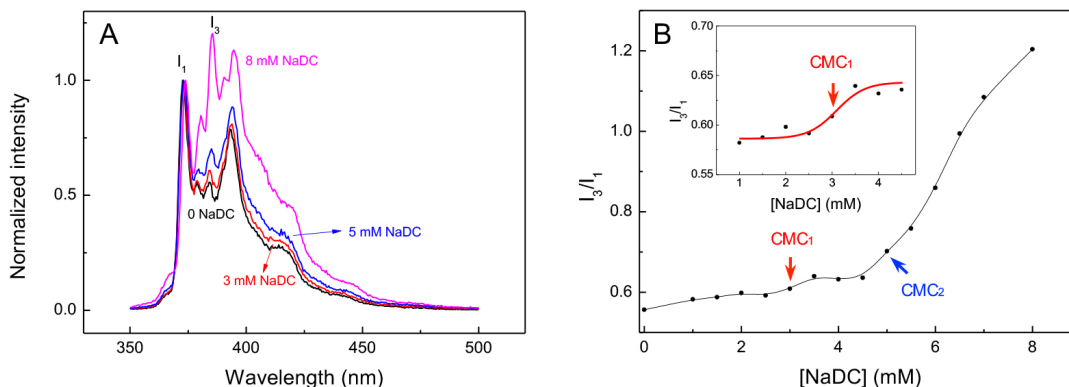


**Figure 5.S2** (A) Fluorescence spectra of pyrene ( $0.3 \mu\text{M}$  in water) with various concentrations of NaDC. (B) Variation of  $I_3/I_1$  of the pyrene fluorescence spectra with the concentration of NaDC. The inset with modified scales shows more clearly the  $\text{CAC}_1$ , and the black and red lines are drawn as visual guides.

## 5.6 References

1. A. Fini; A. Roda; R. Fugazza; B. Grigolo. Chemical Properties of Bile Acids: III. Bile Acid Structure and Solubility in Water. *J. Solution Chem.* **1985**, *14*, 595-603.
2. H. Amenitsch; H. Edlund; A. Khan; E. F. Marques; C. La Mesa. Bile Salts form Lyotropic Liquid Crystals. *Colloids Surf., A* **2003**, *213*, 79-92.
3. E. Carretti; L. Dei; P. Baglioni; R. G. Weiss. Synthesis and Characterization of Gels from Polyallylamine and Carbon Dioxide as Gellant. *J. Am. Chem. Soc.* **2003**, *125*, 5121-5129.
4. E. Carretti; L. Dei; R. G. Weiss; P. Baglioni. A New Class of Gels for the Conservation of Painted Surfaces. *J. Cul. Herit.* **2008**, *9*, 386-393.
5. M. George; R. G. Weiss. Chemically Reversible Organogels via “Latent” Gelators. Aliphatic Amines with Carbon Dioxide and Their Ammonium Carbamates. *Langmuir* **2002**, *18*, 7124-7135.
6. M. George; R. G. Weiss. Chemically Reversible Organogels: Aliphatic Amines as “Latent” Gelators with Carbon Dioxide. *J. Am. Chem. Soc.* **2001**, *123*, 10393-10394.

7. H. Che; M. Huo; L. Peng; T. Fang; N. Liu; L. Feng; Y. Wei; J. Yuan. CO<sub>2</sub>-Responsive Nanofibrous Membranes with Switchable Oil/Water Wettability. *Angew. Chem. Int. Ed. Engl.* **2015**, *54*, 8934-8938.
8. Q. Yan; R. Zhou; C. Fu; H. Zhang; Y. Yin; J. Yuan. CO<sub>2</sub>-Responsive Polymeric Vesicles that Breathe. *Angew. Chem. Int. Ed. Engl.* **2011**, *50*, 4923-4927.
9. Q. Yan; Y. Zhao. CO<sub>2</sub>-Stimulated Diversiform Deformations of Polymer Assemblies. *J. Am. Chem. Soc.* **2013**, *135*, 16300-16303.
10. M. F. Cunningham; P. G. Jessop. An Introduction to the Principles and Fundamentals of CO<sub>2</sub>-Switchable Polymers and Polymer Colloids. *Eur. Polym. J.* **2016**, *76*, 208-215.
11. X. Su; M. F. Cunningham; P. G. Jessop. Use of a Switchable Hydrophobic Associative Polymer to Create an Aqueous Solution of CO<sub>2</sub>-Switchable Viscosity. *Polym. Chem.* **2014**, *5*, 940-944.
12. D. Han; O. Boissiere; S. Kumar; X. Tong; L. Tremblay; Y. Zhao. Two-Way CO<sub>2</sub>-Switchable Triblock Copolymer Hydrogels. *Macromolecules* **2012**, *45*, 7440-7445.
13. Y. Zhang; Z. Chu; C. A. Dreiss; Y. Wang; C. Fei; Y. Feng. Smart Wormlike Micelles Switched by CO<sub>2</sub> and Air. *Soft Matter* **2013**, *9*, 6217.
14. Y. Zhang; Y. Feng; J. Wang; S. He; Z. Guo; Z. Chu; C. A. Dreiss. CO<sub>2</sub>-Switchable Wormlike Micelles. *Chem. Commun.* **2013**, *49*, 4902-4904.
15. Y. Zhang; Y. Feng; Y. Wang; X. Li. CO<sub>2</sub>-Switchable Viscoelastic Fluids Based on a Pseudogemini Surfactant. *Langmuir* **2013**, *29*, 4187-4192.
16. K. Matsuoka; Y. Moroi. Micelle Formation of Sodium Deoxycholate and Sodium Ursodeoxycholate (Part 1). *Biochim. Biophys. Acta, Mol. Cell Biol. Lipids* **2002**, *1580*, 189-199.
17. S. Reis; C. G. Moutinho; C. Matos; B. de Castro; P. Gameiro; J. L. Lima. Noninvasive Methods to Determine the Critical Micelle Concentration of Some Bile Acid Salts. *Anal. Biochem.* **2004**, *334*, 117-126.
18. S. Gouin; X. X. Zhu. Fluorescence and NMR Studies of the Effect of a Bile Acid Dimer on the Micellization of Bile Salts. *Langmuir* **1998**, *14*, 4025-4029.
19. K. Kalyanasundaram; J. K. Thomas. Environmental Effects on Vibronic Band Intensities in Pyrene Monomer Fluorescence and Their Application in Studies of Micellar Systems. *J. Am. Chem. Soc.* **1977**, *99*, 2039-2044.

20. D. Madenci; S. U. Egelhaaf. Self-Assembly in Aqueous Bile Salt Solutions. *Curr. Opin. Colloid Interface Sci.* **2010**, *15*, 109-115.
21. A. V. Verde; D. Frenkel. Simulation Study of Micelle Formation by Bile Salts. *Soft Matter* **2010**, *6*, 3815.
22. S. Mukhopadhyay; U. Maitra. Chemistry and Biology of Bile Acids. *Curr. Sci.* **2004**, *87*, 1666-1683.
23. G. Zhu; J. S. Dordick. Solvent Effect on Organogel Formation by Low Molecular Weight Molecules. *Chem. Mater.* **2006**, *18*, 5988-5995.
24. A. Jover; F. Mejjide; E. R. Nunez; J. V. Tato. Dynamic Rheology of Sodium Deoxycholate Gels. *Langmuir* **2002**, *18*, 987-991.
25. X. Sun; Z. Du; E. Li; X. Xin; N. Tang; L. Wang; J. Yuan. Rheological Properties of the Gels of Biological Surfactant Sodium Deoxycholate/Amino Acids/Halide Salts Systems. *Colloids Surf., A* **2014**, *457*, 345-353.
26. A. Jover; F. Mejjide; E. R. Nunez; J. V. Tato; M. Mosquera; F. R. Prieto. Unusual Pyrene Excimer Formation During Sodium Deoxycholate Gelation. *Langmuir* **1996**, *12*, 1789-1793.
27. D. M. Blow; A. Rich. Studies on the Formation of Helical Deoxycholate Complexes<sup>1,2</sup>. *J. Am. Chem. Soc.* **1960**, *82*, 3566-3571.
28. H. Sobotka; N. Czczowiczka. The Gelation of Bile Salt Solutions. *J. Colloid Sci.* **1958**, *13*, 188-191.
29. G. Li; Y. Hu; J. Sui; A. Song; J. Hao. Hydrogelation and Crystallization of Sodium Deoxycholate Controlled by Organic Acids. *Langmuir* **2016**, *32*, 1502-1509.
30. X. Sun; X. Xin; N. Tang; L. Guo; L. Wang; G. Xu. Manipulation of the Gel Behavior of Biological Surfactant Sodium Deoxycholate by Amino Acids. *J. Phys. Chem. B* **2014**, *118*, 824-832.
31. R. Zangi; M. Hagen; B. J. Berne. Effect of Ions on the Hydrophobic Interaction between Two Plates. *J. Am. Chem. Soc.* **2007**, *129*, 4678-4686.
32. L. W. Diamond; N. N. Akinfiev. Solubility of CO<sub>2</sub> in Water from -1.5 to 100 °C and from 0.1 to 100 MPa: Evaluation of Literature Data and Thermodynamic Modelling. *Fluid Phase Equilib.* **2003**, *208*, 265-290.



33. S. K. Niazi. *Handbook of Pharmaceutical Manufacturing Formulations: Sterile Products*. Niazi, S. K. Eds.; Informa Healthcare USA, Inc.: New York, 2009.

## Chapter 6

### Conclusions and future work

#### 6.1 Conclusions

Molecular gels are gels derived from compounds of low molecular weight (usually  $< 2000 \text{ gmol}^{-1}$ ) in certain solvents. Such molecules self-assemble in specific solvents to form 3-D fibrous networks, immobilize the solvent by surface tension and make the solution to behave solid-like. The driving forces for the formation of such gels are relatively weak supramolecular interactions such as hydrophobic interactions, hydrogen bonding, electrostatic attractions, and van der Waals forces. Molecular gels can be classified as hydrogels and organogels, where the solvents to be gelated are water and organic solvents, respectively. Generally, molecular hydrogels are regarded to be less toxic than molecular organogels, and may be more suitable for biomedical applications. In this work, we have developed two different hydrogelation systems based on bile acids and their derivatives, and studied the properties and formation mechanisms of these hydrogels. A general rule for the relationship between the gelator structure and gelation behavior was also illustrated. Such materials possess advantages such as better degradability and functional diversity when compared with polymeric gels and may be potentially used in areas such as drug delivery and tissue engineering. The fibrillar structures in these gels may also be used as templates for structure directing agents.

##### 6.1.1 Novel molecular hydrogels derived from bile acids

The molecular gels based on bile acids may be obtained at a low gelator concentration, indicating their good gelation ability. Two hydrogelation systems based on bile acids were studied in this thesis. The first one is a cholic acid dimer with two cholic acid units linked via a diethylenetriamine spacer, as discussed in Chapter 3 and 4. It is insoluble in water but become soluble in the presence of selected carboxylic acids, and subsequently self-

assemble to form hydrogels with nanofibers. The addition of carboxylic acids protonated the secondary amine group and formed hydrogen bond with the secondary amide group on the dimer, helping the dissolution of the dimer in water and favoring the self-assembling process. Acids that are either too hydrophobic or too strong cannot induce the gelation of the dimer, due to the low solubility of the formed dimer-acid complex and the lack of hydrogen bonding with the amide group, respectively. Supramolecular interactions such as hydrophobic interaction and hydrogen bonding between the side chain of carboxylic acid in the hydrogels can improve the mechanical strength of the yielded hydrogels. This study showed certain predictability of gelation behavior of the dimer with various acids, which may be helpful in the design of novel functional molecular hydrogels.

The other gelation system is hydrogels of a series of bile salts induced by  $\text{CO}_2$  as discussed in Chapter 5. The bile salts are quite soluble in water and their solubility could be higher than 40 wt%, while the solubility of bile acids is generally poor. Certain bile salts may be partially protonated in the presence of  $\text{CO}_2$  to yield hydrogels. The bile salts self-assemble in water to form micelles with hydroxyl and carboxylate polar groups facing the aqueous media. The formation of hydrogen bonds between the protonated carboxylate groups on the surface of micelles is the primary driving force for the formation of nanofibers and hydrogels. Larger amounts of  $\text{CO}_2$  increase the degree of protonation of the carboxylate groups and the density of hydrogen bonds, leading to the bundling of the nanofibers into thicker nano-shreds and the hydrogels become opaque. Both mechanical strength and transparency of the hydrogels can be improved by the salting-out effect from inorganic salts such as NaCl. Such hydrogels are made of entirely biological compounds, including both bile acids and  $\text{CO}_2$ .

### **6.1.2 A general rule for the formation of molecular gels**

Formation of molecular gels strongly depends on the gelator chemical structures, a slight variation of which may result in the loss of their gelation ability. Enormous efforts have been made in the past decades to understand the basic principles of such gels with self-assembled fibrous 3-D networks. Theories such as hydrophilic-lipophilic balance (HLB) and packing parameters may be used to explain the relationship between the

gelator structure and gelation ability in aqueous systems, while both show their limitations. As a result, the prediction of the gelation ability of a compound with a given structure in a specific solvent is remaining a challenge, and serendipity or trail-and-error is responsible for most of molecular gels reported to date.

In this thesis, by studying the two different gelation systems derived from bile acids, we concluded that a *marginal solubility* in water is a prerequisite for a compound to be a molecular hydrogelator. Insoluble compounds (such as the cholic acid dimer) in water can be made to be marginally soluble by means that favor their dissolution process, such as acid-base reaction (by the addition of carboxylic acids) or the addition of water-miscible organic solvents. In contrast, soluble compounds (bile salts) can be made to be marginally soluble by means that interfere the dissolution process with the help of supramolecular interactions such as protonation (induced by CO<sub>2</sub>) and salting-out effect (by NaCl). The limited or marginal solubility of the species points to the favored direction for the formation of hydrogels. Such a rule may be applicable in the formation of organogels as well.

### 6.1.3 Nematic hydrogels

Certain molecular gels based on bile acids, including organogels and hydrogels, were reported to behave as lyotropic liquid crystals and showed optical textures when observed with a polarized optical microscope. The mechanism for the liquid crystalline structure of molecular gels based on bile acids, however, remains unclear to date.

In this work, a mixture of the cholic acid dimer with formic acid in a molar ratio of 1/1, which was regarded as an organic salt, self-assembled in water to form nanofibers. At low concentrations, the dimer salt yielded a well-dispersed and random-directed 3-D fibrous. The nanofibers in the networks formed ordered aggregate with parallel arrangement when the solution was physically stirred. The randomly directed network immobilizes the solvent when the salt concentration was higher than the critical gelation concentration, leading to the formation of a stable isotropic hydrogel. The nanofibers arranged parallel with each other when the concentration of the dimer salt was high enough, which changed the optical properties of hydrogels and make them behave as

lyotropic liquid crystals. The gelation can be regarded as an intermediate transient state for a solution to crystallize when the solute molecules are more ordered, or to precipitate when the solute molecules are disordered. The nematic hydrogels obtained in this study exemplifies the final state of the system with ordered fine structures/morphologies observed microscopically.

## 6.2 Perspectives

### 6.2.1 Molecular hydrogels induced by ammonia or amines

The *marginal solubility* of gelators was regarded to be a prerequisite of the formation of molecular gels. As shown in Chapter 5, purging CO<sub>2</sub> into aqueous solutions of bile salts may adjust the pH and partially protonate the carboxylate groups on bile salts and reduce the solubility of the solute, resulting in transparent or opaque hydrogels depending on the amount of CO<sub>2</sub> added. One advantage is that CO<sub>2</sub> may be removed by purging an inert gas such as Ar and N<sub>2</sub> into or by mildly heating the mixtures, and the reversible gel-sol phase transition can be repeated several times without any contamination by accumulated chemical by-products.<sup>1-3</sup>

Basic compounds such as ammonia and other compounds bearing amine groups may also be used to change the pH of aqueous solutions.<sup>4-5</sup> Purging or adding them into aqueous solutions may deprotonate compounds with acidic functional groups such as carboxylic acids and improve their solubility in water to form hydrogels. The hydrogelation behavior of a series of organic acids may be tested in the presence of certain amines such as ammonia, methylamine, ethylamine, propylamine, and butylamine. Preliminary gelation tests on a series of bile acids, such as cholic acid (CA), deoxycholic acid (DCA), chenodeoxycholic acid (CDCA) and lithocholic acid (LCA), and fatty acids, such as stearic acid (SA) showed that they could be dissolved in the presence of above-mentioned amines upon heating and yield various aggregates after the subsequently cooling process (Table 6.1). The gelation ability of these two-component systems strongly depends on the chemical structure of both acids and amines. No hydrogel formed by the

relatively hydrophilic bile acids such as CA, DCA, and CDCA under all the conditions tested. LCA and SA are able to form hydrogels with most of amines, while interaction of LCA with butylamine yielded needle-like crystals and the complex of SA and ammonia hydroxide showed a gelation-precipitation transition on the cooling process of a hot solution to room temperature. More detailed tests will be conducted to quantify the concentrations or molar ratio in these two-component systems.

The hydrogelation may be reversed by purging an inert gas or by heating. More specific experiments will be conducted to study how the structure of organic acids and amines affect the gelation ability, as well as the mechanical strength of the yielded hydrogels.

**Table 6.1** Preliminary gelation tests of certain bile acids and a fatty acid in the presence of various amines

	Ammonia	Methylamine	Ethylamine	Propylamine	Butylamine
CA	S	S	S	S	S
DCA	S	S	S	S	S
CDCA	S	S	S	S	S
LCA	OG	OG	OG	OG	C
SA	G-P	TG	TG	TG	TG

S = solution, OG = opaque gel, TG = translucent gel, C = crystal,

G-P = gel upon heating and precipitates at room temperature

### 6.2.2 Two-component molecular hydrogels from bile salts and dopamine

Catechols occur naturally in foods, vegetables, insects, and teas. They are widely used in food and pharmaceuticals and as agrochemical intergradients and stabilizing additives.<sup>6</sup>

<sup>7</sup> The catechol unit may show strong adhesion to inorganic materials. The interaction between catechol and TiO<sub>2</sub> may achieve a bond strength of about 40% that of a covalent bond.<sup>6,8</sup> 3,4-dihydroxy-phenylalanine, a catechol derived amino acid in secreted mussel adhesive proteins, is responsible for the strong adhesion of mussels.<sup>9</sup> Another catechol derivative, dopamine, has also been widely used to make hydrogels, surface coatings,

adhesives, and drug delivery carriers.<sup>10</sup> Dopamine may be easily oxidized in basic aqueous solutions or in the presence of oxidants such as  $\text{NaIO}_4$ , and polymerized afterward to form polydopamine.<sup>11-12</sup> Such a polymer may improve the mechanical properties of hydrogels and make them to be injectable and self-healable.<sup>13-14</sup>

Bile salts may form hydrogels with nanofibers in aqueous solutions in the presence of  $\text{NaCl}$  or acidic compounds such as  $\text{HCl}$  and organic acids.<sup>15-16</sup> In a preliminary experiment we found that sodium deoxycholate (NaDC) can interact with dopamine hydrochloride to form a two-component molecular hydrogel (Fig. 6.1). The color change during the gelation process may indicate the oxidative self-polymerization of dopamine.<sup>12, 17-18</sup> The gelation process may be accelerated by UV irradiation or addition of oxidants such as ammonium persulfate due to the faster polymerization of dopamine.<sup>17, 19</sup> NaDC hydrogel with improved mechanical properties may be obtained to study the interactions between NaDC and dopamine/polydopamine. Such a two-component hydrogelation system based on NaDC and dopamine may be potentially useful for biomedical applications.

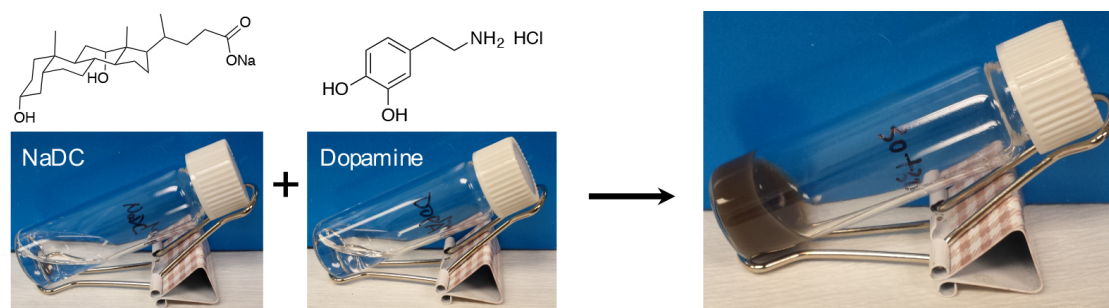


**Figure 6.1** Formation of hydrogels from NaDC and dopamine.

### 6.2.3 Molecular hydrogels based on betulin and its derivatives

Betulin (Fig. 6.2) is an abundant naturally-occurring pentacyclic triterpene alcohol with a lupine skeleton. It is found predominantly in bushes and trees forming the principal extractive (up to 30% of dry weight) of the bark of birch trees.<sup>20-21</sup> It was reported to have antiviral and anti-inflammatory effects and may be used for making novel functional biomaterials.<sup>21-23</sup> Its derivatives, including small molecules and polymers, were

synthesized and show various interesting properties. A polymer derived from betulin exhibits a set of valuable properties such as low toxicity and biological activity.<sup>24</sup> Betulinic acid could be synthesized from betulin in two steps (Fig. 6.2), and it exhibited a variety of biological activities including inhibition of human immunodeficiency virus (HIV), antibacterial, antimalarial, anti-inflammatory, anthelmintic and antioxidant properties.<sup>25</sup>

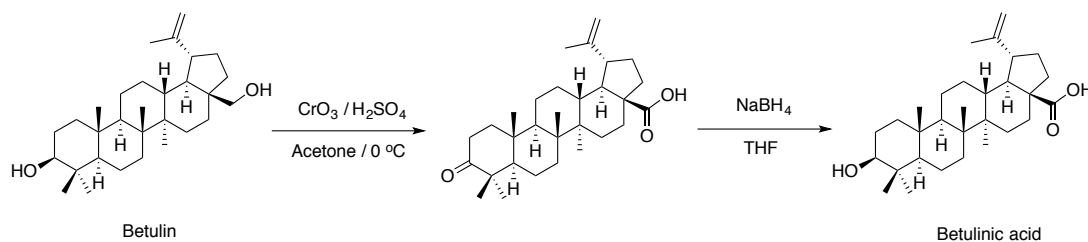


**Figure 6.2** The synthetic route of betulinic acid from betulin.

Bag and Dash<sup>26-27</sup> reported that both molecular organogels and hydrogels via self-assembling could be obtained from betulin and betulinic acid. Betulin self-assembles in organic solvents such as *o*-, *m*- and *p*-xylene, and an aqueous solution with DMSO (1:1) to form molecular gels.<sup>26</sup> Sodium and potassium salts of betulinic acid formed hydrogels in either pure water or the aqueous solutions of DMSO, DMF, ethylene glycol and ethanol at a ratio of 1:1.<sup>27</sup> Therefore, betulin derivatives are promising for making novel molecular gels. The biological activities of betulin and its derivatives may be retained in such gels to facilitate their biomedical applications.

Due to the hydrophobic nature of betulin, introducing hydrophilic units may improve the water-solubility and promote the self-assembling behavior. We proposed a series of compounds based on betulin that may form hydrogels with their synthetic routes (Fig. 6.3). Their gelation behavior may be tested.



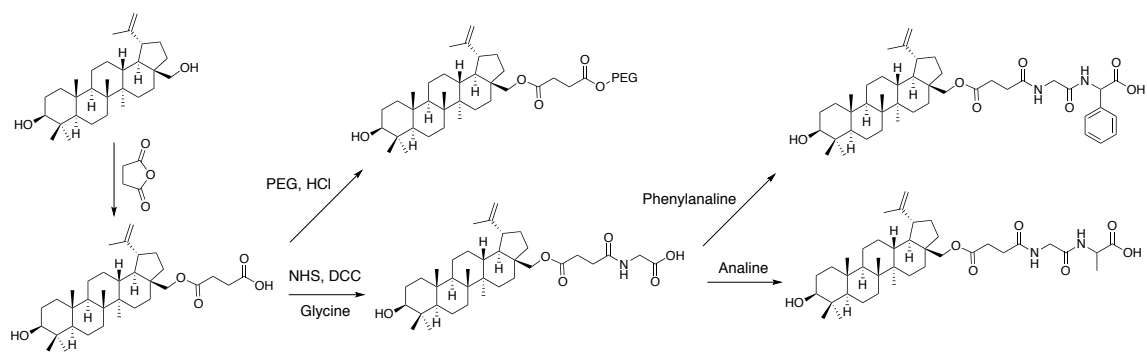


**Figure 6.3** The synthetic route of a series of potential molecular gelators based on betulin.

### 6.3 References

1. T. Yu; R. Cristiano; R. G. Weiss. From Simple, Neutral Triatomic Molecules to Complex Chemistry. *Chem. Soc. Rev.* **2010**, *39*, 1435-1447.
2. D. Han; O. Boissiere; S. Kumar; X. Tong; L. Tremblay; Y. Zhao. Two-Way CO<sub>2</sub>-Switchable Triblock Copolymer Hydrogels. *Macromolecules* **2012**, *45*, 7440-7445.
3. Q. Yan; Y. Zhao. Block Copolymer Self-Assembly Controlled by the "Green" Gas Stimulus of Carbon Dioxide. *Chem. Commun.* **2014**, *50*, 11631-11641.
4. H. Basit; A. Pal; S. Sen; S. Bhattacharya. Two-Component Hydrogels Comprising Fatty Acids and Amines: Structure, Properties, and Application as a Template for the Synthesis of Metal Nanoparticles. *Chem. Eur. J.* **2008**, *14*, 6534-6545.
5. A. Pal; H. Basit; S. Sen; V. K. Aswal; S. Bhattacharya. Structure and Properties of Two Component Hydrogels Comprising Lithocholic Acid and Organic Amines. *J. Mater. Chem.* **2009**, *19*, 4325-4334.
6. Y.-G. Jia; X. X. Zhu. Nanocomposite Hydrogels of LAPONITE® Mixed with Polymers Bearing Dopamine and Cholic Acid Pendants. *RSC Adv.* **2016**, *6*, 23033-23037.
7. E. Faure; C. Falentin-Daudré; C. Jérôme; J. Lyskawa; D. Fournier; P. Woisel; C. Detrembleur. Catechols as Versatile Platforms in Polymer Chemistry. *Prog. Polym. Sci.* **2013**, *38*, 236-270.
8. H. Lee; N. F. Scherer; P. B. Messersmith. Single-Molecule Mechanics of Mussel Adhesion. *Proc. Natl. Acad. Sci. U. S. A.* **2006**, *103*, 12999-13003.

9. J. Wu; L. Zhang; Y. Wang; Y. Long; H. Gao; X. Zhang; N. Zhao; Y. Cai; J. Xu. Mussel-Inspired Chemistry for Robust and Surface-Modifiable Multilayer Films. *Langmuir* **2011**, *27*, 13684-13691.
10. X. Zhao; M. Zhang; B. Guo; P. X. Ma. Mussel-inspired Injectable Supramolecular and Covalent Bonds Crosslinked Hydrogels with Rapid Self-healing and Recovery via a Facile Approach Under Metal-free Conditions. *J. Mater. Chem. B* **2016**.
11. C. Lee; J. Shin; J. S. Lee; E. Byun; J. H. Ryu; S. H. Um; D. I. Kim; H. Lee; S. W. Cho. Bioinspired, Calcium-Free Alginate Hydrogels with Tunable Physical and Mechanical Properties and Improved Biocompatibility. *Biomacromolecules* **2013**, *14*, 2004-2013.
12. A. Postma; Y. Yan; Y. Wang; A. N. Zelikin; E. Tjipto; F. Caruso. Self-Polymerization of Dopamine as a Versatile and Robust Technique to Prepare Polymer Capsules. *Chem. Mater.* **2009**, *21*, 3042-3044.
13. L. Li; B. Yan; J. Yang; L. Chen; H. Zeng. Novel Mussel-Inspired Injectable Self-Healing Hydrogel with Anti-Biofouling Property. *Adv. Mater.* **2015**, *27*, 1294-1299.
14. N. Holten-Andersen; M. J. Harrington; H. Birkedal; B. P. Lee; P. B. Messersmith; K. Y. Lee; J. H. Waite. pH-Induced Metal-Ligand Cross-Links Inspired by Mussel Yield Self-Healing Polymer Networks with Near-Covalent Elastic Moduli. *Proc. Natl. Acad. Sci. U. S. A.* **2011**, *108*, 2651-2655.
15. A. Jover; F. Mejjide; E. R. Nunez; J. V. Tato. Dynamic Rheology of Sodium Deoxycholate Gels. *Langmuir* **2002**, *18*, 987-991.
16. G. Li; Y. Hu; J. Sui; A. Song; J. Hao. Hydrogelation and Crystallization of Sodium Deoxycholate Controlled by Organic Acids. *Langmuir* **2016**, *32*, 1502-1509.
17. X. Du; L. Li; J. Li; C. Yang; N. Frenkel; A. Welle; S. Heissler; A. Nefedov; M. Grunze; P. A. Levkin. UV-Triggered Dopamine Polymerization: Control of Polymerization, Surface Coating, and Photopatterning. *Adv. Mater.* **2014**, *26*, 8029-8033.
18. W. Zheng; H. Fan; L. Wang; Z. Jin. Oxidative Self-Polymerization of Dopamine in an Acidic Environment. *Langmuir* **2015**, *31*, 11671-11677.
19. Q. Wei; F. Zhang; J. Li; B. Li; C. Zhao. Oxidant-Induced Dopamine Polymerization for Multifunctional Coatings. *Polym. Chem.* **2010**, *1*, 1430.

20. S. Alakurtti; T. Makela; S. Koskimies; J. Yli-Kauhaluoma. Pharmacological Properties of the Ubiquitous Natural Product Betulin. *Eur. J. Pharm. Sci.* **2006**, *29*, 1-13.
21. J. J. Tang; J. G. Li; W. Qi; W. W. Qiu; P. S. Li; B. L. Li; B. L. Song. Inhibition of SREBP by a Small Molecule, Betulin, Improves Hyperlipidemia and Insulin Resistance and Reduces Atherosclerotic Plaques. *Cell Metab.* **2011**, *13*, 44-56.
22. O. Salin; S. Alakurtti; L. Pohjala; A. Siiskonen; V. Maass; M. Maass; J. Yli-Kauhaluoma; P. Vuorela. Inhibitory Effect of the Natural Product Betulin and Its Derivatives Against the Intracellular Bacterium Chlamydia Pneumoniae. *Biochem. Pharmacol.* **2010**, *80*, 1141-1151.
23. M. Laavola; R. Haavikko; M. Hamalainen; T. Leppanen; R. Nieminen; S. Alakurtti; V. M. Moreira; J. Yli-Kauhaluoma; E. Moilanen. Betulin Derivatives Effectively Suppress Inflammation in Vitro and in Vivo. *J. Nat. Prod.* **2016**, *79*, 274-280.
24. M. N. Gorbunova; G. F. Krainova; I. A. Tolmacheva; V. V. Grishko. New Polymeric Derivatives of Betulin. *Russ. J. Appl. Chem.* **2012**, *85*, 1137-1141.
25. P. Yogeewari; D. Sriram. Betulinic Acid and Its Derivatives: A Review on their Biological Properties. *Curr. Med. Chem.* **2005**, *12*, 657-666.
26. B. G. Bag; S. S. Dash. Hierarchical Self-Assembly of a Renewable Nanosized Pentacyclic Dihydroxy-triterpenoid Betulin Yielding Flower-Like Architectures. *Langmuir* **2015**, *31*, 13664-13672.
27. B. G. Bag; S. S. Dash. Self-Assembly of Sodium and Potassium Betulinates into Hydro- and Organo-Gels: Entrapment and Removal Studies of Fluorophores and Synthesis of Gel–Gold Nanoparticle Hybrid Materials. *RSC Adv.* **2016**, *6*, 17290-17296.